UILU-ENG-2000-2001

CIVIL ENGINEERING STUDIES

STRUCTURAL RESEARCH SERIES NO. 629

ISSN: 0069-4274

MINIMUM LIFE-CYCLE COST STRUCTURAL DESIGN AGAINST NATURAL HAZARDS

By
YONG-JOONG KANG
and
YI-KWEI WEN

A Report on a Research Project
Sponsored by the
NATIONAL SCIENCE FOUNDATION
(Under Grant NSF CMS-95-10243
and University of Illinois Research Board)

DEPARTMENT OF CIVIL AND ENVIRONMENTAL ENGINEERING
UNIVERSITY OF ILLINOIS AT URBANA-CHAMPAIGN
URBANA, ILLINOIS
JANUARY 2000

50272–101

REPORT DOCUMENTATION PAGE	1. REPORT NO. UILU-ENG-2000-2001	2.	3. Recipient's Accession No.

4. Title and Subtitle

Minimum Life-Cycle Cost Structural Design Against Natural Hazards

5. Report Date

January 2000

6.

7. Author(s)

Y.-J. Kang and Y. K. Wen

8. Performing Organization Report No.

SRS 629

9. Performing Organization Name and Address

University of Illinois at Urbana-Champaign
Department of Civil and Environmental Engineering
205 N. Mathews Avenue
Urbana, Illinois 61801-2352

10. Project/Task/Work Unit No.

11. Contract(C) or Grant(G) No.

NSF CMS-95-10243
Univ. of Illinois Research Board

12. Sponsoring Organization Name and Address

National Science Foundation
4201 Wilson Boulevard
Arlington, VA 22230

13. Type of Report & Period Covered

14.

15. Supplementary Notes

16. Abstract (Limit: 200 words)

A methodology is developed for determination of design criteria for structures under single and multiple hazards. Emphasis is on consideration of the uncertainties in the hazards and structural capacity, and costs, i.e., initial (construction) cost, costs of consequences of various structural limit-states including deaths and injuries, and discounting of cost over time. Optimal structural strength and target reliability are obtained by minimizing the expected life-cycle cost. Sensitivity of optimal design to important loading and structural parameters is also investigated. It is found that, for a single hazard, the optimal design depends primarily on the limit state consequences (costs), and to a lesser extent on the structural life. For multiple hazards, the optimal design is controlled by the hazard with large uncertainty and severe failure consequences. The methodology is then applied to the design of a 9-story office building against earthquakes in Los Angeles. The seismic hazards are based on USGS data and FEMA 273 provisions. The structural response is evaluated via an equivalent nonlinear SDOF system. Cost estimates are based on findings in recent FEMA reports. The optimal structural strength is found to be higher than the strength according to current design. The application is further extended to design against both winds and earthquakes in Seattle, Charleston and Boston. Both structural and building envelope (glass window) limit states are considered for winds. It is found that one hazard often dominates in the optimal design and uniform reliability against different hazards, a commonly accepted notion, is not required. The method and results are useful in developing next generation codes and standards.

17. Document Analysis a. Descriptors

Uncertainty, Nonlinear Response, Life-Cycle Cost, Optimal Design, Sensitivity Analysis, Seismic Load, Wind Load, Limit State, Expected Failure Cost, Cost of Death and Injury, Envelope Failure, Windborne Missiles

b. Indentifiers/Open-Ended Terms

c. COSATI Field/Group

18. Availability Statement	19. Security Class (This Report)	20. No. of Pages
Release Unlimited	UNCLASSIFIED	190
	21. Security Class (This Page) UNCLASSIFIED	22. Price

(See ANSI–Z39.18)

OPTIONAL FORM 272 (4–77)
Department of Commerce

ACKNOWLEDGEMENTS

This report is based on the thesis of Dr. Yong-Joong Kang submitted in partial fulfillment of the requirement for the Ph.D. degree in Civil Engineering at the University of Illinois at Urbana-Champaign. Financial supports by the National Science Foundation under grant NSF CMS-95-10243 and University of Illinois Research Board are gratefully acknowledged.

The comments and suggestions of Professors Douglas A. Foutch, William L. Gamble and Liang Y. Liu are gratefully appreciated.

TABLE OF CONTENTS

LIST OF TABLES

LIST OF FIGURES

CHAPTER 1

INTRODUCTION AND BACKGROUND

1.1 Introduction

The large number of structural failures observed after recent earthquakes and hurricanes, e.g., the Northridge earthquake and the Hyogoken-Nanbu earthquake, hurricane Hugo and hurricane Andrew, indicated the need for new concepts and methodologies of design to improve building performance. According to a report by Structural Engineers Association in California (SEAOC, 1995), current building codes in seismically active regions of the United States ensure life-safety protection in buildings that have been properly designed and constructed. However, they appear to be less reliable against property damage in moderate events. Fortunately, very few lives were lost in buildings that were designed according to recent building codes, but the structural engineering profession and public policy makers considered the economic loss to be too large for such moderate events. Therefore, a new building design methodology is needed that in addition to protecting life safety can also reduce property damage and economical impact to an acceptable level. The method should be applicable to design of new buildings as well as rehabilitation of existing buildings.

In 1992, the SEAOC board of directors initiated the Vision 2000 Committee and proposed "Performance Based Seismic Engineering of Buildings" to develop a framework for a next generation building design code. Since then, many multi-level performance-based design concepts and methods have been proposed; notable examples are the NEHRP Guidelines for the Seismic Rehabilitation of Buildings (FEMA-273, 1997), the FEMA/SAC Steel Project (1997) and the Building Standard Law in Japan (Hiraishi et al, 1998). Most of the proposals recommend multi-level building

performance check using response spectra or time histories according to given probability (or return period) levels to account for uncertainty in the seismic demand.

The selection of the seismic hazards, or more specifically, the associated return periods and the corresponding structural performance levels, however, has largely been based on professional experience and judgement. For example, the major building codes, such as the Uniform Building Code, BOCA code and the Standard Building Code, have been based mostly on experience with structures in past earthquakes and recent research results. Because of the large uncertainty in loading and resistance in structures, determination of the design loads in code revisions requires careful considerations. The uncertainty can be attributed to a large number of factors e.g., characteristics of loads, structural resistance, and structural response behavior. They all have serious implications in the long-term performance of the structure. Also, to develop a more comprehensive performance goal in a performance-based design, various costs due to hazards over the life of the structure obviously need to be taken into consideration. The same is true when retrofit is needed for existing structures.

In general, a structure designed for a lower level of load will have a higher risk of failure. On the other hand, a structure designed for a higher load and improved performance costs more. Therefore, the design load should be selected to achieve a balance between structural performance and cost. The need for this balance is more apparent in the design of a temporary structure whose failure may cause serious consequences such as deaths and injuries. Generally speaking, the level of load demand is less than that for a permanent structure because of shorter exposure time, hence lower probability of severe load. If lower design intensity is used, the structure nevertheless may fail even during its (short) life and cause severe consequences. Hence, design based on probability alone can not solve this problem. Therefore, a more comprehensive method is needed, in which the uncertainty in loading and resistance and various cost and lifetime factors are all taken into consideration, to establish an optimal target level of safety and design load. The basic concept is illustrated in Figure 1.1. A structure designed for a lower load will have a lower initial cost, but large expected failure cost. On the

other hand, making the structure stronger reduces the expected failure cost at the price of large initial cost. The optimal design level can be determined at the point of the minimum total cost. This optimal design level can be used as a target value in design.

1.2 Background and Previous Works

Probabilistic method and reliability analysis have been used successfully in developing codes and standards during the last few decades. Notable examples are the Minimum Design Loads for Buildings and Structures of ASCE (1995), the Recommended Practice 2A – Load and Resistance Factor Design (LRFD) for Offshore Structures of American Petroleum Institute (1990), and the LRFD method being developed for a new bridge code by the American Association of State Highway and Transportation Officials. In these procedures, the design goal is generally to satisfy a target reliability level against a prescribed limit state. The target reliability is inferred from what is implied in current practice and acceptable to the profession at the time. The required design resistance is then determined from the load and resistance factor design (LRFD) format such that the target reliability level is satisfied. All procedures are intended for design of new and regular facilities with normal design life span. The target reliability, however, may be different for different load combinations.

In design of new structures or retrofitting of existing structures, economics is an importance consideration. To incorporate such considerations, one needs to consider reliability and costs of various structure limit states that may occur throughout the life-cycle of a structure and arrive at an optimal design. Most studies on time-invariant reliability-based structural optimization do not consider multiple limit states, cost of limit states, discounting of cost over time, or structural lifetime.

The design procedure based on optimization considering cost and benefit is generally referred to as level IV reliability-based design. Early works include, among

others, Liu, et al (1972, 1976) and, Rosenblueth (1976). Liu, et al (1972) proposed a mathematical formulation of a seismic design on the basis of minimum life-cycle cost. Based on his research findings, Rosenblueth made a strong argument for design based on optimization as the only rational procedure to ensure long term benefit to the society.

Vanmarcke and Angelides (1983) presented an approach for quantifying risk and reliability and a review of the shortcoming of existing methods for assessing risk in offshore engineering. A reliability based approach to optimum structural design was presented by Surahman and Rojiani (1983), in which the optimal structure is based on a minimization of the total expected cost as the sum of the initial building cost and the loss due to failure. Jones (1985) developed an integer programming formulation for the minimum cost design of precast, prestressed concrete and simple supported beams and designed a box girder for a multi-beam highway bridges. Frangopol (1985) developed a new formulation related to multi-criteria optimization and showed comparative results when different criteria are used for the optimum design of a structure under service and ultimate reliability constraints. Neely and Neathammer (1989) of the U.S. Army Construction Engineering Research Laboratory (CERL) developed several methods for determining life-cycle cost of facilities and described the benefits and operation of the system. Costa (1990) suggested that the design of structural systems must be based on the consideration of the ratio of expectation of benefit to be gained by rendering a system safer to cost increase.

For the cost-effectiveness analysis of active control of structures, Wen and Ang (1991) and Wen and Shinozuka (1994) investigated the expected life-cycle cost of structural system under earthquake loads, with and without active control. Recent developments in reliability-based optimization and applications to design of structural systems can be found in Frangopol and Corotis (1994). Chang (1995) explored the need of multi-disciplinary approach to address important systems-level infrastructure problems based on a cost-effective need considerration. Using damage cost data of Mexico City after the 1985 earthquake, Ang and Leon (1997) obtained optimal risks for damage control and life safety based on a life cycle cost analysis. Several FEMA (US Federal

Emergency Management Agency) studies (e.g., FEMA 1992, 1996) dealt with design decision in rehabilitation of existing buildings. A standard benefit/cost model was developed for the seismic rehabilitation of existing buildings. Field data in nine cities were collected to support the model.

More recent literatures on estimation of earthquake loss emphasize the importance of anticipating earthquake losses. For example, King, et al (1997) developed a comprehensive methodology for evaluating the socio-economic impacts of large earthquakes. Werner, et al (1997) also developed a procedure for loss estimation due to earthquakes of highway systems. McCormack, et al (1997) developed a loss estimation model based on ATC-13 and the scoring system developed by ATC-21 through surveying of the seismic hazards for about 30,000 nonresidential buildings in Portland and Oregon. Rojahn, et al (1997) conducted a study (ATC-36) of updating and converting the ATC-13 data and methodology to either geographic information system (GIS) or non-GIS software applications in Salt Lake County, Utah. Whitman, et al (1997) summarized the development of a GIS-based regional loss estimation methodology for the United States. Brookshire, et al (1997) suggested the earthquake loss estimation methodology for direct and indirect economic losses. Olshansky (1997) emphasized the role of earthquake hazard maps in loss estimation because local-scale seismic hazard maps are an important component of loss estimation by providing information on possible site effects. Shinozuka, et al (1997) emphasized the methodological advances and insights from the loss estimation for Memphis, Tennessee, in the NCEER buildings and lifelines loss estimation projects. HAZUS (1998) program for the FEMA-NIBS methodology for earthquake loss estimates the economic losses due to damage to buildings, essential facilities and social consequences such as casualties and shelter needs in a city or region after a "scenario earthquake". All these researches are emphasize the importance of economic loss and need of rational methods to estimate loss due to earthquake.

This brief review indicates that designs based on optimization with consideration of cost and loss have been gaining more attention. Most studies have been dealing with optimal design of structure members. System performance, various limit states and

consequence of failure, as well as discounting cost over time have not been investigated on a comprehensive and systematic basis. Development of a rational methodology based on a life-cycle cost consideration is still needed.

1.3 Objective and Scope

The purpose of this study is to develop life-cycle cost based design criteria for civil structure. The objectives are:

1. Develop a methodology for determination of design criteria based on consideration of loading and resistance uncertainty and life-cycle cost.
2. Investigate parameters that effect the life-cycle cost and study of sensitivity of optimal design loads to load and structural parameters.
3. Perform a feasibility study of application of life-cycle cost based design criteria to realistic structures against earthquakes and winds.

1.4 Organization

In Chapter 2, system parameters that are important in development of a life-cycle cost based design criteria are investigated including lifetime, discount ratio, limit state, failure probability, initial cost and failure cost. The formulation proposed by Wen and Ang (1991) and Wen and Shinozuka (1994) is adopted and extended for multiple loads. The analytical formulation allows closed form solutions of total expected cost for multi-limit states under multiple loads. Numerical results of design for the case of a simple state under one and two loads representing earthquake and wind loads, are obtained and parametric studies are carried out.

Chapter 3 describes the application of the minimum life-cycle cost criteria to design against seismic loads and it shows the feasibility of the proposed method. The definition of limit state follows those in FEMA 227 (1992), FEMA 273 (1997), SEAOC (1995) and Maison and Bonowitz (1998). Twelve 9-story buildings are designed in Los

Angeles for different intensities of seismic load according to the NEHRP 97 provisions. Nonlinear inelastic push-over analyses by DRAIN-2DX structural analysis program (Prakash et al., 1993: Powell, 1993) are carried out for nonlinear inelastic response and IGRESS2 program (Ghaboussi, 1989) is used to calculate the drift ratio for each structure. The initial cost of each structure is calculated according to 1998 Building Construction Cost Data (BCCD) considering only structural components. USGS data (1999), FEMA 273 (1997) procedures and equivalent SDOF method by Collins et al. (1996) are used for structural response and failure probability. A correction factor is used for considering the uncertainty in structural capacity. The cost function is composed of damage cost, relocation cost, content loss cost, economic loss cost, injury and death cost. The mean damage index and cost values in FEMA 227 (1992) are used to calculate the cost functions. A sensitivity analysis of the optimal design to change in design life, death and injury cost, structural capacity uncertainty and discount rate is also carried out. In addition to Los Angeles, three more cities, Seattle, Charleston and Boston are considered to examine the dependence of design on geographical location.

In Chapter 4, the minimum life-cycle cost design criteria is applied to wind load. Building limit states due to winds can be described in term of structural failure (large deflection) and building envelope failure (glass or cladding failure due to wind and missile debris effects). Since wind effects causing these two types of building failure are different, two separate design wind load intensities, for to the strength of structure and strength of glass windows are considered. The response of structural frame to the wind load is calculated according to the procedures proposed in ASCE 7-98. The limit states and cost functions are the same as those considered in the earthquake load. For developing design criteria for building envelope failure, twelve glass types according to thickness, are considered. Failure probabilities by the wind pressure and missile debris effects are calculated. Failure probability, total expected life-cycle cost and the optimal design intensity are determined. A sensitivity analysis to lifetime, discount rate and missile availability is also carried out.

In Chapter 5, the proposed method is applied to design against multiple loads. The optimal design intensity of the structure against earthquake and wind loads is calculated. Sensitivity analysis to lifetime, discount rate and injury and death cost is carried out.

Chapter 6 summarizes the significant conclusions from this study and recommendations for future study.

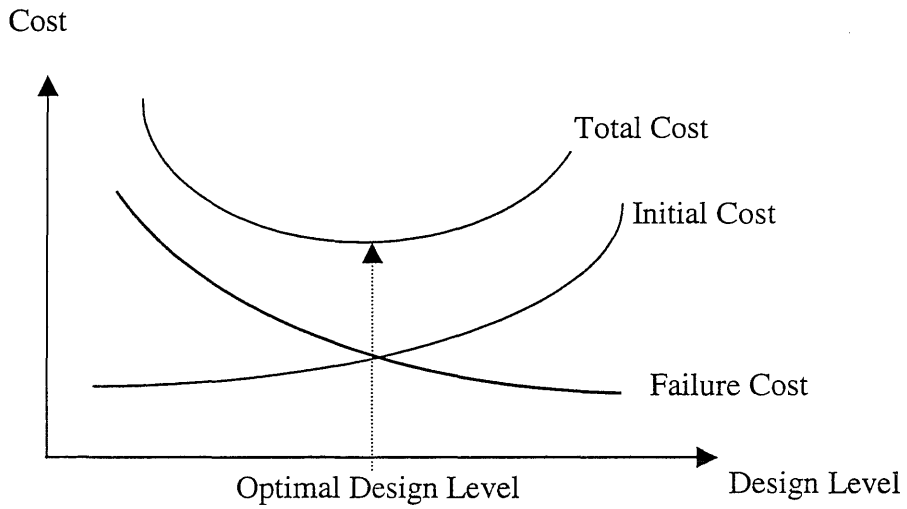

Figure 1.1 Cost and optimal design level

CHAPTER 2

ANALYTICAL FORMULATION AND PARAMETRIC STUDY

2.1 Introduction

In this chapter, cost functions used in the past are first reviewed to identify important parameters in developing an analytical procedure to estimate expected life-cycle cost. The formulation proposed by Wen and Ang (1991) and Wen and Shinozuka (1994) is adopted and extended to design under multiple hazards. This procedure allows consideration of important factors affecting design decision such as lifetime, discount rate, limit state, failure probability, initial cost and failure cost. Numerical results are obtained of design for the case of a simple single limit state under one or two hazards. A parametric study is then carried out to examine the sensitivity of optimal design to important design variables.

2.2 Review of Previous Cost Models

Various cost functions have been tried by previous researchers. Russell and Choudhary (1980) proposed the general cost model for fabricators and contractors including profit and overhead. This simple cost function was established for construction management. Vanmarcke and Angelides (1983) proposed a cost function for offshore structure with considering interest rate, design life, and discount rate.

The cost functions for structural member optimization were proposed by Tao and Corotis (1994), Frangopol et al (1997) and Thoft-Chistensen (1998). Tao and Corotis (1994) modeled their cost matrix for Markov decision process (MDP) for bridge design. Frangopol et al (1997) proposed an objective function to be minimized. In their cost function, expected total cost is composed of initial cost, inspection coat, total expected

inspection cost, cost of repair, expected cost of routine maintenance, and expected cost of failure, but is oriented toward maintenance, inspection and repair for the bridge. Thoft-Chistensen (1998) proposed a cost function for life-cycle cost evaluation of concrete highway bridge. Life-cycle cost includes initial cost, the expected repair costs (inspection, maintenance and repair costs) and the expected failure costs.

The cost functions for the design of a whole structure were proposed by Surahman and Rojiani (1983), Frangopol (1985), FEMA 227 (1992), Warszawaski et al. (1996), and Ang and Leon (1997). Surahman and Rojiani (1983) proposed the objective function for cost optimization with upper and lower bounds on the total expected cost. Frangopol (1985) introduced new formulations for a multi-criteria optimization in structural frame design. In FEMA report (227, 1992), an expected annual cost equation was proposed. to satisfy life-safety earthquake standards. The cost equation consists of building damage, rental losses, relocation expenses, personal and proprietor's income losses, business inventory losses and personal property losses. This cost model was established for benefit-cost analysis for the seismic rehabilitation of buildings. It has multi-limit states according to Modified Mercalli Intensity (MMI) ranging from VI to XII. Warszawski et al (1996) proposed a cost function in economic evaluation of design codes to the seismic design of buildings. Their cost function considers total life-cycle cost was annualized and multiplied by discount ratio. Ang and Leon (1997) divided expected life-cycle cost into those related to life safety and damage control or prevention. For life safety, the total expected life-cycle cost consists of the initial cost function; the replacement cost of the collapsed or demolished structure; loss of contents (total); the economic loss caused by structural collapse; cost of all injuries (disabling and non-disabling), and cost of human fatality. For damage control or prevention, the replacement cost and cost of injury and human fatality are replaced by the cost of non-disabling injury caused by structural damage. This cost function also considers discount ratio and occurrence rate of earthquake. The damage index (Park, Ang and Wen, 1984) for reinforced concrete element is used to assess structural damage.

The brief review suggests that the following need to be considered in establishing appropriate lifecycle cost for building structures. (1) cost functions: initial cost, maintenance cost and failure cost as functions of design variables; failure cost should include damage cost, replacement cost, loss of contents, economic loss, and cost of death and injury, (2) important system parameters: discount rate, lifetime, occurrence rate and intensity of hazards, and (3) multiple limit states for severe natural hazards.

2.3 Analytical Formulation

The major considerations in a life cycle cost analysis of a constructed facility are proper treatment of loading and resistance uncertainties, consideration of costs. Costs should include those of construction, maintenance and operation, repair, damage and failure consequence (loss of revenue, deaths and injuries, etc.), and discount over time of future loss/cost. It is reasonable to assume there are only a small number of limit states to be considered and the loadings which can cause the facility to reach these limit states are due to severe natural and man-made hazards which occur infrequently. Taking into account all these factors, the formulation of Wen and Ang (1991) and Wen and Shinozuka (1994) is used in this study and extended to a structure with multiple limit states under multiple hazards. The expected total cost over a time period (t), which is the design life of a new facility or the remaining life of a retrofitted facility, can be expressed as a function of t and the design variable vector $\boldsymbol{X}$ as follows:

$$E\,[C(t,X)] = C_0(X) + E\,[\sum_{i=1}^{N(t)}\sum_{j=1}^{k} C_j e^{-\lambda t_j} P_{ij}(X,t_i)] + \int_0^t C_m(X)\, e^{-\lambda\tau} d\tau \qquad (2.1)$$

in which C_0 = the construction cost for new or retrofitted facility; $\boldsymbol{X}$ = design variable vector, e.g., design loads and resistance, or load and resistance factors associated with nominal design loads and resistance; i= number of severe loading occurrences due occurrences and joint occurrence of different hazards such as live, wind, and seismic loads; t_i = loading occurrence time; a random variable; $N(t)$ = total number of severe

loading occurrences in t, a random variable; C_j = cost in present dollar value of j-th limit state being reached at the time of the loading occurrence including costs of damage, repair, loss of service, and deaths and injuries; $e^{-\lambda t}$ = discounted factor of over time t, λ = constant discount rate per year; P_{ij} = probability of j-th limit states being exceeded given the i-th occurrence of a single hazard or joint occurrence of different hazards; k = total number of limit states under consideration; and C_m=operation and maintenance cost per year.

If hazard occurrences can be modeled by a Poisson Process with occurrence rate of ν per year and the resistance is time-invariant, Equation (2.1) can be evaluated in closed form. The solutions and a parametric study are given in the following.

2.3.1 For a Single Hazard

If there is a single hazard and only one limit state is considered, according to Wen and Ang (1991), Equation (2.1) can be evaluated in closed form

$$E[C(t,X)] = C_0 + C_f P_f \frac{\nu}{\lambda}(1-e^{-\lambda t}) + \frac{C_m}{\lambda}(1-e^{-\lambda t}) \tag{2.2}$$

in which C_f is failure cost and P_f is failure probability given the occurrence of the hazard. The hazard intensity is assumed to follow an exponential distribution with a mean value of 1.0. Assuming that the initial cost is proportional to the design intensity and the maintenance cost is not considered, Equation (2.2) can be rewritten as

$$E[C(t,X)] = (aX + C)\cdot e^{-X}\cdot\frac{\nu}{\lambda}(1-e^{-\lambda t}) - aX \tag{2.3}$$

in which a is constant, C is initial cost and $\boldsymbol{X}$ is design intensity.

If a single hazard and multi-limit state is considered, Equation (2.1) can be written as

$$E[C(t,X)] = C_0 + (C_1 P_1 + C_2 P_2 + ... + C_k P_k)\frac{\nu}{\lambda}(1-e^{-\lambda t}) + \frac{C_m}{\lambda}(1-e^{-\lambda t}) \tag{2.4}$$

in which C_k = k-th limit-state failure cost and P_k = k-th limit-state probability.

2.3.2 For Multiple Hazards

Most civil systems are subjected to more than one hazard. One needs to consider the random occurrence in time of the loads and combinations of loads and load effects. Time-variant loadings are properly treated as random processes and the probability of limit state under combined loadings, $P_{ij}(\boldsymbol{X}, t_i)$ in Equation (2.1), is evaluated according to the event based load coincidence method (Wen, 1990).

If there are multi-hazards and multi-limit state is considered, Equation (2.1) can be written as

$$E[C(t,X)] = C_0 + C_F\frac{(1-e^{-\lambda t})}{\lambda} + \frac{C_m}{\lambda}(1-e^{-\lambda t}) \tag{2.5}$$

in which, C_F is the expected limit state cost given by

$$C_F = \sum_{l=1}^{k} C_l[\sum_{i=1}^{n}\nu_i P_l^i + \sum_{i=1}^{n-1}\sum_{j=i+1}^{n}\nu_{ij}P_l^{ij} + \sum_{i=1}^{n-2}\sum_{j=i+1}^{n-1}\sum_{k=j+1}^{n}\nu_{ijk}P_l^{ijk} + ...] \tag{2.6}$$

where,

$\nu_{ij} = \nu_i\nu_j(\mu d_i + \mu d_j)$, coincidence rate of hazards i and j;

$\nu_{ijk} = \nu_i\nu_j\nu_k(\mu d_i\mu d_j + \mu d_j\mu d_k + \mu d_i\mu d_k)$, coincidence rate of hazards i, j and k;

P_l^{ij} = probability of limit-state l given the coincidence of hazards i and j;

P_l^{ijk} = probability of limit-state l given the joint occurrence of hazards i, j and k;

μd_i = mean duration of hazard i.

2.3.3 Closed Form Solution for Two-Hazards

Consider the case of two such time-varying loads whose intensities follow an exponential distribution. The load effect under consideration is assumed to be a linear function of the load intensities

$$X = c_1 X_1 + c_2 X_2 \tag{2.7}$$

The strength of the system is also assumed to a linear function of the design load intensities

$$Y = c_1 Y_1 + c_2 Y_2 \tag{2.8}$$

In many design situations, the capacity is controlled by one design load and is given by

$$Y = \max(c_1 X_1 + c_2 X_2) \tag{2.9}$$

If the maintenance cost is not considered, the total expectation cost can be expressed as

$$E[C(t,Y)] = C_0(Y) + \left[\begin{array}{l} \nu_1 \cdot e^{-\left(\frac{c_1 Y_1 + c_2 Y_2}{c_1 \mu_{X_1}}\right)} + \nu_2 \cdot e^{-\left(\frac{c_1 Y_1 + c_2 Y_2}{c_2 \mu_{X_2}}\right)} + \frac{\nu_1 \nu_2 (\mu_{d_1} + \mu_{d_2})}{c_2 \mu_{X_2} - c_1 \mu_{X_1}} \\ \times \left(c_2 \cdot \mu_{X_2} \cdot e^{-\left(\frac{c_1 Y_1 + c_2 Y_2}{c_2 \mu_{X_2}}\right)} - c_1 \cdot \mu_{X_1} \cdot e^{-\left(\frac{c_1 Y_1 + c_2 Y_2}{c_1 \mu_{X_1}}\right)} \right) \end{array} \right] \cdot \frac{C}{\lambda}(1 - e^{-\lambda t}) \tag{2.10}$$

where ν_1 and ν_2 are occurrence rates for X_1 and X_2, μ_{d1} and μ_{d2} are mean duration of hazards X_1 and X_2.

If the hazard intensities are normal distribution and the other variables are the same as above, the total expectation cost can be written as

$$E[C(t,Y)] = C_0(Y) + \left\{ \begin{array}{l} \nu_1 \left[1 - \Phi\left(\dfrac{\dfrac{c_1 Y_1 + c_2 Y_2}{c_1} - \mu_{X_1}}{\sigma_{X_1}} \right) \right] + \\ \nu_2 \left[1 - \Phi\left(\dfrac{\dfrac{c_1 Y_1 + c_2 Y_2}{c_2} - \mu_{X_2}}{\sigma_{X_2}} \right) \right] + \nu_1 \nu_2 (\mu_{d_1} + \mu_{d_2}) \times \\ \left[1 - \Phi\left(\dfrac{c_1 Y_1 + c_2 Y_2 - (c_1 \mu_{X_1} + c_2 \mu_{X_2})}{\sqrt{c_1^2 \sigma_{X_1}^2 + c_2^2 \sigma_{X_2}^2}} \right) \right] \end{array} \right\} \cdot \frac{C}{\lambda}(1 - e^{-\lambda t}) \tag{2.11}$$

In the above analysis, method of load coincidence (Wen, 1990) is used. The facility is assumed to be restored to its original condition after each limit state has been reached. The design decision is then made based on the criterion that the expected total life cycle cost should be minimized with respect to the design variable vector $\boldsymbol{X}$. Although for many systems, the operation and maintenance cost (such as heating cost for building) over the lifetime may be high, their dependence on the design variables under consideration in this study would be generally weak. The problem to be solved in the optimization is primarily that of balance between construction cost and expected failure (limit state) costs. Depending on problems under investigation, proper constraints may be also introduced in the above minimization problem. The constraints may be in the form of limits of design variables or minimum acceptable reliability levels for limit states, or both. The viability and advantage of the formulation given Equation (2.1) is illustrated by a simple example as follows.

2.4 Parametric Study and Numerical Result

2.4.1 Optimal Design Under a Single Hazard

Under a single hazard modeled by a Poisson process with an occurrence rate of ν per year and for a resistance that is time-invariant, a closed form analytical solution of the expected life cycle cost given by Equation. (2.2) can be obtained. It greatly facilitates the determination of the optimal solution as a function of design life and other important parameters. A parametric study has been carried out for the optimal design intensity against seismic hazard under the condition that: (1) the hazard has an intensity described by an exponential distribution with a mean value of 1.0; (2) the resistance uncertainty is ignored and a single limit state of design intensity being exceeded is considered; and (3) the initial cost is proportional to the design intensity X and the maintenance cost is not considered. The expected total cost as a function of the lifetime t can be obtained as Equation (2.3) and the optimal (minimum expected cost) solution can be determined from Equation (2.3) without difficulty.

The close form solution allows easy sensitivity studies of the optimal design intensity to the load parameters, structural life and failure consequence.

Figure 2.1 shows the optimal design intensity (arbitrary unit) as a function of design life and cost of limit state being reached (arbitrary unit). Under the condition that the failure cost C = 20, which is of the same order of the construction cost (e.g., only repair and replacement costs need to be considered), the design intensity is 1.2 for a facility of a design life of 5 years. Compared with a design intensity is 3.2 for a life of 50 years, the reduction is almost a factor of three. On the other hand, when the failure cost C=100, which is about five times of the construction cost (e.g., failure consequences such as human death and injuries are included in the consideration), the design intensity reduces only from 4.4 to 3.0. The design intensity based on a criterion of equal life-time probability of exceedance (10%) is also shown in the figure. It is seen that it would lead

to under-design for a system of short life and high failure consequence and over-design for a system of long life and low failure consequences.

Figure 2.2 shows the dependence of design intensity of failure consequence. When the failure consequence is large, a high design intensity is needed, even for facility with short design life. In this case, the additional initial cost ensures much less failure cost and hence saving in the long run. An equal (10%) life time probability of exceedance criterion would lead to design intensity of 2.25, 3.63 and 4.55 for t = 5, 20 and 50 years respectively independent of the failure consequence. The example shows that a rational, quantitative design decision can be made based on results of such a minimum life-cycle cost analysis which can not be obtained based on judgment and experience or consideration of probability alone.

2.4.2 Optimal Design Under Two Hazards

The simple Poisson process is a good approximate model for occurrence of many severe natural and man-made hazards which allows closed form evaluation of the expected costs. Analytical solution of the expected cost, even approximate in nature, will facilitate significantly the ensuing minimization problem. The case of two such time-varying loads whose intensities follows exponential distribution is considered.

The optimal solution can be determined from the above equation. A 3-D and a contour plot of the expected lifecycle total cost are shown in Figure 2.3 and Figure 2.4. It can be seen (Figure 2.4) that the point where combination of the two design load intensities gives the minimum expected lifecycle cost can be determined. The dependence of the optimal solution on the loading and resistance parameters and the lifetime are similar to that of the single load case and will be illustrated in the following.

2.4.3 Numerical Results for Two Hazards

Numerical examples are carried out. The system parameters are given in Table 2.1. As can be seen by comparison of the parameters, $X_1(t)$ occurs much more frequently and has a longer duration, where as $X_2(t)$ is more intense and variable with a mean and a

standard deviation twice those of $X_1(t)$. The k1 and k2 values are chosen to be 1.2 and 1.5 respectively such that the initial cost will increase slightly faster than a linear function with the design load intensity, and more so for X2(t). In other words, design for $X_2(t)$ is more expensive. The discount rate is assumed to be 5% per year. It is similar to the situation of design for both winds and earthquakes. Consider first the case of the system capacity given by Equation (2.10). Because of the extremely small probability of coincidence the two loads, the contribution of the simultaneous occurrence of the two loads is negligible. The optimal design intensities for both loads as function of the structural life are shown in Figure 2.5 for three different values of cost of failure (limit state reached). The range of C from 20 to 50 represents the case of considering only cost of replacement of the structure, whereas the range from 100 to 500 represents the case where costs of loss of revenue, injuries, and death are also included. The solid lines are design loads of $X_1(t)$ and the dotted lines are those of $X_2(t)$ for different costs of failure consequence. The resultant annual limit state probabilities of the optimal design under each load as function of the structural life are calculated and shown in Figure 2.6. Because of the dominance of $X_2(t)$, the overall (target) limit state probability is almost the same as that under $X_2(t)$ only. The reciprocal of the probability is the return period for the optimal design in terms of one load only. For example, for a structure with a useful life of 50 years, if only structure damage is considered (C=20), the optimal return period of $X_2(t)$ for design is 43 years. It increases to 690 years if revenue loss, injury and death are also considered (C=500). The initial costs (solid lines) and the minimized expected life-cycle cost (dotted lines) as functions of structural life for different values of cost of failure are shown in Figure 2.7.

For the case of capacity controlled by one load (Equation (2.9)), it was found that the expected life-cycle cost generally converges to two local minima that are the same as when the two loads are considered separately. As expected, the optimal solution with respect to $X_2(t)$ is the global minimum. The optimal system design capacity and the target failure probabilities show only small differences from those given in Figures 2.5 and 2.6. One can conclude from results shown in Figures 2.5, 2.6, and 2.7 that:

1. The optimal design loads increase with the structural life but the increase is small for structural life longer than 50 years. They are highly dependent on the failure consequences (costs).
2. The optimal failure probability under $X_2(t)$ only is consistently and considerably (by at least one order of magnitude) higher than that under $X_1(t)$ only owing to the fact that the former is more intense, more variable and more expensive to design against. In other words, because of the widely different characteristics of the two hazards, uniform reliability against both loads is not necessary and would not be cost-effective.
3. The dominance of one load has important implications in design for multiple hazards, namely, that considering the dominant hazard such as earthquake only in the life-cycle cost analysis may be sufficient for a cost-effective design.
4. When cost of failure consequence is large (e.g. 500) and exposure time is long (e.g. 100 years), large initial cost is justified by the fact that it keeps the expected lifetime failure cost small (e.g. less than 20).

2.5 Summary

In this chapter, previous cost functions are reviewed and discussed. The analytical formulation proposed by Wen and Ang (1991) and Wen and Shinozuka (1994) is adopted and extended for multiple loads. Closed form solutions of design for a single limit state under a single hazard as well as for multiple limit states under multiple hazards are derived. Finally, parametric studies are carried out taking advantage of the tractable analytical formulation. Numerical results of design for the case of a simple single limit state under one and two hazards representing earthquakes and winds are obtained.

Table 2.1 Load, load effect, and cost parameters

Hazards	Mean Occurrence Rate (ν)	Mean Intensity (μ_X)	Mean Duration (μ_D)_	Load Effect Coefficient (c)	Cost Multiplier (d)
$X_1(t)$	5 per year	1.0	0.001 year	1.0	2.0
$X_2(t)$	0.2 per year	2.0	0.00005 year	2.0	2.0

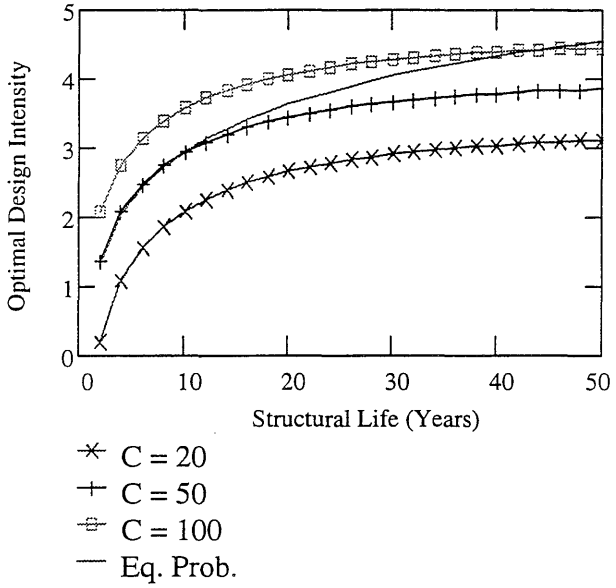

Figure 2.1 Optimal design intensity as a function of design life for λ = 0.05/yr, ν = 0.2/yr and a(initial cost per unit design intensity) = 5.

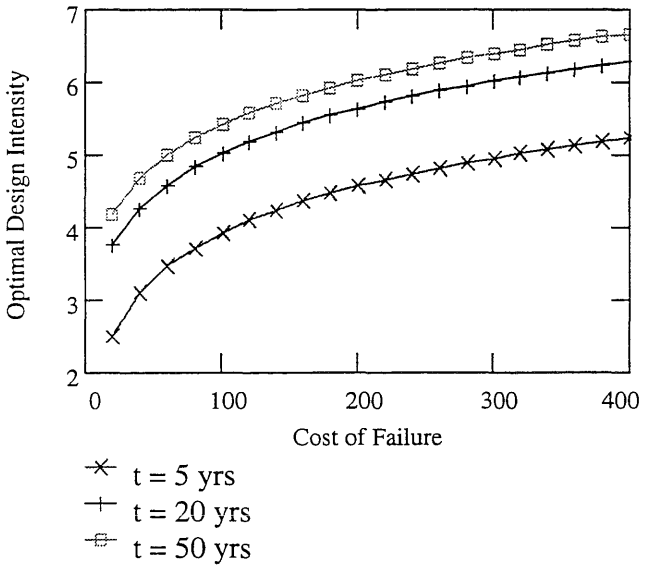

Figure 2.2 Optimal design intensity as a function of cost of failure for λ = 0.05/yr, ν = 0.5/yr and a(initial cost per unit design intensity) = 5.

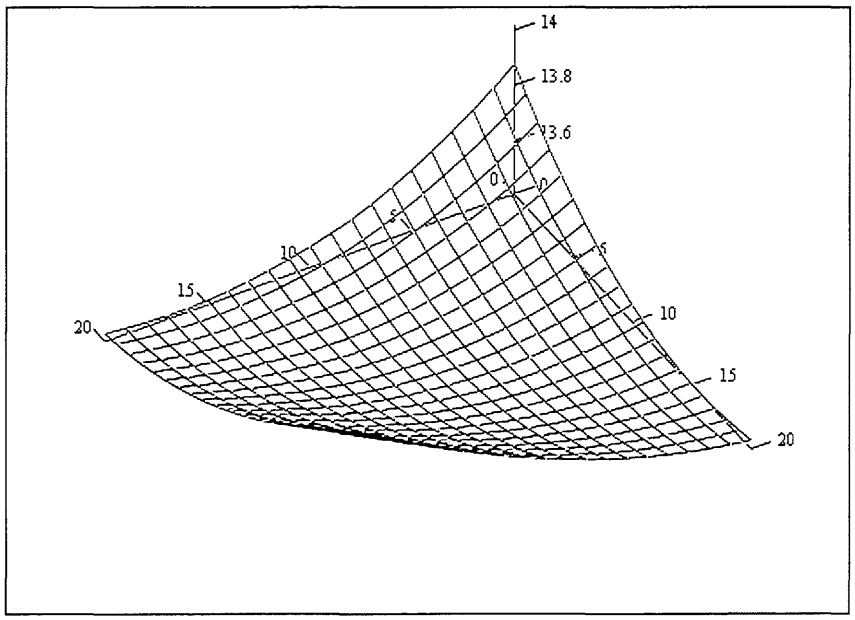

Figure 2.3 Expected total lifecycle cost as function of design variables.

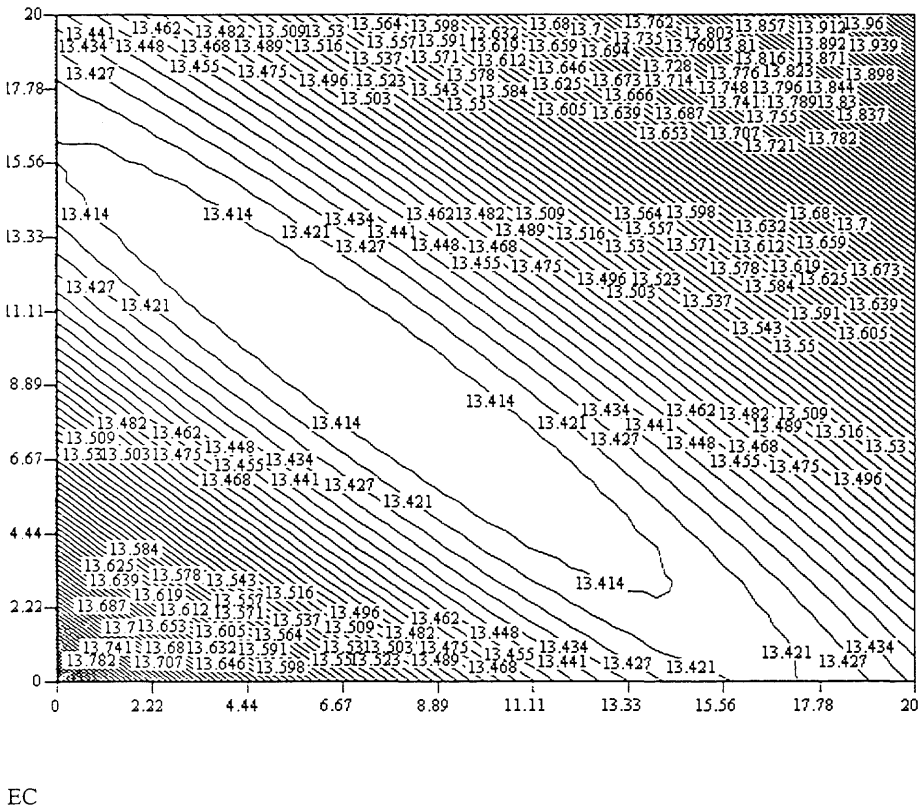

Figure 2.4 Contour of expected total lifecycle cost as function of design variables.

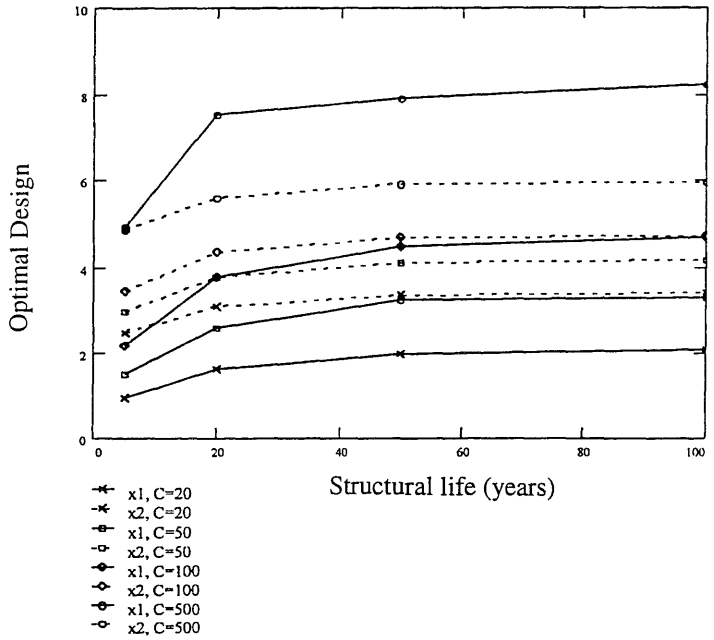

Figure 2.5 Optimal values of design variable X_1 and X_2 as function of structural life. C is cost of failure of limit state.

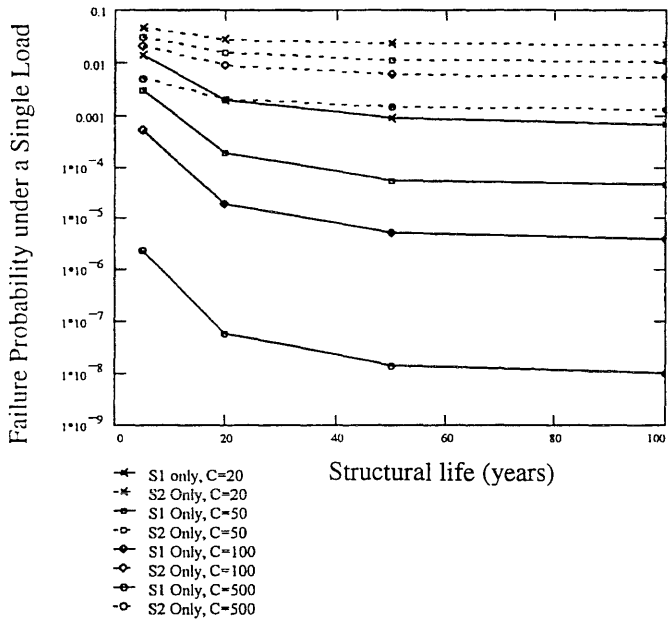

Figure 2.6 Annual limit state probability under one load only as function of structural life. C is cost of failure of limit state.

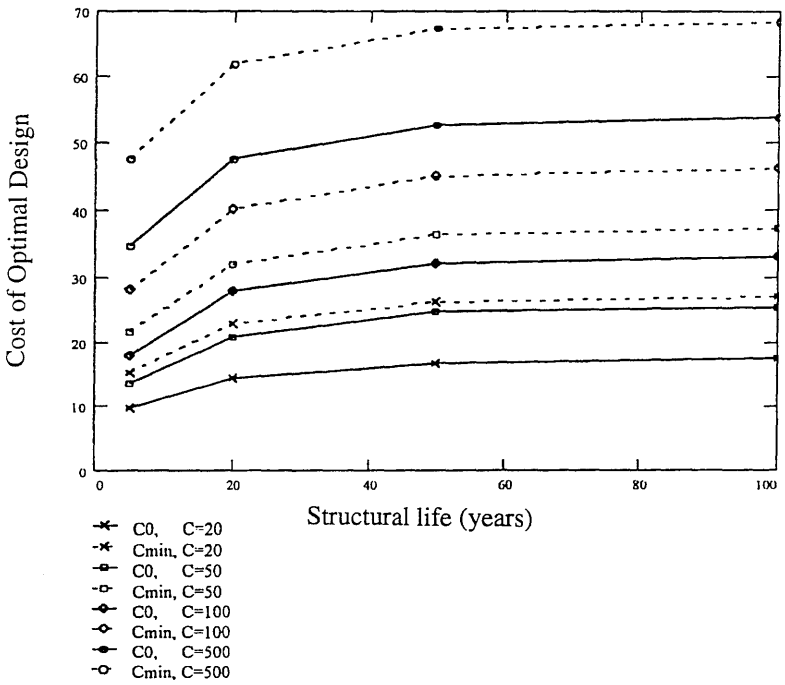

Figure 2.7 Initial and life-cycle costs of optimal design as function of structural life. C is cost of failure of limit state.

CHAPTER 3

APPLICATION TO SEISMIC DESIGN

3.1 Introduction

In this chapter, the proposed method is applied to seismic loads and demonstrated by an example of determination of optimal design load intensity. For this purpose, twelve 9-story buildings are designed for a wide range of load intensity according to the NEHRP 97 provisions. Seismic hazard is described by uniform hazard spectral accelerations according to USGS (1999) and FEMA 273 (1997). Structural limit state is described in terms of drift ratio according to FEMA 227 (1992), FEMA 273 (1997), SEAOC (1995), and Maison and Bonowitz (1998).

To determine the probability of exceedance of a given drift ratio limit, an equivalent SDOF method by Collins et al (1996) is used and the computer software DRAIN-2DX (1992) and IGRESS2 (1989) are used for nonlinear push-over analysis to determine the equivalent SDOF system parameters. The equivalent SDOF system is then used to evaluate the ductility factors and the drift ratios. Soil factors and bias factors are considered. A correction factor is also used to account for the uncertainty in structural capacity.

The initial cost of each structure is calculated according to the 1998 Building Construction Cost Data (BCCD). Nonstructural costs are not considered. The expected failure cost for each structure depends on the probabilities of exceedance of drift ratio under future seismic loads. The failure cost function consists of damage cost, relocation cost, content loss cost, economic loss cost, and cost of injury and death. The mean damage index and cost values of FEMA 227 (1992) are used to calculate the cost functions. The total expected life-cycle cost is calculated by summation of initial cost and expected failure cost. The minimum total expected life-cycle cost is determined by a

numerical procedure using a polynomial fit of the expected cost. A sensitivity analysis of the optimal design to change in design life, death and injury cost, structural capacity uncertainty and discount rate is also carried out. The locations considered are Los Angeles, California, Seattle, Washington, Charleston, South Carolina and Boston, Massachusetts, and the results are compared. Figure 3.1 and 3.2 show overall procedures for calculating the total expected life-cycle cost and failure probability of each limit state.

3.2 Definition of Limit State

Structural limits states vary according to performance requirements and load types. Most of present codes, including UBC, ABC, NEHRP, emphasize life safety only. Building damages, however, also cause serious consequences such as economic loss and need to be considered.

Whitman et al. (1975) proposed five limit states according to overall building damage as shown in Table 3.1. In FEMA (Federal Emergency Management Agency) report (FEMA 227 and 228, 1992) description of limit states were proposed according to damage states as shown in Table 3.2. Quantitative measures of damage in terms of structural response are needed in describing the performance level for calculation of the failure probability and failure cost.

A performance based design was introduced in the SEAOC (Structural Engineering Association of California) report (1995), in which five performance levels are categorized according to overall building damage. A quantitative measure in terms of permissible transient drift was used to describe structural performance.

NEHRP Guidelines for the Seismic Rehabilitation of Buildings (FEMA 273, 1997) also proposed performance levels according to overall damage. In general, building performance is a combination of the performance of both structural and nonstructural components. Structural performance and damages can be divided into those of vertical and horizontal elements, and nonstructural performance levels and damage can be

divided into those of architectural components, mechanical system, electrical system, plumbing systems and contents.

In vertical elements, performance levels are divided into several parts according to structural types, i.e., concrete walls, steel moment frames, braced steel frame, unreinforced masonry infill walls, unreinforced masonry (noninfill) walls, reinforced masonry walls, wood stud walls, precast concrete connections, and foundations. Horizontal elements are categorized into four fields, i.e., metal deck diaphragms, wood diaphragms, concrete diaphragms, and precast diaphragms.

Structural performance levels for steel moment frames in vertical elements of structural performance levels and damage are shown in Table 3.3. This Table shows only three drift ratios according to performance levels. These values are intended to be qualitative descriptions of the approximate behavior of structures meeting the indicated levels.

Yun and Foutch (1998) investigated and analyzed the incipient collapse of steel moment frame building, and found a large variation in drift ratio according to building story (height), year built, structural type, and connection type. For example, the local drift ratio for collapse depends on connection type, beam depth and built year, the global drift ratio for collapse depends on connection type and structural type.

Maison and Bonowitz (1998) also pointed out this issue in their opinion paper, where two performance levels, i.e., Life Safety (LS) and Collapse Prevention (CP), are addressed. They found that the drift limits of most codes and guidelines do not adequately address the issues of life safety and collapse prevention and some set the same limits for all building types. Drift ratio limits according to various sources were summarized as shown in Table 3.4. Expectations are that SAC guidelines due in 2000 would set different limits for new and existing buildings, different connection types, and different analysis procedures.

Based on a study of performance of three buildings of similar heights in Northridge earthquake, Maison and Bonowitz (1998) proposed following drift ratio limits for existing WSMF (Welded Steel Moment Frame) buildings of moderate redundancy:

Life Safety (LS) limit: Story Drift Ratio (SDR) = 0.025

Collapse Prevention (CP) limit: SDR = 0.050

Based on the above review, seven limit states and six permissible drift ratios are assumed as shown in Table 3.5.

3.3 Structural Modeling and Response Analysis

3.3.1 Modeling of Structures

A 9-story office building in downtown Los Angeles, California is selected for study. This building has a 75 ft. by 150 ft. plan and a height of 119 ft. shown in Figure 3.3. This structure is classified as a Special Moment Resisting Frame (SMRF) and a commercial building for professional, technical, and business services. The main reason for choosing this building is for easy comparison of results with 9-story building studied in SAC Steel Project and building of the same configuration in K. Collins (1995).

Twelve buildings designated as S1 to S12 are designed according to NEHRP 97 provisions for a wide range of design intensity. S4 corresponds to current design. The beam and column member sizes of each frame are shown in Table 3.6 and 3.7, and the members for S4 are also shown in Figure 3.4. Compared with the model for the SAC Steel Project, the differences in member sizes can be attribute to the difference in the structural configuration and the differences between 97 NEHRP and 94 UBC shown above. The 9-story building in the SAC Steel Project has a 150 ft. by 150 ft. plan and 122 ft. height and was designed based on 1994 UBC. The differences in design base shear between 1997 UBC and 1997 NEHRP are shown in Figure 3.5.

All frames satisfy the limitation of drift ratio by 97 NEHRP Provisions. The allowable story drift, Δ_s, is given by

$$\Delta_s = 0.020 \cdot h_{sx} \tag{3.1}$$

where h_{sx} is the story height below level x. The Story drift ratio from the equivalent lateral force for S4 is shown in Figure 3.6. All frames also satisfy requirements of LRFD (Load & Resistance Factor Design) manual of AISC (American Institute of Steel Construction), i.e., for width-thickness ratio, column-beam moment ratio, shear strength of panel zone, and panel zone thickness. The computer program IGRESS2 (An Interactive Graphic Environment for Steel Structures Analysis and Computer-Aided Design, 1989) is used to calculate the drift ratio and to carry out the structural analysis.

Table 3.8 shows the vertical loads used in this study; where dead loads on the floor and the roof, are 76 psf and 67 psf, respectively, and live loads on the floor and the roof are 45 psf and 16 psf, respectively. The effect of seismic load for load combinations also follows 97 NEHRP provisions.

Finally, characteristics of the twelve structures are summarized according to periods and system yield force coefficients (Sy) as shown in Table 3.9. The system yield force coefficient (Sy) is defined as the ratio of system yield force (Vy) to weight of structure (W), which is used as a measure of system resistance. It will be used as a structural design variable in the optimization analysis.

3.3.2 Drift Ratio Calculation

In order to determine limit state probability and expected failure cost, structural response analyses are carried out. The program DRAIN-2DX (Prakash et al., 1993) is used to determine the structural periods, system yield forces and global displacements by performing a nonlinear static push-over analysis. For probabilistic response analysis of the system, an equivalent single-degree-of freedom (SDOF) system is used.

According to Collins et al. (1996), the response of a MDOF nonlinear system can be approximated by that of an equivalent nonlinear SDOF system based on the results of a static push-over analysis. The maximum for linear elastic and nonlinear inelastic response in terms of interstory drift ratio of the MDOF system can be obtained as

$$\Delta = N_s^{DRIFT} \cdot \frac{\beta_{LG}}{H} \cdot P^* \cdot f \cdot C_e \cdot \left[g\left(\frac{T^*}{2\pi}\right)^2 \right] \tag{3.2}$$

and

$$\Delta = N_u^{DRIFT} \cdot \frac{\beta_{LG}}{H} \cdot \mu \cdot D_y \tag{3.3}$$

in which N_s^{DRIFT} and N_u^{DRIFT} are bias factors for connection of the errors introduce by the SDOF system, β_{LG} is the equivalent system parameter, H is the total structure height, P^* is the excitation scale factor, f is the site soil factor, C_e is elastic force coefficient determined from the response spectra, g is the acceleration of gravity expressed in appropriate units, μ is ductility factor for the SDOF system and D_y is global yield displacement determined from the static push-over analysis.

In this study, a bias factor of 0.96 and 0.90 is used for linear elastic and nonlinear inelastic responses, respectively, 0.64 is used as the site soil factor. β_{LG}, P^* and μ are determined by Equation (A.12), (A.8) and (A.25), respectively. Details for determining these factors are given in Appendix A.

The uniform hazards response spectra in USGS (1999) and FEMA 273 (1997) can be used directly to calculate the C_e values. The National Seismic Hazard Mapping Project of USGS (U.S. Geological Survey) provides maps for peak ground acceleration (PGA) and spectral acceleration (S_a) for 2%, 5%, and 10% probability of exceedance (PE) in 50 years at a given site. Table 3.10 shows PGA and PE at a site of 118° west longitude, 34° north latitude in Los Angeles. Probability of S_a for other probability level, e.g., 50% and 75% in 50 years, can be obtained using the procedure in FEMA 273 (1997).

The spectral accelerations at a period of one second are 0.19393g and 0.14344g for 50% and 75% probability of exceedance in 50 years, respectively. Figure 3.7 shows the probability of exceedance of one-second spectral acceleration for the Los Angeles site.

Drift ratios for all twelve structures are calculated as shown in Table 3.11. Figure 3.8 shows the probability of exceedance of interstory drift ratio in 50 years for structures S2, S4 and S12.

3.4 Calculation of Limit State Probability

3.4.1 Generalized Extreme Value Distribution (GEVD)

The Generalized extreme value distribution (GEVD) by Maes and Breitung (1993) is used to fit the probability of exceedance of drift ratio. It is a distribution of three parameters. GEVD is given by:

$$F(x) = \exp\left\{-\left[1-\frac{\gamma(x-\alpha)}{\beta}\right]^{\frac{1}{\gamma}}\right\} \tag{3.4}$$

where α, β, and γ are the distribution parameters which determine the type of the distribution. If $\gamma = 0$, the distribution is a type I or Gumbel distribution, whereas the case $\gamma < 0$ corresponds to a type II or Frechet distribution and the case $\gamma > 0$ represents a type III or Weibull distribution.

Figure 3.9 shows fittings of the drift ratio and annual probability of exceedance for S2 and S4 by GEVD.

3.4.2 Correction Factor for Capacity and Model Uncertainty

The effect of resistance uncertainty can be included in the reliability evaluation using a correction factor. The effect of model and resistance uncertainty on reliability has been investigated by Der-Kirureghian (1989) and Maes (1996). The uncertainty includes inaccuracies in structural modeling and probabilistic modeling such as those in the inelastic response models, distribution selection, and parameter estimation for a given random variable. The general effect of modeling uncertainty is obviously a decrease in reliability. Its effect on the reliability can be incorporated by a correction factor defined as the ratio of the limit state probability with consideration of the model uncertainty to that in which the model uncertainty has been ignored (Wen and Foutch, 1997). It is a very convenient tool for both performance and reliability evaluation and for the development

of reliability-based design when model uncertainty is present but can not be accurately quantified at the time. For example, one can treat the model uncertainty separately by first neglecting its effects in the reliability analysis and reliability-based design formulation, and recover it using the correction factor which can be continually updated as more information on model uncertainty becomes available.

The correction factor method for reliability evaluation and reliability-based design is illustrated in the following for the case that both the seismic load and resistance uncertainty can be modeled by log-normal random variables. It is assumed that the resistance is equal to a nominal resistance R. multiplied by a model uncertainty factor M. Nominal resistance R is a deterministic quantity, and a model uncertainty factor M is a random variable with a mean (bias) μ_M = 1.0 (no bias) and a coefficient of variation δ_M. In other words, the uncertainty in the resistance is represented by a single model uncertainty factor M. The seismic loading has a mean value of μ_L and a coefficient of variation of δ_L. It can be shown that the correction factor for probability of failure for the case of a single uncertain parameter is reduced to

$$C_F \approx 1+\frac{1}{2}S^2\delta_M^2 \tag{3.5}$$

in which S is the sensitivity coefficient. Under the assumption that both capacity and demand are log-normal, S can be calculated from (Wen and Foutch, 1997):

$$S = \frac{ln\,R-\lambda}{\varsigma^2} \tag{3.6}$$

where R is the deterministic system resistance ignoring the uncertainty, λ and ζ are the log-normal distribution parameters in the seismic hazard (spectral acceleration) distribution. It is seen that the correction factor increases proportionally to the square of the coefficient of variation of the model uncertainty and depends on the seismic hazard statistics and system resistance level. For Los Angeles, λ and ζ are equal to -4.238 and 1.202, respectively. Figure 3.10 shows fitting spectral acceleration and annual probability of exceedance assuming lognormal distribution. The sensitivity coefficients S and

correction factor C_F are shown in Table 3.12 and 3.13, respectively. Figure 3.11 shows the difference in annual probability of exceedance with and without the correction factor.

3.4.3 Limit State Probability given Occurrence of an Earthquake

In Equation (2.4) for a single hazard and multi-limit states, if the maintenance cost, C_m, is not considered, one obtains

$$E[C(t,X)] = C_0 + (C_1P_1 + C_2P_2 + \ldots\ldots + C_kP_k)\frac{\nu}{\lambda}(1-e^{-\lambda t}) \tag{3.7}$$

in which P_k is k^{th} limit state probability given the earthquake occurrence. P_k can be obtained in terms of probability of exceedance in t years as follows:

Let $P_t\ (\Delta>\Delta_a)$ be the probability that Δ, the drift ratio, is greater than Δ_a in t years. Assuming the earthquake occurrences can be modeled by a Poisson Process with occurrence rate of ν per year, $P_t\ (\Delta>\Delta_a)$ can be obtained as follows:

$$P_t(\Delta > \Delta_a) = 1 - e^{-\nu \cdot P_f(\Delta>\Delta_a)\cdot t} \tag{3.8}$$

One can solve for P_f from Equation (3.8)

$$P_f(\Delta > \Delta_a) = -\frac{1}{\nu \cdot t}\left[\ln(1 - P_t(\Delta > \Delta_a)\right] \tag{3.9}$$

There are 6 limit drift ratios for the seven limit states considered as shown in Figure B.1. Therefore, based on Equation (3.9), Equation (3.7) can be expressed as follows:

$$\begin{aligned} E[C(t,X)] = C_0 + \Bigg\{ & C_{II}\cdot\frac{1}{t}[G_t(\Delta_{II}) - G_t(\Delta_I)] + C_{III}\cdot\frac{1}{t}\left[G_t(\Delta_{III}) - G_t(\Delta_{II})\right] \\ & + \ldots\ldots + C_{VII}\cdot\frac{1}{t}\left[-G_t(\Delta_{VI})\right]\Bigg\}\cdot\frac{1}{\lambda}(1-e^{-\lambda t}) \end{aligned} \tag{3.10}$$

where $G_t(\Delta_i) = ln\ [1\text{-}P_t\ (\Delta > \Delta_i)]$ and $P_t\ (\Delta > \Delta_i)$ is probability of Δ exceeding Δ_i in t years. If annual probability of exceedance is used, $G_a(\Delta_i) = ln\ [1\text{-}P_a\ (\Delta > \Delta_i)]$, Equation (3.10) can be rewritten as follows:

$$E[C(t,X)] = C_0 + \left\{C_{II}\cdot\left[G_t(\Delta_{II}) - G_t(\Delta_I)\right] + \ldots\ldots + C_{VII}\cdot\left[-G_t(\Delta_{VI})\right]\right\}\cdot\frac{1}{\lambda}(1-e^{-\lambda t}) \tag{3.11}$$

Details are given in Appendix B. Table 3.14 shows limit state probability for each structure.

3.5 Cost Function Estimation

3.5.1 Initial Cost

Initial cost is the construction cost for new or retrofitted facility, in general, the initial cost in Equation (2.4) can be obtained according to the design intensity variables. In this study, the initial costs for the twelve structures are calculated using 1998 Building Construction Cost Data (BCCD). Since the nonstructural component cost has on affect on the optimal design intensity as shown in Figure C.1, the nonstructural items are not considered. The major initial cost items, therefore, are steel, shear connectors, metal decking, welded wire fabric, concrete (light weight), beam fireproofing, and column fireproofing. Steel costs are calculated according to 1998 Building Construction Cost Data (BCCD), and the other costs are calculated according to 1996 Means BCCD by Georgetown Laboratory Cost Estimate. The steel cost consists of the bare cost (material, labor and equipment costs) and overhead and profit (O & P).

For the calculation of the initial cost, a location factor is needed to adjust from the national average to Los Angeles by using following equation:

$$Cost\ in\ City\ A = \frac{Index\ for\ City\ A}{100} \times National\ Average\ Cost \tag{3.12}$$

According to 1998 BCCD, the city index is 111.2 for Los Angeles. To convert 1996 Means BCCD to 1998 costs, the historical cost index is needed. The historical index converts national average building costs in a given year to that of a different year by the following formula:

$$Cost\ in\ 1998 = \frac{Index\ for\ 1998}{Index\ for\ 1992} \times Cost\ in\ 1992 \tag{3.13}$$

For example, according to 1998 BCCD, the index for 1998 and the index for 1996 are 100 and 96.3, respectively. Thus, the historical cost index to convert the average building cost from 1996 to 1998 is 1.038.

Table 3.15 shows design spectral response acceleration (S_{D1}), the corresponding seismic response coefficient (C_s), system yield force coefficient (S_y) and the initial cost. Figure 3.12 (a) and (b) show initial cost as function of seismic response coefficients (C_s) and system yield force coefficient (S_y), respectively. Details for calculation of initial cost are presented in Appendix B.

According to Rosenblueth and Jara (1990), the initial cost is proportional to the power of the design base shear coefficient as follows:

$$C = C_0 \max\left\{1, [1 + C(x-a)^b]\right\} \tag{3.14}$$

where C_0 is a constant, x is the design base shear coefficient, and a, b, and c are parameters.

The values of C_0, a, b and C are found to be 2.079×10^6, 0.05, 1.091 and 6.547, respectively, for the initial cost as a function of C_s and 1.789×10^6, 0.063, 1.077 and 2.574 as function of S_y, similar to the values, $a = 0.05$, $b = 1.1$, by Rosenblueth and Jara (1990) based on a study of ten-story reinforced concrete structures. The fitting results in Figure 3.13 show that both b values are greater than 1. This means that initial cost increases faster than a linear function of the seismic response coefficients (C_s) or system yield force coefficient (S_y). Therefore the initial cost will be high when the design intensity is large.

3.5.2 Failure Costs

The cost vector in Equation (2.4) consists of damage cost, loss of contents, relocation cost, economic loss, cost of injury and cost of human fatality. It can be formulated as follows:

$$C_j = C_j^{dam} + C_j^{con} + C_j^{rel} + C_j^{eco} + C_j^{inj} + C_j^{fat} \tag{3.15}$$

in which j is j-th limit state, C_j^{dam} = the damage/repair cost function, C_j^{con} = the loss of contents, C_j^{rel} = the relocation cost, C_j^{eco} = the economic loss caused by a structural damage, C_j^{inj} = the cost of injuries, and C_j^{fat} = the cost of human fatality. Factors in estimating the cost function are based on FEMA reports (1992). Each function is obtained as follows:

3.5.2.1 Damage/Repair Cost Function

Damage/repair cost is evaluated as a function of the mean damage index. Damage cost is estimated by floor area and replacement cost. A value of \$85/ft^2 is used for the replacement cost based on the typical replacement value of buildings in FEMA 227 (ATC-13) for medium rise office buildings for commercial, professional, technical and business services.

3.5.2.2 Loss of Contents

Loss of contents is evaluated as a function of the mean damage index. Contents costs are obtained from floor area times unit contents cost depending on the social function classification, at \$28.9/ft^2.

3.5.2.3 Relocation Cost

Relocation costs may be incurred when building damage requires repairs and the pre-earthquake function of the facility is partially or fully lost. Total relocation costs depend on gross leasable area, relocation costs per square foot per month, and estimated loss of function times. A typical relocation cost of \$1.50/month/ft^2 is suggested in FEMA handbook No. 174 (1989).

3.5.2.4 Economic Loss

Economic loss is divided into two parts, rental cost and income loss. Average rental rates for the buildings under consideration are given on a per square foot per month basis.

Rental rates vary widely with social function classification, but are intrinsically local because they depend on local economic conditions including vacancy rate, the desirability of the neighborhood, and the desirability of the buildings. Rental incomes to building owners may be lost until functionality is restored after earthquake damage.

In this study, the rental cost for Los Angeles is based on the data of example in FEMA 228 (1992), where \$0.61/month/ft^2 is suggested for Seattle. If location factor based on 1998 BCCD is applied to this rate, the average rental cost is \$0.58/month/ft^2.

In this study, income is defined as personal and proprietor's income. Disruption of income depends on occupancy and social function of the building. Income loss occurs when building damage disrupts commercial activity. The two critical parameters to be estimated are (1) the level of income generated by the enterprise, and (2) the length of time of disruption. Like rental income and relocation costs, income losses are expected to be proportional to the duration of complete or partial loss of function. Loss of function depends on expected central damage factors and social function classification.

According to FEMA 228 (1992), when social function classification is commercial, professional, technical and business services, income loss rate is \$100/year/ft^2.

Rental income is evaluated from rental rate and loss of rental time; the income loss comes from income rate and out-of-business time.

3.5.2.5 Injury Cost Function

Total injury cost is calculated from floor area multiplied by expected injury rate (depending on limit state), occupancy rate and cost per person. An occupancy rate of 2 persons/1,000 ft^2 is used based on social function classification data, and cost per person is divided into minor injury cost (\$1,000/person) and serious injury cost (\$10,000/ person).

3.5.2.6 Value of Life

The economic value of human life is an important and difficult issue. The value range is also wide. According to Scanlan (1980), values have ranged from $1.1 million per life (Dept. of Agriculture) to $8 million per life (Environmental Protection Agency). Four principal methods can be used to derive the value of life. They are the human capital approach, the court awards approach, the risk-cost method, and the willingness-to-pay approach. The summaries of these approaches are in FEMA 228 (1992).

Keech et al. (1989) reviewed 25 updated studies for the Federal Aviation Administration, and defines the social value of early death as including foregone taxes, and medical, emergency, legal, court, and public assistance administration costs. The total of these costs, which is the social value of a statistical life, was estimated at $1,740,000 in 1987 dollars.

Cost of human fatality is evaluated from death cost per person and expected death rate. Total death cost is calculated from floor area, number of occupants, death rate and death cost per person. A death cost of $1,740,000/person suggested in FEMA report (FEMA 227, 1992) is used.

3.5.3 Calculation of Failure Cost

3.5.3.1 Discount Rate

The discount rate is used to calculate the present value of benefits that will occur in the future. Increasing the discount rate lowers the present value of future benefits. Conversely, assuming a lower discount rate raises the present value of future benefits.

The choice of an appropriate discount rate is one of the most difficult aspects of benefit-cost analysis. According to Young and Howe (1988), there are three general approaches to establishing a discount rate to evaluate public investments. They are the cost of capital and two "market failure" alternatives – the Social Time Preference and the Social Opportunity Cost approaches.

The various approaches to determining appropriate discount rates yield values in the range of 3% to 6%. According to FEMA 227 (1992), for public sector considerations, a discount rate of 3 or 4% is reasonable; for private sector considerations, slightly higher rates of 4 to 6% is reasonable. In this study, 5% is used for the discount rate.

3.5.3.2 Calculation of Failure Cost

Above mentioned cost functions and basic costs are summarized in Table 3.16. All costs are given in 1992 US dollars. Thus the historical cost index is needed to convert national average building cost at a particular time to the approximate building costs for some other time by using Equation (3.23). According to 1998 BCCD, the index for 1998 and the index for 1992 are 100 and 86.9, respectively. Thus, the historical cost index is 1.151 to convert average building costs from 1992 to 1998.

To calculate the expected failure cost, the probability of damage in percent according to limit state is needed. The central damage factor in FEMA 227 (1992) is used for this purpose. Table 3.17 shows the general damage description and central damage factors corresponding to different limit states.

Earthquake damage may render buildings unfit for their normal functions until repairs are made or until destroyed buildings are replaced. Rents and other incomes may be lost during this loss of function interval and relocation costs may also be incurred. Consensus opinions about expected loss of function and restoration times were developed in ATC-13. Loss of function depends on damage state and social function classification. Weighted statistics for loss of function and restoration time of social function classifications for professional business service is presented in Table 3.18.

Death and injury rates increase with increasing damage to buildings and will vary depending on the design, construction and condition of individual buildings. Consensus values of death and injury rates for seven damage states considered in FEMA 227 (ATC-13) are summarized in Table 3.19.

Failure cost can be calculated by using cost function, basic costs, central damage factor, loss of function, and death and injury rates. The results of cost calculations for each limit state are given in Table 3.20.

3.6 Calculation of Total Expected Life-Cycle Cost

By adding initial cost and total expected failure cost, the total expected life-cycle cost can be calculated based on Equation (3.11). Total failure cost is obtained from the cost functions multiplied by the limit state probabilities of Table 3.14. A constant discount rate λ of 0.05 is used. Figure 3. 14 shows the result of total expected life-cycle cost for t = 50years as function of design system yield force coefficient (S_Y).

3.7 Determination of Optimal Design Intensity

A polynomial equation is used to determine the optimal point corresponding to the minimum expected life-cycle cost in Figure 3.14. Figure 3.15 shows the polynomial fit and the optimal point for the life-cycle cost with (w/) and without (w/o) considering injury and death of humans. The optimal system yield force coefficient (S_y) and corresponding life-cycle costs (C) are S_y = 0.189, C = \$2,934,000 when human injury and death cost are not included and are S_y = 0.194, C = \$3,044,000 when human injury and death cost are included. The corresponding target limit state probability is therefore approximately given by that of structure No.7 (S_y=0.188) without consideration of injury and death of humans in Table 3.21, and given by the structure between No 7 (S_y=0.188) and No 8 (S_y=0.213) when injury and death are considered. The current design according to NEHRP 97 is close to the structure between No. 4 (S_y=0.115) and No. 5 (S_y=0.140).

3.8 Sensitivity Analysis

A sensitivity analysis of the optimal design is carried out to change in design life, death and injury cost, structural capacity uncertainty and discount rate. The results are shown in Figure 3.16. The results indicate that the optimal design intensity is not sensitive at all to structural capacity uncertainty, and it is not sensitive to assumption of death and injury cost primarily due to the small probability of such occurrences. The design is moderately dependent on the discount rate for a long life span (T > 50 years) and much more sensitive to design life change. The optimal design system yield coefficient increases from 0.133 for T = 5 years to 0.198 for T = 100 years.

3.9 Applications to Other Locations

To examine the dependence of the optimal design load on location, the method is applied to design in Seattle, Boston, and Charleston, in regions of various degree of seismicity. Charleston is specially selected because of high wind condition due to hurricanes.

To determine the minimum total expected life-cycle cost for these cities, the same procedure for Los Angeles that is shown in Figure 3.1 is used. Spectral acceleration can be obtained according to USGS data FEMA 273 procedure. Table 3.22 shows the spectral accelerations at 1 second period for four cities. Spectral accelerations and probability of exceedance in 50 years for each city are compared in Figure 3.17.

In the calculation of failure probability, different value of the seismic hazard parameters μ_l and δ_l, are used for the correction factor, C_F. They are 0.003 and 18.31 for Seattle, 0.00145 and 7.866 for Charleston and 0.00058 and 7.810 for Boston.

To calculate the initial cost, city cost indexes of 105.5, 77.6, and 116.7 are used for Seattle, Charleston, and Boston, respectively. Initial costs of structures each city are shown in Table 3.23 based on 1998 BCCD.

Figure 3.18 to 3.20 shows the expected life-cycle cost as functions of system yield force coefficient for the building at Seattle, Boston and Charleston, respectively. The minimum total expected life-cycle cost is determined. In the case of Boston, the total expected cost increases monotonically because of low seismicity at Boston area indicating that even S_1 exceeds the optimal design requirement.

The optimal system yield force coefficients for each city are summarized in Table 3.24. Figure 3.21 shows the optimal design intensities of system yield force coefficients with and without considering injury and death cost for the three cities. The difference in optimal system yield force coefficient is small for Los Angeles, while the differences are large for Seattle and Boston.

Table 3.25 shows the values of S_1 that are used in the calculation of current design intensity. These values come from 1997 NEHRP maps and USGS data. Figure 3.23 shows the comparison between design intensity based on current design value and optimal design intensity based on life-cycle cost for the case of 50 years lifetime. All optimal design intensities based on total life-cycle cost are higher than current design intensity. The result also shows that the difference between optimal design intensity based on life-cycle cost and current design intensity depends on site; the difference is large for Los Angeles, while the difference is small for Seattle and Charleston.

A sensitivity analysis of the optimal design is also carried out. Figure 3.24 to 3.25 shows the result of sensitivity analysis to lifetime, discount rate, system uncertainty, and injury and death cost function for Seattle and Charleston, respectively. The results indicated that the optimal design intensity is not sensitive to structural capacity uncertainty. The design is moderately dependent on discount rate for long life span (T > 50 years) and more sensitive to design life change. For example, the optimal design system yield coefficient increases from 0.052 for T = 5 years to 0.111 for T = 100 years for Seattle and from 0.017 for T = 5 years to 0.100 for T = 100 years for Charleston.

It is clear that, for Seattle and Boston, the optimal design intensity is much more sensitive to the injury and death cost function, while the optimal design intensity is not sensitive at Los Angeles, as shown in Figure 3.21 and Figure 3.26.

The differences in contribution of injury and death cost to the total expected life-cycle cost for different locations are due to the characteristics of the seismic hazard (in terms of spectral acceleration) as shown by the example in Figure 3.27. Because of the much flatter hazard curve at Charleston at the tail, the percentage contribution of the expected injury and death cost to the total expected life-cycle cost is much larger than that at Los Angles, as indicated by the probability of injury and death relation to that of damage for these two cities.

For example, the difference in expected damage costs with and without injury and death cost for S4 structure at Los Angeles is $246,600 and the difference at Charleston is $175,330. Even though the difference at Charleston is smaller, it accounts for 12% of the change in the total expected life-cycle cost while it is only 7% at Los Angeles. This indicates that injury and death cost plays a much more important role at Charleston than at Los Angeles.

3.10 Summary

The proposed methodology for determination of minimum life-cycle cost design criteria is demonstrated by application to design of a steel building against seismic load.

Several conclusions can be drawn from the results:

1. The optimal system yield force coefficients (S_y) with and without considering injury and death cost at Los Angeles are 0.194 and 0.189. They are 0.109 and 0.089 for Seattle and 0.097 and 0.051 for Charleston, respectively.
2. At Los Angeles, the optimal design intensity for 50 years lifetime is larger than design intensity based on the current design code (1997 NEHRP), while at Seattle and Charleston, the differences are relatively small.
3. The sensitivity results analysis indicates that the optimal design intensity is not sensitive to structural capacity uncertainty. It also indicates that the optimal design intensity moderately depends on discount rate and design life.

4. The optimal design intensity is not sensitive to the injury and death cost at Los Angeles, but is at Seattle and Charleston due to the difference in the characteristics of seismic hazard at these locations.

Table 3.1 Damage description of damage level by Whitman et al (1975).

Performance level	Overall Building Damage
I	No Damage
II	Light Damage
III	Moderate Damage
IV	Heavy Damage
V	Total Damage or Collapse

Table 3.2 Description of damage state (FEMA 227, 1992).

Damage State	Description of Damage State
None	No Damage
Slight	Limited localized minor damage not requiring repair
Light	Significant localized damage of some components generally not requiring repair
Moderate	Significant localized damage of many components warranting repair
Heavy	Extensive damage requiring major repairs
Major	Major widespread damage that may result in the facility being razed, demolished, or repaired
Destroyed	Total destruction of the majority of the facility

Table 3.3 Structural performance levels and damage-vertical elements (FEMA 273, 1997).

Element	Type	Structural Performance Levels		
		Collapse Prevention S-5	Life Safety S-3	Immediate Occupancy S-1
Steel Moment Frames	Primary	Extensive distortion of beams and column panels. Many fractures at moment connections, but shear connections remain intact.	Hinges form. Local buckling	Minor local yielding at a few places. No fractures. Minor buckling or observable permanent distortion of members.
	Secondary	Same as primary.	Extensive distortion of beams and column panels. Many fractures at moment connections, but shear connections remain intact.	Same as primary.
	Drift	5% transient or permanent	2.5% transient; 1% permanent	0.7% transient; negligible permanent

Table 3.4 Story drift ratio limits for a 9-story steel frame buildings by Maison and Bonowitz (1998).

Reference	Intended Use	Immediate Occupancy	Life Safety (or better)	Collapse Prevention
FEMA 178 (1992)	Existing frames	none	.027	none
FEMA 310 (1998)	Existing steel frames	.015	.025	none
FEMA 273 (1997)[1]	Rehabilitated steel frames	.007	.025	.050
FEMA/NIBS (Kircher et al., 1997)[1]	Loss estimation, 4-7	.008	.020	.053
FEMA/NIBS[1]	Loss estimation, 8+story steel frames	.006	.015	.040
FEMA 222 (1995)	New frame buildings	none	.020	none
SEAOC (1998a)	New buildings	none	.020	none
SEAOC (1998a) Commentary	New buildings, nonlinear time history analysis	none	.010	none
SEAOC Vision 2000 (SEAOC, 1996)	New buildings	.005	.015	.025
SEAOC PBSE Guidelines (1998b)	New steel frames	.0075	.020	none
UBC 1997 (ICBO, 1997)	New buildings	none	.020	none
IBC 2000 (ICC, 1998)	New frame buildings	none	.020	none

[1] Anticipated value, not acceptability criteria.

Table 3.5 General damage description of the performance level and drift ratio.

Performance level	Damage State	Permissible Drift Ratio (%)
I	None	$\Delta < 0.2$
II	Slight	$0.2 < \Delta < 0.5$
III	Light	$0.5 < \Delta < 0.7$
IV	Moderate	$0.7 < \Delta < 1.5$
V	Heavy	$1.5 < \Delta < 2.5$
VI	Major	$2.5 < \Delta < 5.0$
VII	Destroyed	$\Delta > 5.0$

Table 3.6 Member size for a 9-story building (Beam).

Floor	9	8	7	6	5	4	3	2	1
S1	W14×22	W16×26	W18×35	W18×35	W18×50	W18×50	W18×50	W18×50	W18×50
S2	W14×34	W18×35	W21×50	W24×55	W24×68	W24×68	W24×68	W24×68	W24×68
S3	W18×35	W21×50	W24×68	W24×84	W27×84	W27×84	W30×90	W30×90	W30×90
S4	W21×44	W21×57	W24×84	W27×84	W30×99	W30×99	W30×99	W30×108	W30×108
S5	W18×50	W24×55	W30×90	W30×99	W33×118	W33×118	W33×118	W33×118	W33×118
S6	W21×44	W24×68	W30×99	W30×108	W36×135	W36×135	W36×135	W36×135	W36×135
S7	W24×55	W24×76	W30×108	W33×118	W36×135	W36×150	W36×150	W36×150	W36×150
S8	W24×55	W24×84	W30×116	W33×130	W36×160	W36×160	W36×160	W40×167	W40×167
S9	W24×62	W24×84	W33×118	W33×141	W40×167	W40×167	W40×167	W40×167	W40×167
S10	W24×62	W27×84	W33×130	W33×141	W40×167	W40×167	W40×183	W40×183	W40×183
S11	W27×84	W27×102	W36×170	W36×170	W36×232	W36×232	W36×232	W36×256	W36×256
S12	W30×90	W30×108	W36×194	W36×194	W36×300	W36×300	W36×300	W36×300	W36×300

Table 3.7 Member size for a 9-story building (Column).

Floor	9	8	7	6	5	4	3	2	1
S1	W14×53	W14×159	W14×159	W14×176	W14×176	W14×193	W14×193	W14×193	W14×193
	W14×68	W14×176	W14×176	W14×193	W14×193	W14×211	W14×211	W14×233	W14×233
S2	W14×68	W14×176	W14×176	W14×193	W14×193	W14×211	W14×211	W14×211	W14×211
	W14×68	W14×193	W14×193	W14×211	W14×211	W14×233	W14×233	W14×257	W14×257
S3	W14×82	W14×193	W14×193	W14×211	W14×211	W14×233	W14×233	W14×233	W14×233
	W14×90	W14×211	W14×211	W14×233	W14×233	W14×257	W14×257	W14×283	W14×283
S4	W14×132	W14×211	W14×211	W14×233	W14×233	W14×257	W14×257	W14×257	W14×257
	W14×132	W14×233	W14×233	W14×257	W14×257	W14×283	W14×283	W14×311	W14×311
S5	W14×132	W14×233	W14×233	W14×257	W14×257	W14×283	W14×283	W14×283	W14×283
	W14×132	W14×257	W14×257	W14×283	W14×283	W14×311	W14×311	W14×342	W14×342
S6	W14×132	W14×257	W14×257	W14×283	W14×283	W14×311	W14×311	W14×311	W14×311
	W14×132	W14×283	W14×283	W14×311	W14×311	W14×342	W14×342	W14×370	W14×370
S7	W14×132	W14×283	W14×283	W14×311	W14×311	W14×342	W14×342	W14×342	W14×342
	W14×159	W14×311	W14×311	W14×342	W14×342	W14×370	W14×370	W14×398	W14×398
S8	W14×132	W14×311	W14×311	W14×342	W14×342	W14×370	W14×370	W14×370	W14×370
	W14×159	W14×342	W14×342	W14×370	W14×370	W14×398	W14×398	W14×426	W14×426
S9	W14×145	W14×342	W14×342	W14×370	W14×370	W14×398	W14×398	W14×398	W14×398
	W14×176	W14×370	W14×370	W14×398	W14×398	W14×455	W14×455	W14×500	W14×500
S10	W14×145	W14×370	W14×370	W14×398	W14×398	W14×426	W14×426	W14×426	W14×426
	W14×193	W14×398	W14×398	W14×426	W14×426	W14×500	W14×500	W14×550	W14×550
S11	W14×159	W14×370	W14×370	W14×455	W14×455	W14×500	W14×500	W14×500	W14×500
	W14×283	W14×398	W14×398	W14×500	W14×500	W14×605	W14×605	W14×665	W14×665
S12	W14×176	W14×426	W14×426	W14×550	W14×550	W14×605	W14×605	W14×605	W14×605
	W14×233	W14×500	W14×500	W14×605	W14×605	W14×730	W14×730	W14×808	W14×808

Table 3.8 Design vertical loads.

Load		Floor (psf)	Roof (psf)
Dead Load	Concrete Slab with Decking	42	42
	Insulation and Membrane	0	11
	Ceiling	10	10
	Mechanical and Electrical	4	4
	Structural Steel	Calculated	Calculated
	Partition	20	0
	Total	76	67
Exterior Wall and Facade		30	30
Live Load		45	16

Table 3.9 Characteristics of twelve structures.

Structure	Period (T) (Sec.)	Weight (W) (kips)	System Yield Force (Vy) (kips)	System Yield Force Coefficient (Sy)
S1	4.335	5046.0	167.2	0.033
S2	3.159	5089.1	309.9	0.061
S3	2.542	5137.6	479.0	0.093
S4	2.323	5183.0	597.5	0.115
S5	2.062	5223.8	732.5	0.140
S6	1.883	5267.4	887.9	0.169
S7	1.772	5311.8	999.3	0.188
S8	1.664	5356.1	1139.4	0.213
S9	1.572	5398.7	1241.1	0.230
S10	1.500	5440.3	1331.8	0.245
S11	1.343	5572.3	1789.0	0.321
S12	1.200	5730.4	2339.0	0.408

Table 3.10 Peak ground acceleration (PGA) and spectral acceleration (SA) in terms of probability of exceedance in 50 years at Los Angeles by USGS (1999).

PGA and SA	10% PE in 50 years	5% PE in 50 years	2% PE in 50 years
PGA	48.48927	64.78114	89.54587
SA at 0.2 sec.	119.3100	149.2870	194.6149
SA at 0.3 sec.	115.5928	139.5881	190.6932
SA at 1.0 sec.	44.30749	60.75126	85.97154

Table 3.11 Drift ratio and probability of exceedance in 50 years for a 9-story building at Los Angeles.

Structure	2%/50yrs	5%/50yrs	10%/50yrs	50%/50yrs	75%/50yrs
S1	3.963	2.884	2.151	0.897	0.663
S2	2.682	1.951	1.451	0.633	0.468
S3	2.118	1.537	1.137	0.495	0.366
S4	2.018	1.459	1.075	0.428	0.316
S5	1.811	1.306	0.846	0.370	0.274
S6	1.596	1.148	0.779	0.341	0.252
S7	1.485	1.066	0.700	0.306	0.227
S8	1.436	1.028	0.659	0.288	0.213
S9	1.313	0.939	0.618	0.271	0.200
S10	1.237	0.884	0.593	0.260	0.192
S11	1.195	0.703	0.513	0.225	0.166
S12	1.052	0.638	0.466	0.204	0.151

Table 3.12 Sensitivity coefficients for drift ratio limit.

Structure	Sensitivity Coefficients, S, for drift ratio limit (%)					
	0.2	0.5	0.7	1.5	2.5	5.0
S1	0.629	1.414	1.660	2.152	2.444	2.802
S2	0.693	1.641	1.898	2.388	2.671	3.016
S3	1.031	1.827	2.065	2.538	2.818	3.163
S4	1.183	1.935	2.155	2.593	2.852	3.172
S5	1.303	2.031	2.247	2.678	2.935	3.254
S6	1.419	2.117	2.327	2.747	2.998	3.308
S7	1.477	2.157	2.364	2.779	3.028	3.339
S8	1.534	2.194	2.393	2.796	3.039	3.339
S9	1.589	2.234	2.431	2.829	3.069	3.370
S10	1.623	2.260	2.457	2.857	3.099	3.401
S11	1.735	2.352	2.548	2.950	3.194	3.498
S12	1.814	2.417	2.607	2.999	3.236	3.537

Table 3.13 Correction factors for drift ratio limit.

Structure	Correction Factors, C_F, for drift ratio limit (%)					
	0.2	0.5	0.7	1.5	2.5	5.0
S1	1.03	1.13	1.18	1.30	1.39	1.51
S2	1.03	1.17	1.23	1.37	1.46	1.59
S3	1.07	1.22	1.28	1.42	1.51	1.65
S4	1.09	1.24	1.30	1.44	1.53	1.65
S5	1.11	1.27	1.33	1.46	1.56	1.69
S6	1.13	1.29	1.35	1.49	1.58	1.71
S7	1.14	1.30	1.36	1.50	1.59	1.72
S8	1.15	1.31	1.37	1.51	1.60	1.72
S9	1.16	1.32	1.38	1.52	1.61	1.74
S10	1.17	1.33	1.39	1.53	1.62	1.75
S11	1.20	1.36	1.42	1.56	1.66	1.79
S12	1.21	1.38	1.44	1.58	1.68	1.81

Table 3.14 Limit state probability for each structure.

Structure	I	II	III	IV	V	VI	VII
S1	0.7390438	0.2080010	0.0039446	0.0238673	0.0039446	0.0016940	0.0005613
S2	0.7665259	0.2029989	0.0018062	0.0146956	0.0018062	0.0007242	0.0002247
S3	0.8772452	0.1038269	0.0010623	0.0087138	0.0010623	0.0004084	0.0001161
S4	0.9108208	0.0748556	0.0008334	0.0061838	0.0008334	0.0003442	0.0001111
S5	0.9316501	0.0571870	0.0006032	0.0046464	0.0006032	0.0002441	0.0000763
S6	0.9476833	0.0433666	0.0004580	0.0035230	0.0004580	0.0001856	0.0000581
S7	0.9543546	0.0375435	0.0004020	0.0030917	0.0004020	0.0001623	0.0000505
S8	0.9602357	0.0323532	0.0003695	0.0027040	0.0003695	0.0001537	0.0000502
S9	0.9653242	0.0279516	0.0003229	0.0023592	0.0003229	0.0001340	0.0000437
S10	0.9680778	0.0255945	0.0002903	0.0021757	0.0002903	0.0001183	0.0000372
S11	0.9759903	0.0188761	0.0002001	0.0016030	0.0002001	0.0000781	0.0000228
S12	0.9804204	0.0150924	0.0001605	0.0012684	0.0001605	0.0000633	0.0000189

Table 3.15 Design response spectral acceleration, seismic response coefficient, and system yield force coefficient versus initial cost for each structure.

Structure	Design Response Spectral Acceleration (S_{D1})	Seismic Response Coefficient (C_s)	System Yield Force Coefficient (Sy)	Initial Cost ($)
S1	0.1	0.01	0.033	1,694,100
S2	0.2	0.02	0.061	1,787,310
S3	0.3	0.03	0.093	1,893,040
S4	0.4	0.04	0.115	1,990,200
S5	0.5	0.05	0.140	2,079,460
S6	0.6	0.06	0.169	2,172,750
S7	0.7	0.07	0.188	2,267,430
S8	0.8	0.08	0.213	2,360,870
S9	0.9	0.09	0.230	2,470,200
S10	1.0	0.10	0.245	2,577,640
S11	1.2	0.12	0.321	2,880,170
S12	1.5	0.156	0.408	3,234,730

Table 3.16 Cost functions, equations and basic cost given by FEMA 227 and 228.

Function	Cost	Equation	Basic Cost
C_j^{dam}	Damage/ Repair	Replacement Cost × Floor Area × Mean Damage Index	\$85/sqft for replacement cost
C_j^{con}	Loss of contents	Unit Contents Cost × Floor Area × Mean Damage Index	\$28.9/sqft for unit contents cost
C_j^{rel}	Relocation	Relocation Cost × Gross Leasable Area × Loss of Time	\$1.5/month/sqft
C_j^{eco}	Economic Loss	Rental Cost(C_j^{ren}) + Income Cost(C_j^{inc})	
C_j^{ren}	Rental	Rental Rate × Gross Leasable Area × Loss of Function	\$0.58/month/sqft
C_j^{inc}	Income	Rental Rate × Gross Leasable Area × Out of Business	\$100/year/sqft
C_j^{inj}	Injury	Injury Cost per person × Expected Injury Rate	\$1,000(minor), \$10,000(serious)
C_j^{fat}	Human Fatality	Death Cost per person × Expected Death Rate	\$1,740,000/person

Table 3.17 General damage description of the limit-state level and central damage factor (%) by FEMA 227.

Limit State Level	Damage State	Damage Factor Range (%)	Central Damage Factor (%)
I	None	0	0
II	Slight	0-1	0.5
III	Light	1-10	5
IV	Moderate	10-30	20
V	Heavy	30-60	45
VI	Major	60-100	80
VII	Destroyed	100	100

Table 3.18 Weighted statistics for loss of function and restoration time (days) of social function classifications from ATC-13.

Damage State	Central Damage Factor	Mean Time (days) of Total Loss of Function to Restore
I	0	0
II	0.5	3.4
III	5	12.08
IV	20	44.72
V	45	125.66
VI	80	235.76
VII	100	346.93

Table 3.19 Expected injury and death rates for existing building by FEMA 227 (1992).

Damage State	CDF (%)	Fraction Injured		Fraction Death
		Minor	Serious	
I	0	0	0	0.000001
II	0.5	0.00003	0.000004	0.00001
III	5	0.003	0.00004	0.0001
IV	20	0.003	0.0004	0.001
V	45	0.03	0.004	0.001
VI	80	0.3	0.04	0.01
VII	100	0.4	0.4	0.2

Table 3.20 Results of damage cost calculation for Los Angeles.

Limit State Level	C^{dam}	C^{con}	C^{rel}	C^{eco}	
				C^{ren}	C^{inc}
I	0	0	0	0	0
II	66,091	22,471	26,437	10,222	144,858
III	660,915	224,711	93,928	36,319	514,672
IV	2,643,658	898,844	347,719	134,451	1,905,309
V	5,948,231	2,022,399	977,065	377,798	5,353,781
VI	10,574,633	3,595,375	1,833,144	708,816	10,044,623
VII	13,218,291	4,494,219	2,697,542	1,043,050	14,781,053

Limit State Level	C^{inj}		C^{fat}	Sum I	Sum II
	minor	serious			
I	0	0	0	0	0
II	8	11	487	270,079	270,586
III	84	112	4,867	1,530,544	1,535,606
IV	839	1,119	48,667	5,929,981	5,980,605
V	8,391	11,188	486,666	14,679,274	15,185,518
VI	83,908	111,877	4,866,658	26,756,591	31,819,034
VII	111,877	1,118,772	97,333,164	36,234,155	134,797,968

Table 3.21 Total expected life-cycle cost for Los Angeles.

Structure	Sy	E[C(t)] (w/)	E[C(t)](w/o)	IC	EFC (w/)	EFC (w/o)
S1	0.033	9,171,741	7,938,465	1,694,104	7,477,637	6,244,360
S2	0.061	5,903,026	5,398,852	1,787,307	4,115,719	3,611,544
S3	0.093	4,204,167	3,938,284	1,893,037	2,311,130	2,045,247
S4	0.115	3,717,062	3,479,882	1,990,199	1,726,863	1,489,683
S5	0.140	3,388,486	3,217,905	2,079,455	1,309,032	1,138,450
S6	0.169	3,166,573	3,036,709	2,172,747	993,825	863,962
S7	0.188	3,135,837	3,022,851	2,267,425	868,412	755,426
S8	0.213	3,106,887	3,002,254	2,360,868	746,019	641,385
S9	0.230	3,156,596	3,059,940	2,470,200	686,397	589,741
S10	0.245	3,195,594	3,112,515	2,577,641	617,953	534,875
S11	0.321	3,311,822	3,260,073	2,880,165	431,657	379,908
S12	0.408	3,581,107	3,538,385	3,234,728	346,379	303,657

Table 3.22 Locations and spectral accelerations at one second period for four cities.

City	Location	Spectral Acceleration (S_a) in 50 years				
		2%	5%	10%	50%	75%
Los Angeles	34.00° N, 118.00° W	0.859715	0.607513	0.443075	0.193932	0.143438
Seattle	47.61° N, 122.33° W	0.559750	0.322340	0.220632	0.036372	0.018836
Charleston	32.80° N, 79.97° W	0.417614	0.170861	0.071923	0.016012	0.009253
Boston	42.33° N, 71.08° W	0.087823	0.048669	0.028276	0.006295	0.003638

Table 3.23 Initial cost for each city.

Structure	Seattle	Charleston	Boston
S1	1,607,266	1,182,217	1,777,895
S2	1,695,692	1,247,258	1,875,708
S3	1,796,002	1,321,040	1,986,667
S4	1,888,183	1,388,844	2,088,635
S5	1,972,864	1,451,130	2,182,306
S6	2,061,375	1,516,234	2,280,213
S7	2,151,199	1,582,304	2,379,573
S8	2,239,853	1,647,512	2,477,638
S9	2,343,580	1,723,808	2,592,377
S10	2,445,514	1,798,785	2,705,132
S11	2,732,530	2,009,899	3,022,619
S12	3,068,919	2,257,328	3,394,719

Table 3.24 Optimal system yield force coefficient for each city.

City	Los Angeles	Seattle	Charleston
With Injury and Death	0.198	0.109	0.097
Without Injury and Death	0.193	0.089	0.051

Table 3.25 Spectral response acceleration (% of gravity) at one second period, S_1, by 1997 NEHRP maps and USGS (1999) for each city.

City	Los Angeles	Seattle	Charleston	Boston
S_1 by 1997 NEHRP	76	54	40	9
S_1 by USGS	85.97	55.98	41.76	8.78

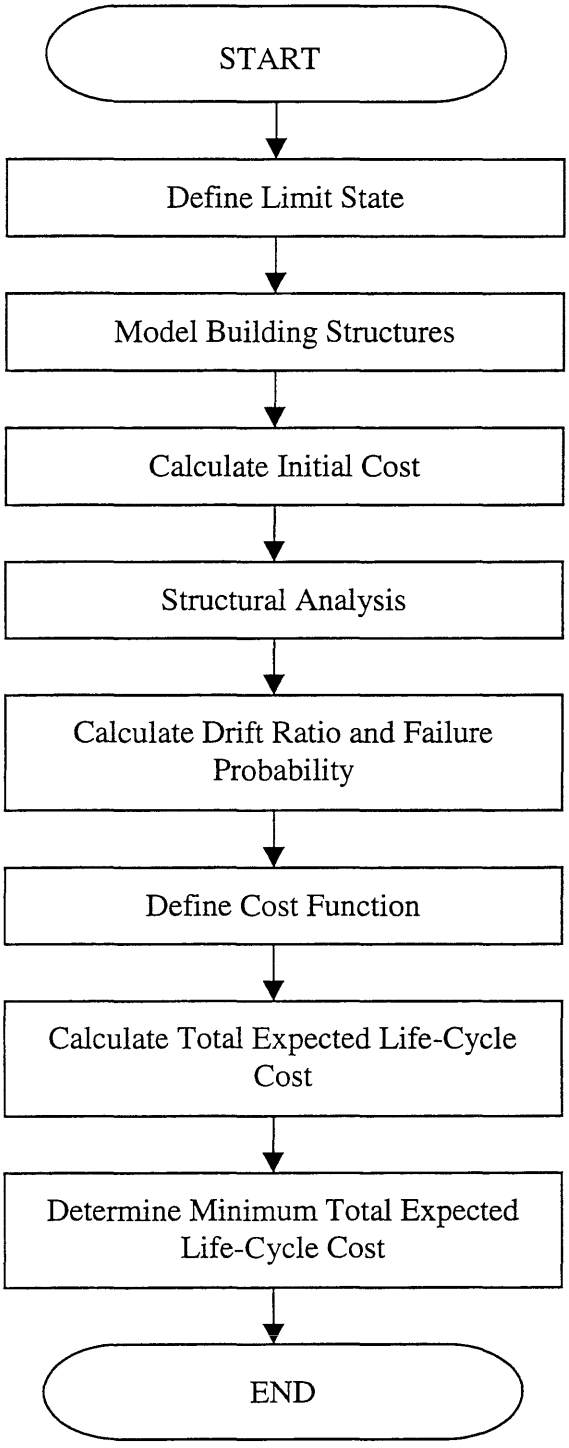

Figure 3.1 Procedure to determine minimum total expected life-cycle cost.

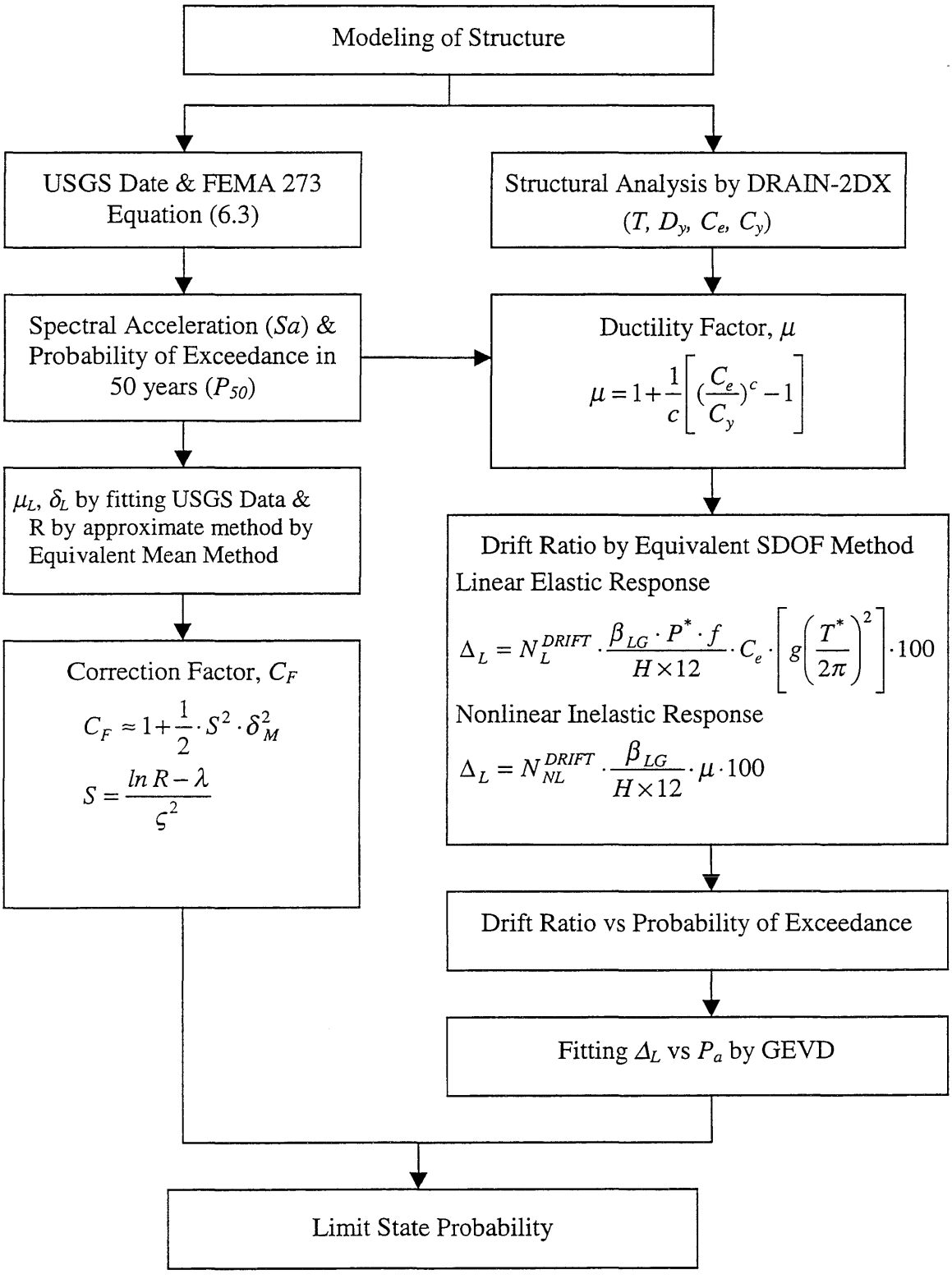

Figure 3.2 Procedure to calculate the limit state probability.

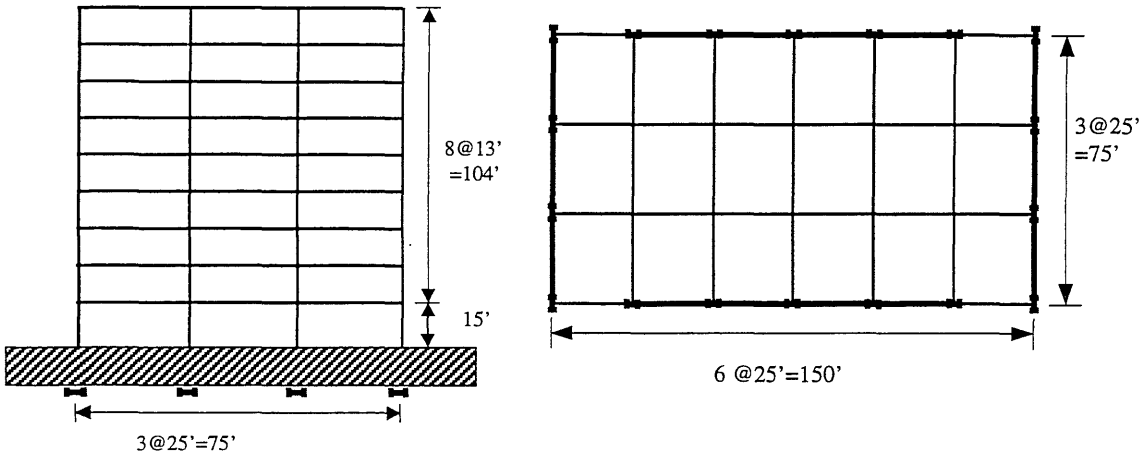

Figure 3.3 Plan and elevation of 9-story steel building

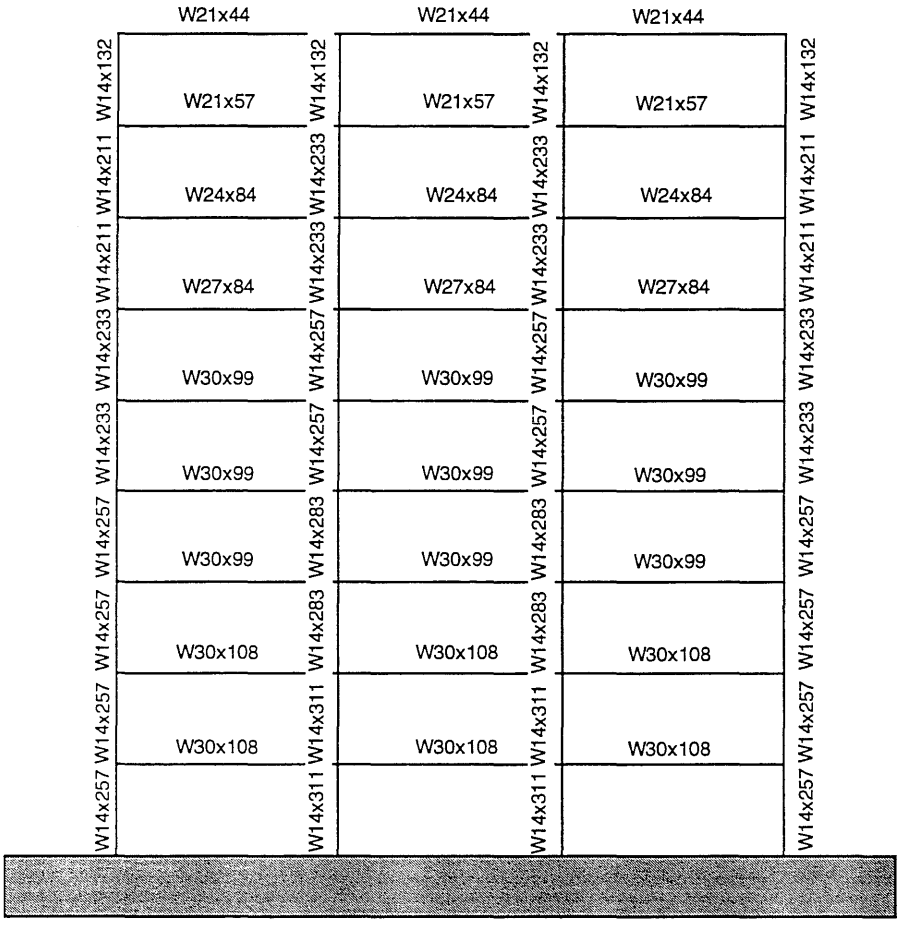

Figure 3.4 Member sizes for structure S4

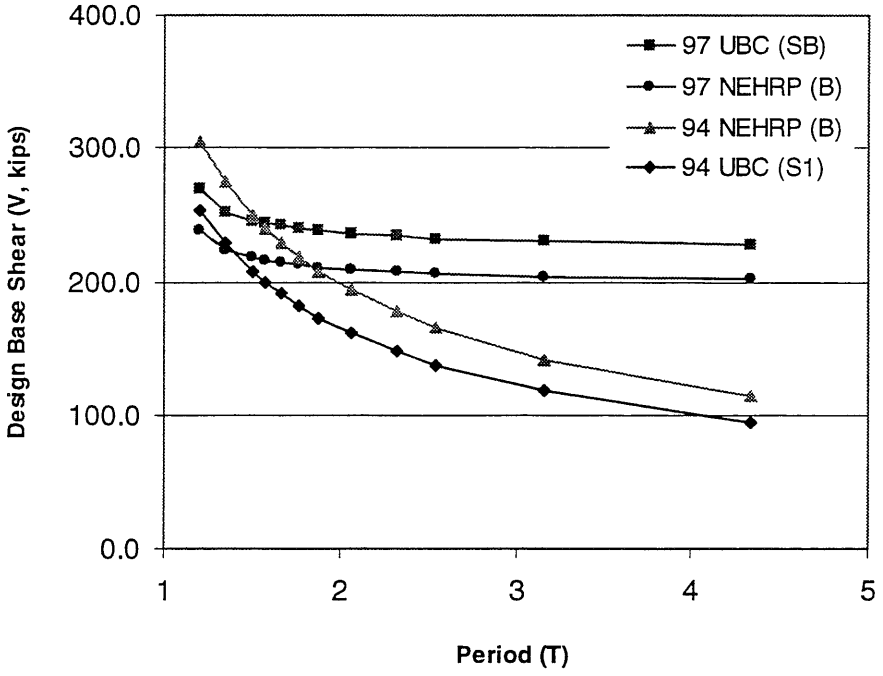

Figure 3.5 Design base shear (V) for each structure according to 4 different codes.

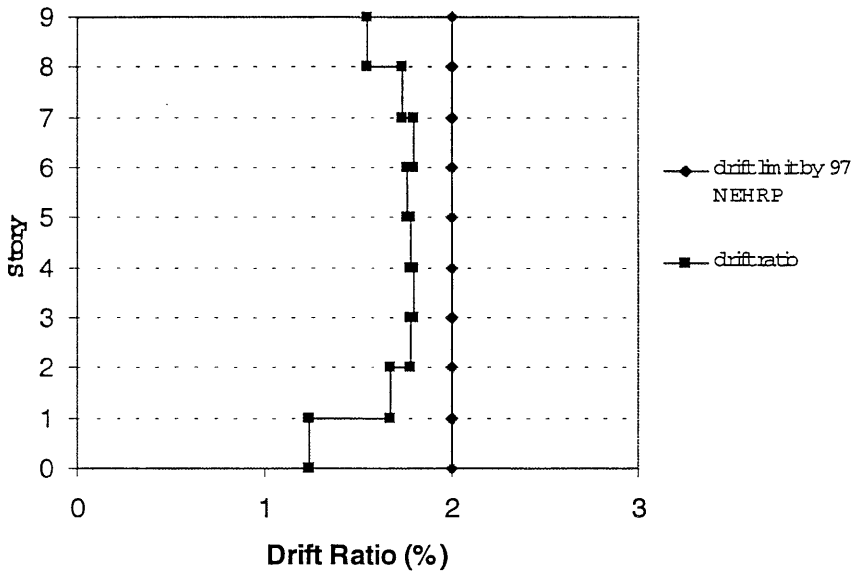

Figure 3.6 Interstory drift ratio (%) of S4 and drift limit by 1997 NEHRP provisions.

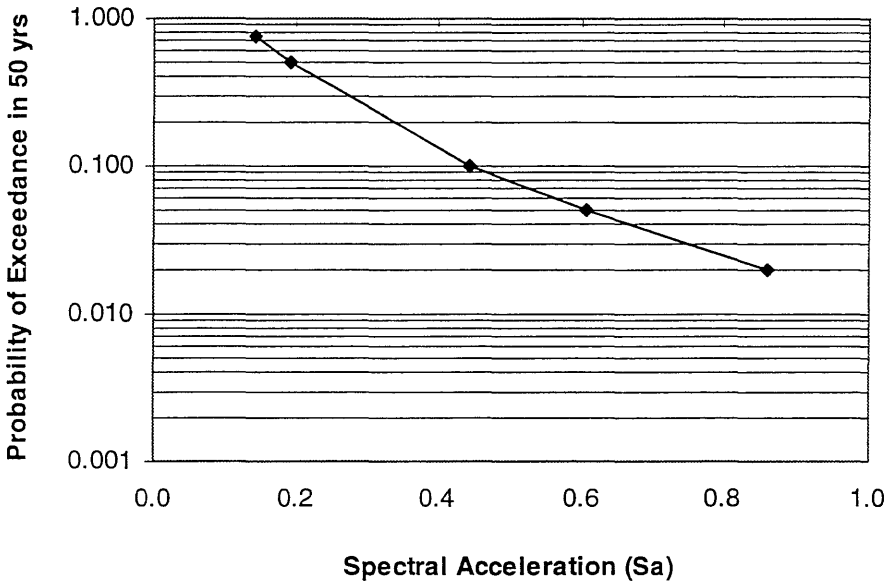

Figure 3.7 Probability of exceedance of spectral 1-sec. acceleration (Sa) in 50 years at Los Angeles site.

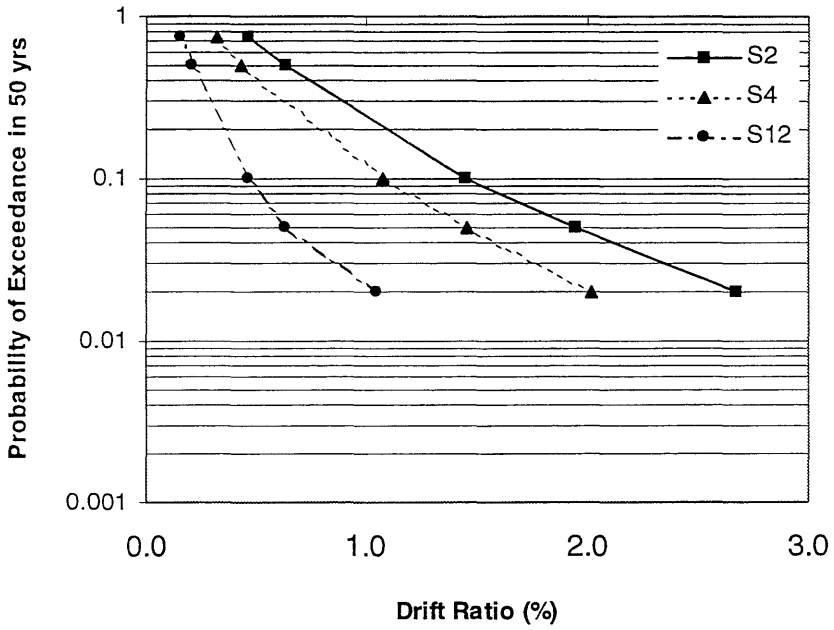

Figure 3.8 Interstory drift ratio (%) and probability of exceedance in 50 years for S2, S4 and S12.

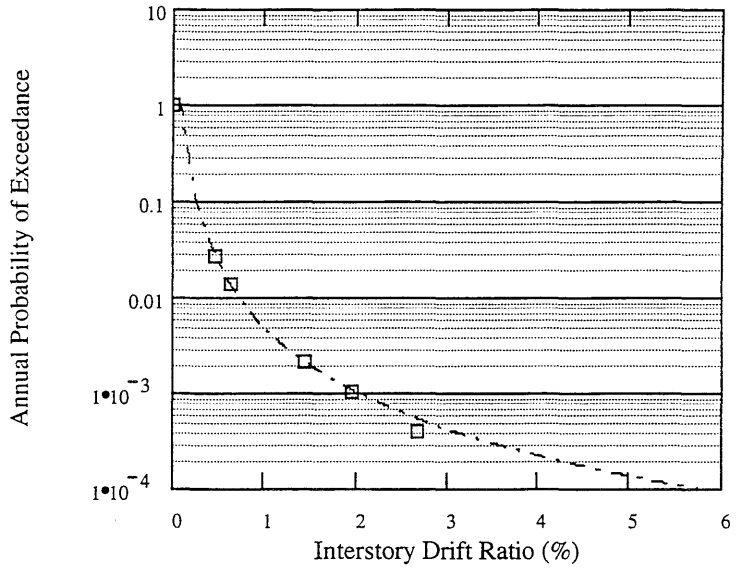

(a) S2

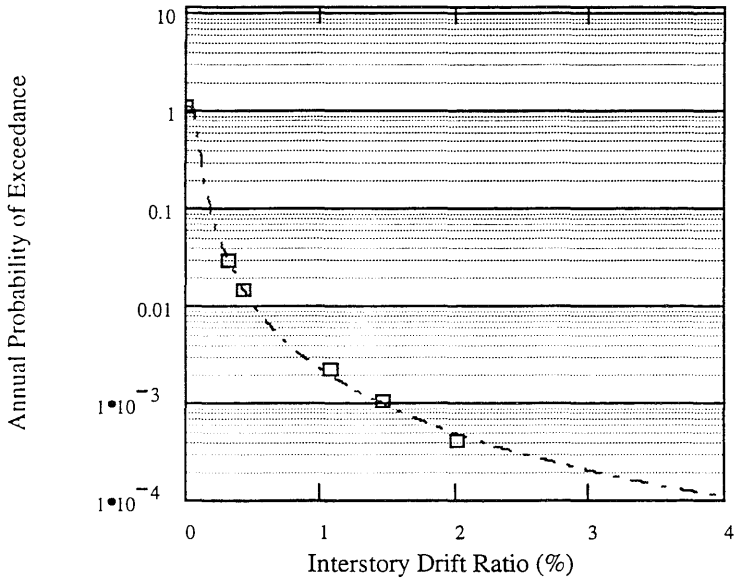

(b) S4

Figure 3.9 Interstory drift ratio and annual probability of exceedance by generalized extreme value distribution (GEVD) for S2and S4.

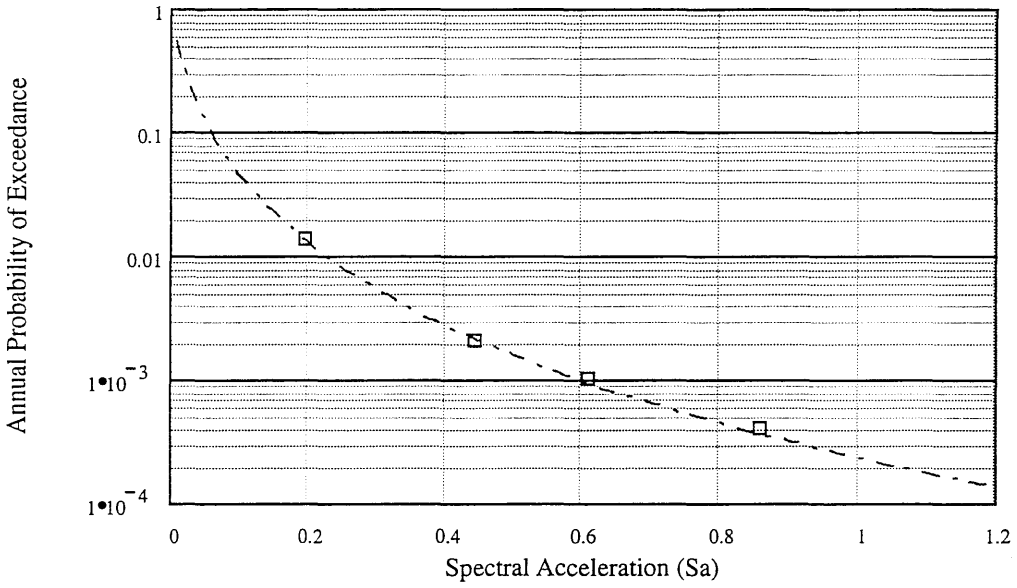

Figure 3.10 Spectral acceleration (Sa) and annual probability of exceedance assuming lognormal distribution.

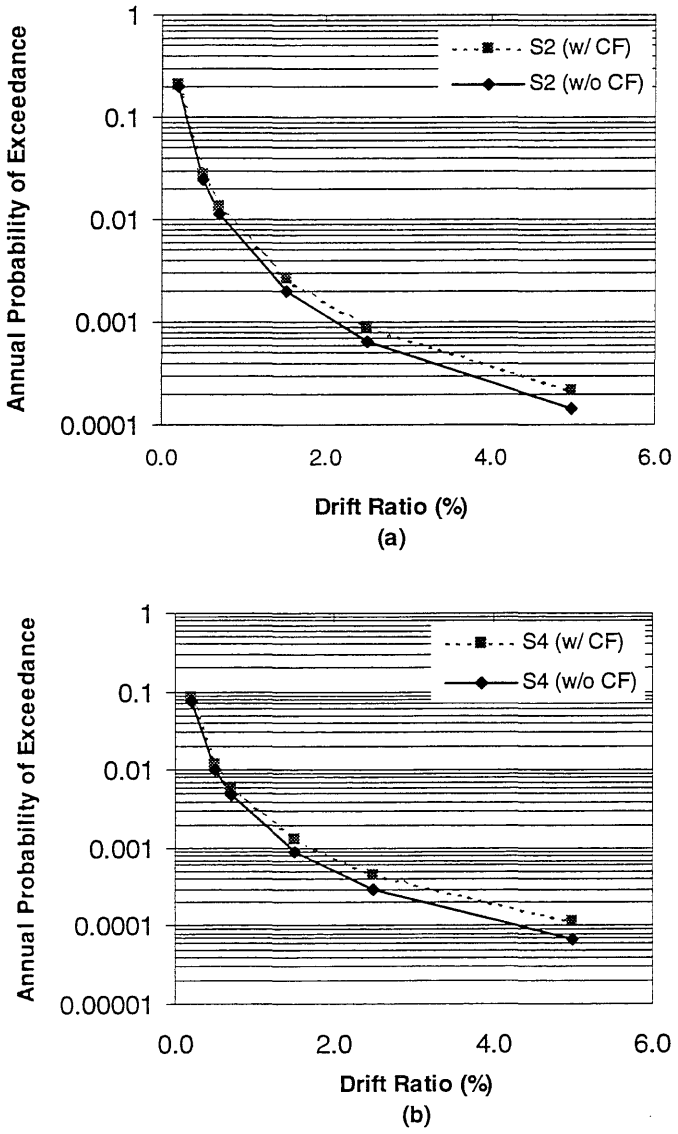

Figure 3.11 Annual probability of exceedance of drift ratio with(w/) and without(w/o) correction factor for S2 and S4.

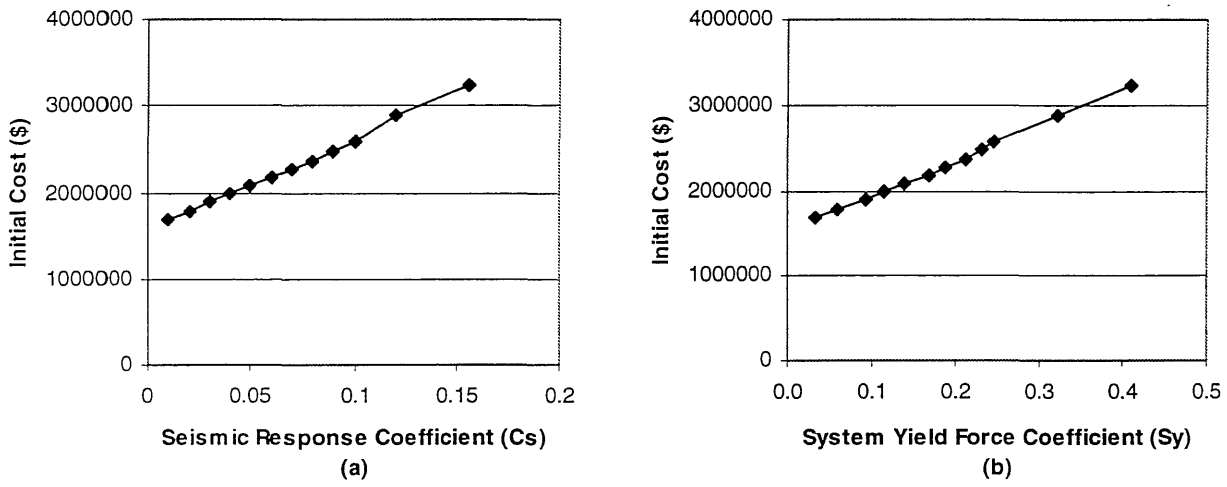

Figure 3.12 Initial cost as function of (a) seismic response coefficient (Cs). (b) system yield force coefficient (S_y).

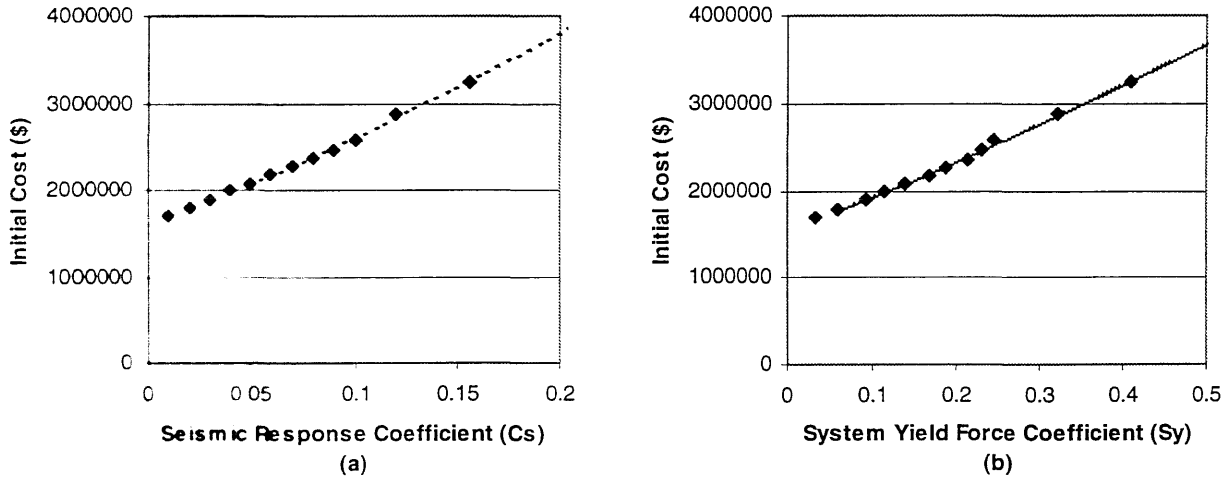

Figure 3.13 Fitting initial cost according to the equation by Rosenblueth and Jara (1990) as function of (a) seismic response coefficient (Cs). (b) system yield force coefficient (S_y).

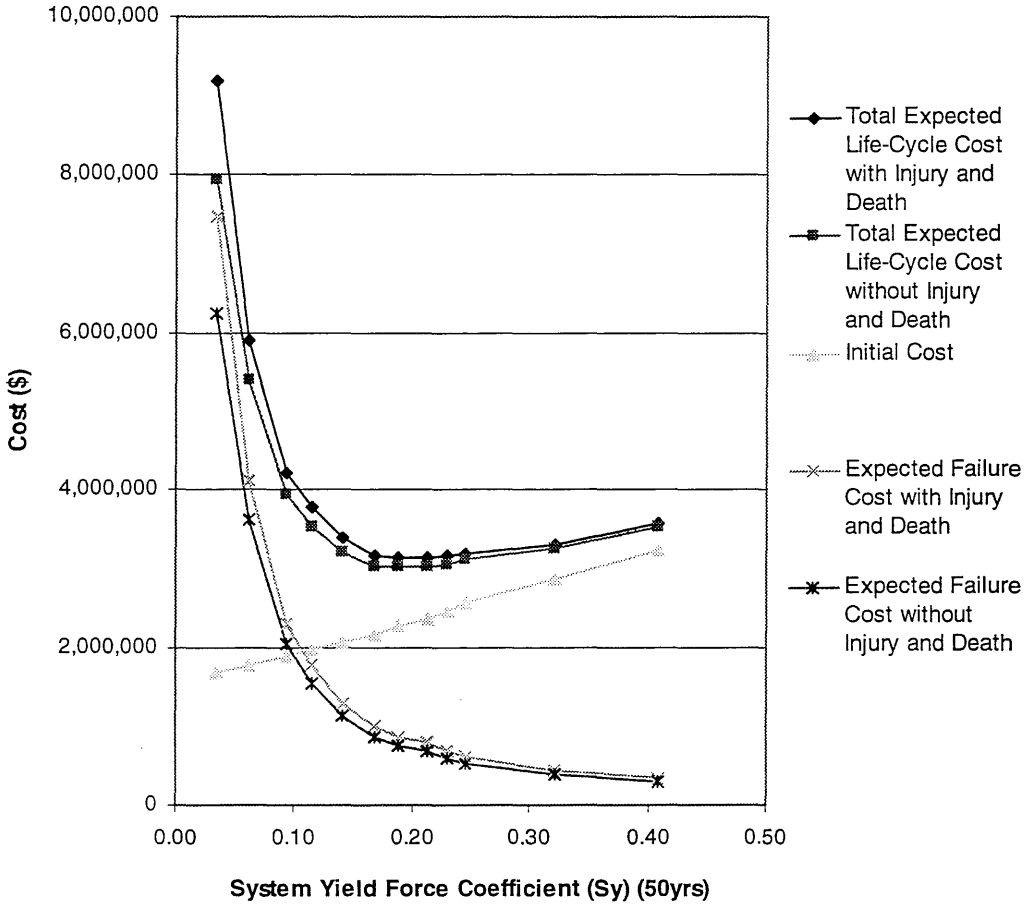

Figure 3.14 Total expected life-cycle cost as function of system yield force coefficient at Los Angeles for t = 50 years, $\lambda = 0.05$.

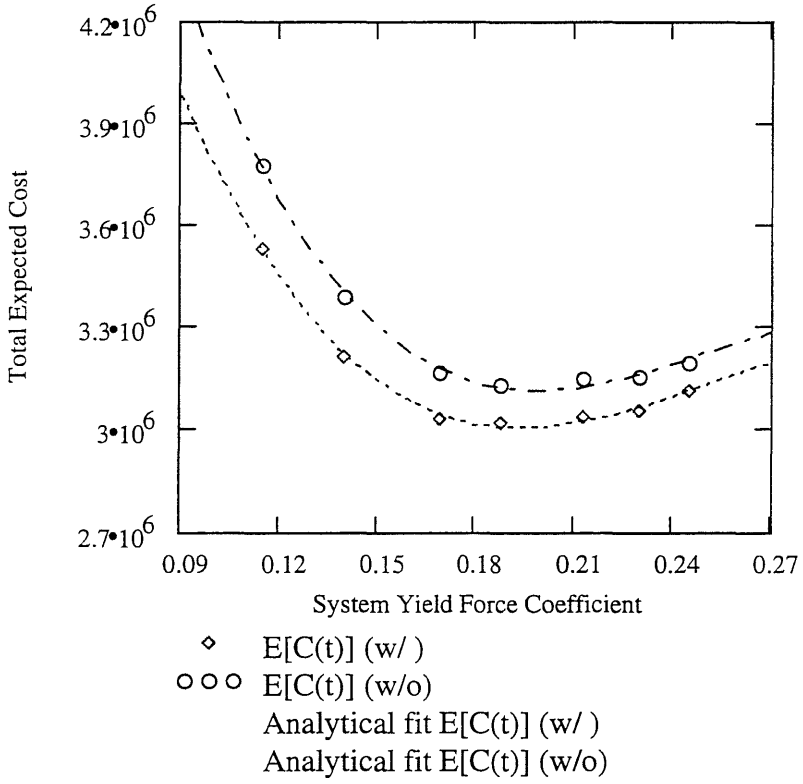

Figure 3.15 Polynomial fit of total expected life-cycle cost as function of system yield force coefficient at Los Angeles for t=50 years and ν=0.05.

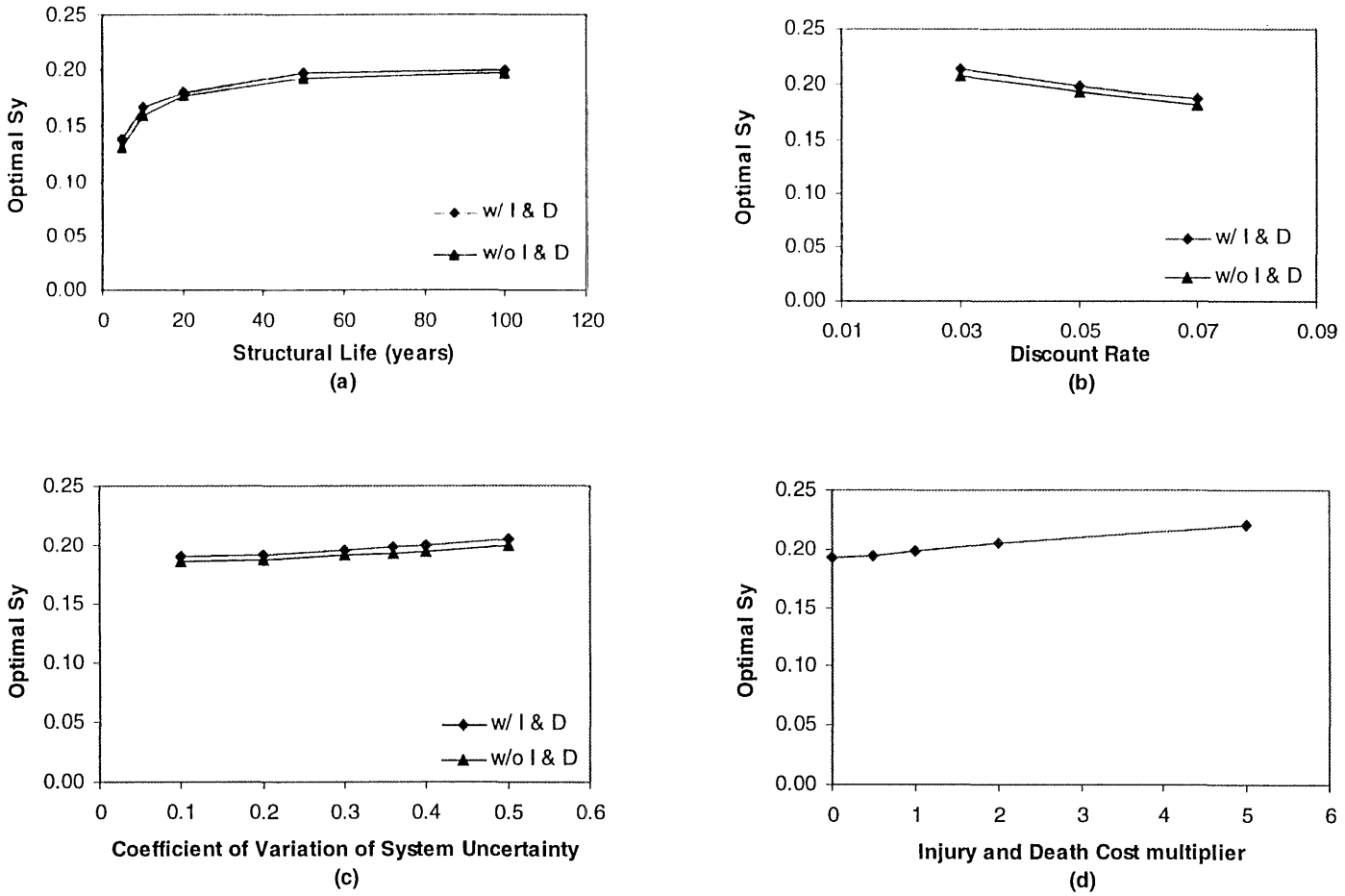

Figure 3.16 Sensitivity of optimal design to (a) structural lifetime (b) discount rate (c) coefficient of variation of system uncertainty and (d) injury and death cost at Los Angeles.

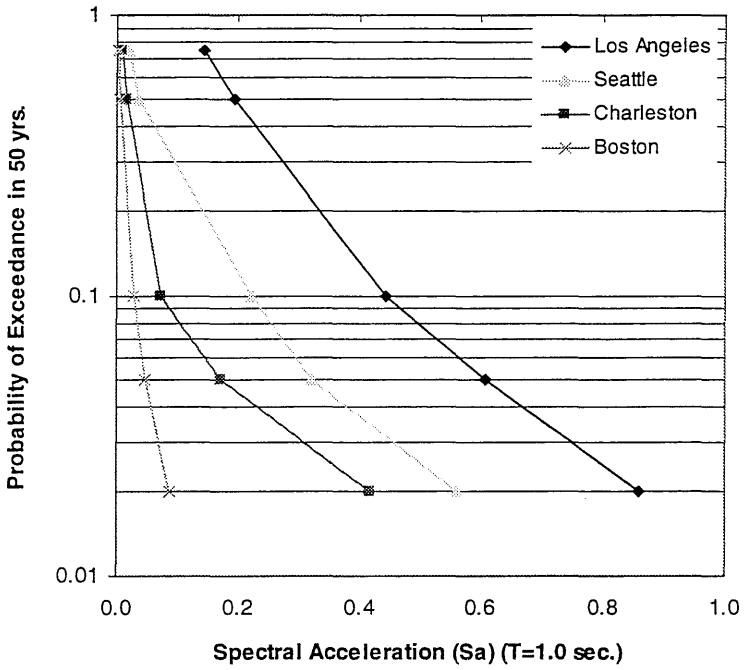

Figure 3.17 Probability of exceedance of spectral acceleration at a one second and in 50 years for each city.

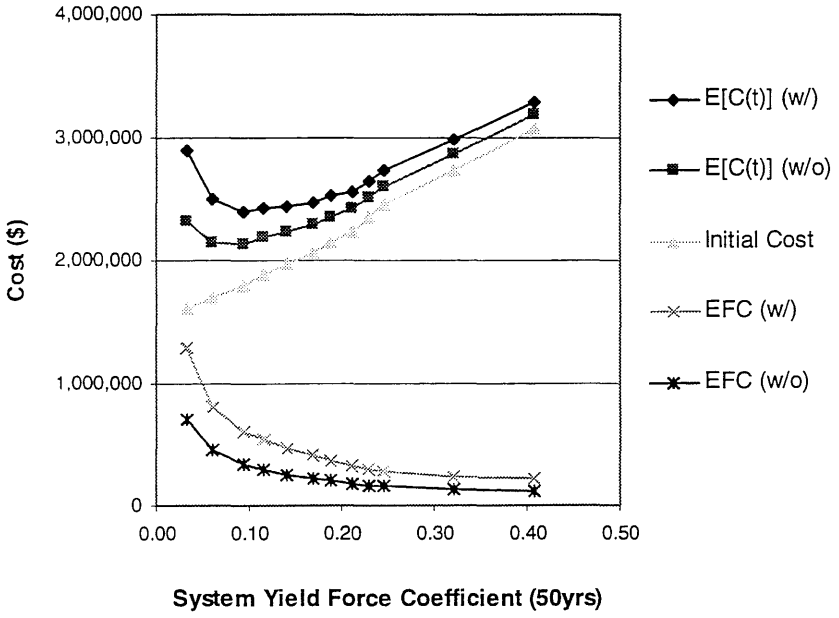

Figure 3.18 Total expected life-cycle cost as function of system yield force coefficient at Seattle for t=50 years and λ=0.05.

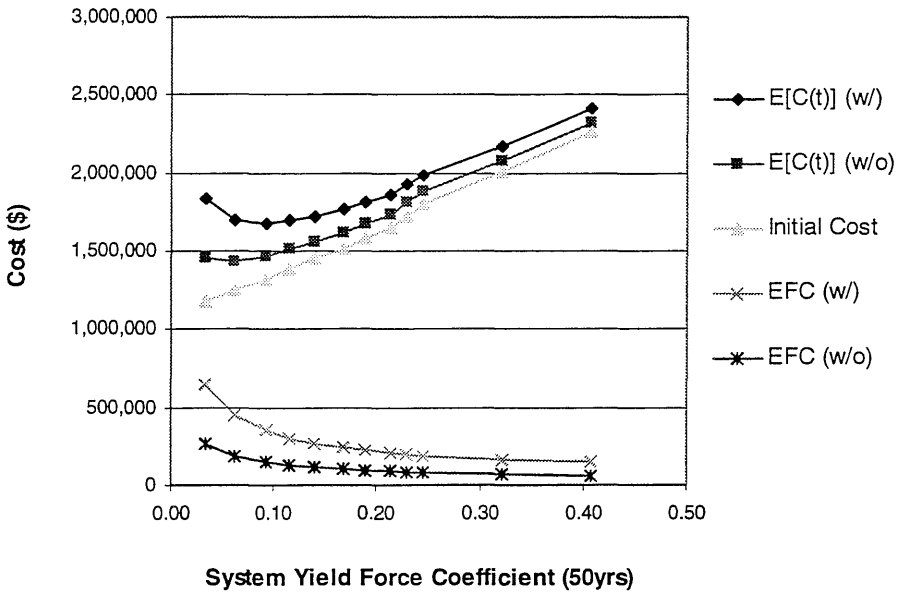

Figure 3.19 Total expected life-cycle cost as function of system yield force coefficient at Charleston for t=50 years and λ=0.05.

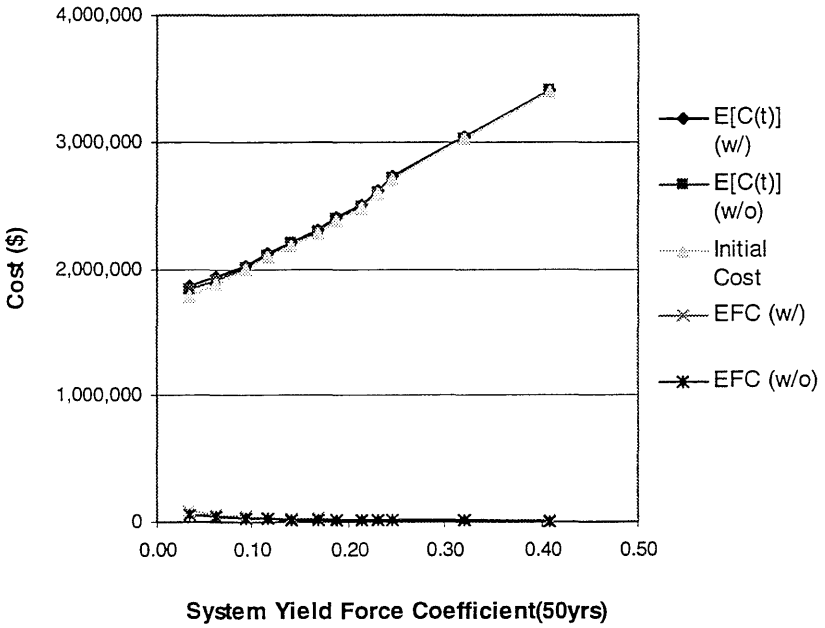

Figure 3.20 Total expected life-cycle cost as function of system yield force coefficient at Boston for t=50 years and λ=0.05.

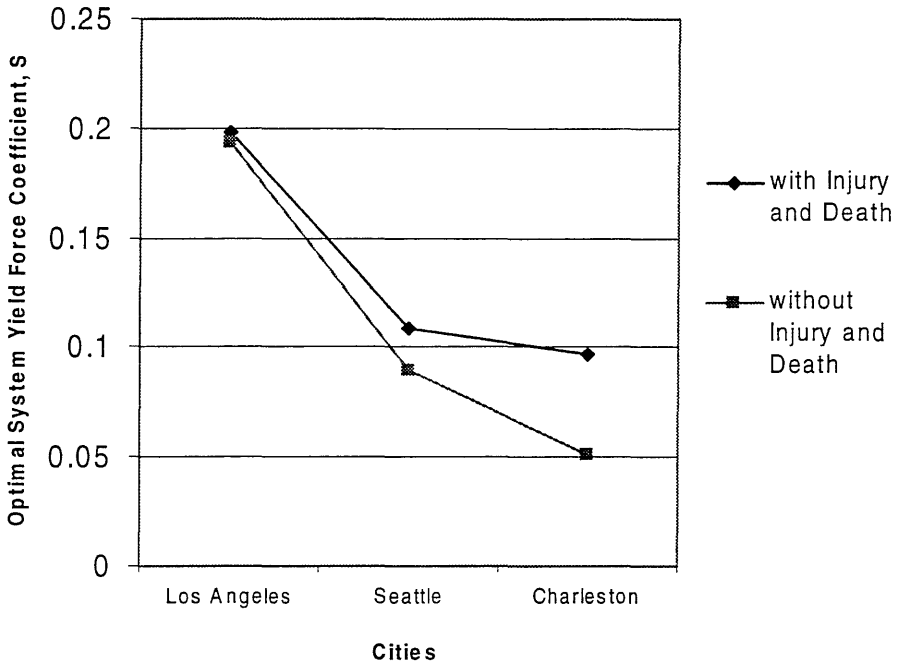

Figure 3.21 Comparison of optimal system yield force coefficient (Sy) with and without injury and death cost at 3 cities.

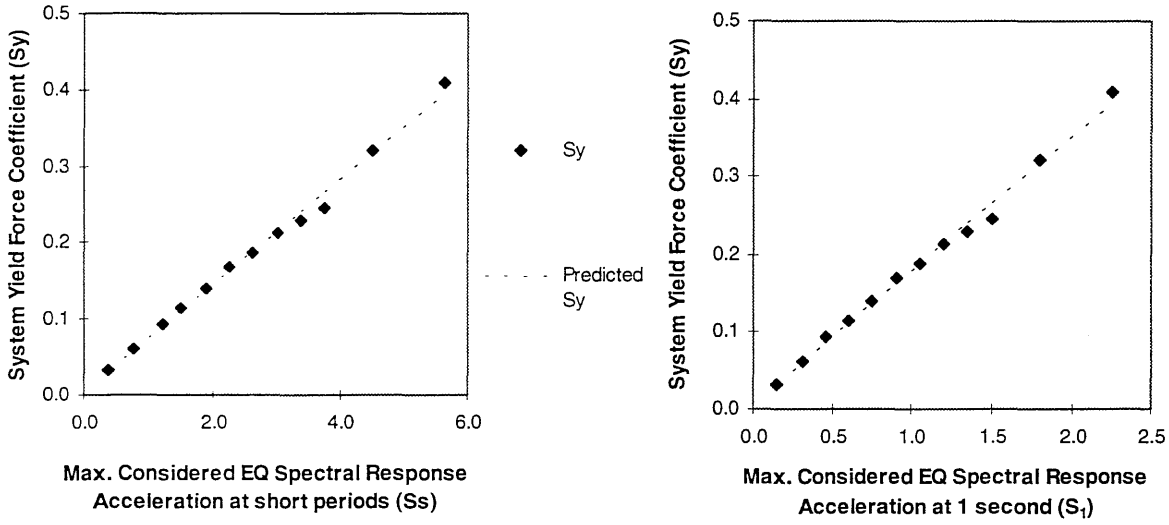

Figure 3.22 Regression for system yield force coefficient (S_y) and Maximum Considered Earthquake spectral response acceleration at short period and at a one second.

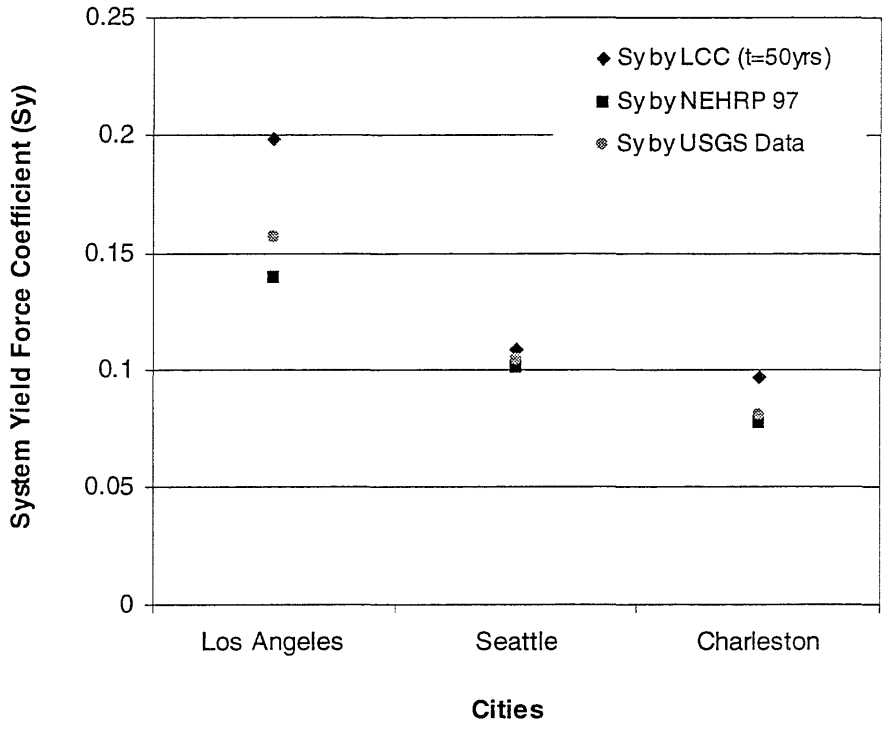

Figure 3.23 Comparison of optimal system yield force coefficients for each city by Life-Cycle Cost (LCC) with these based on NEHRP 1997 provisions and USGS data.

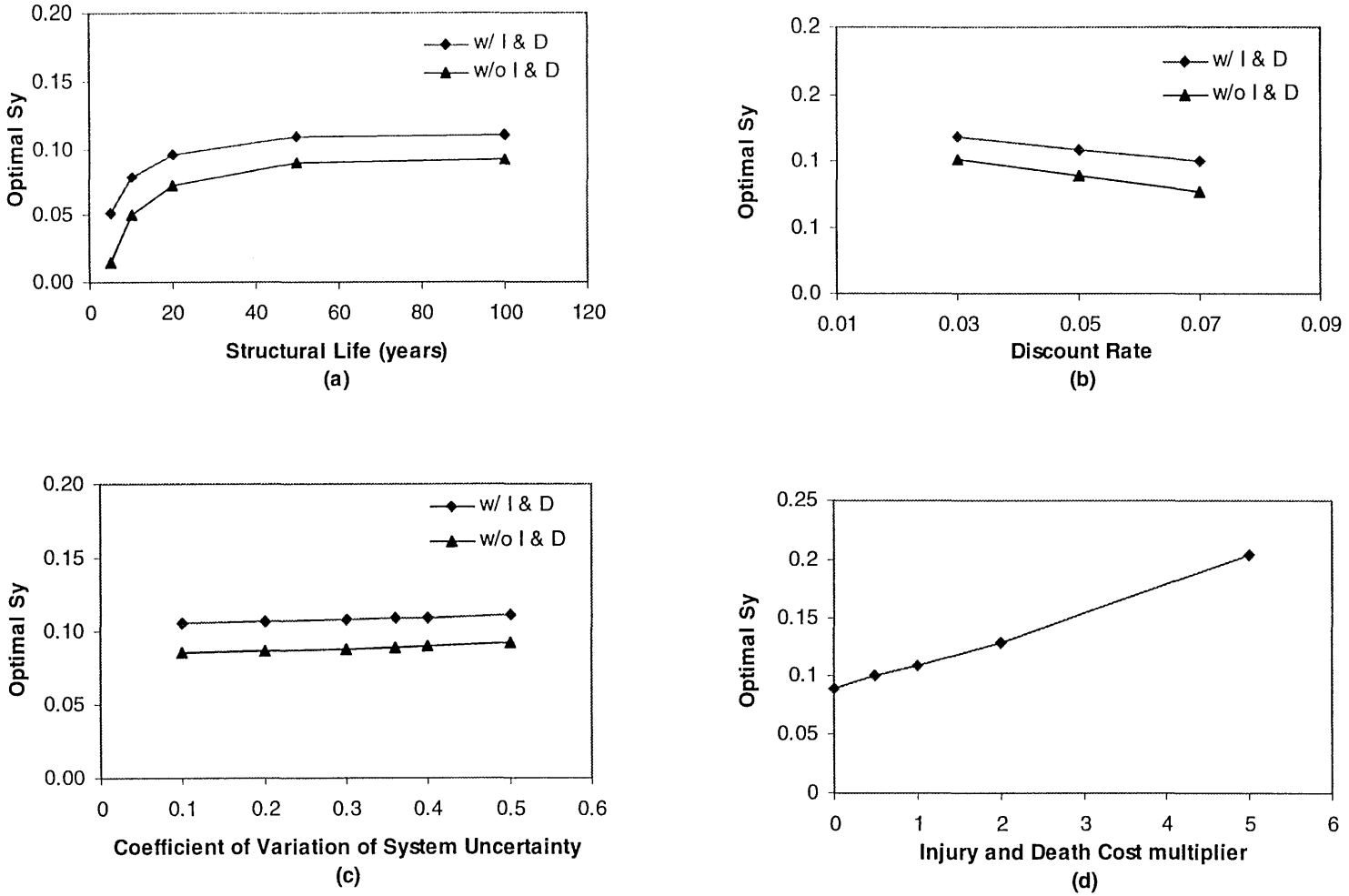

Figure 3.24 Sensitivity of optimal design to (a) life-time (b) discount rate (c) coefficient of variation of system uncertainty (d) injury and death cost at Seattle.

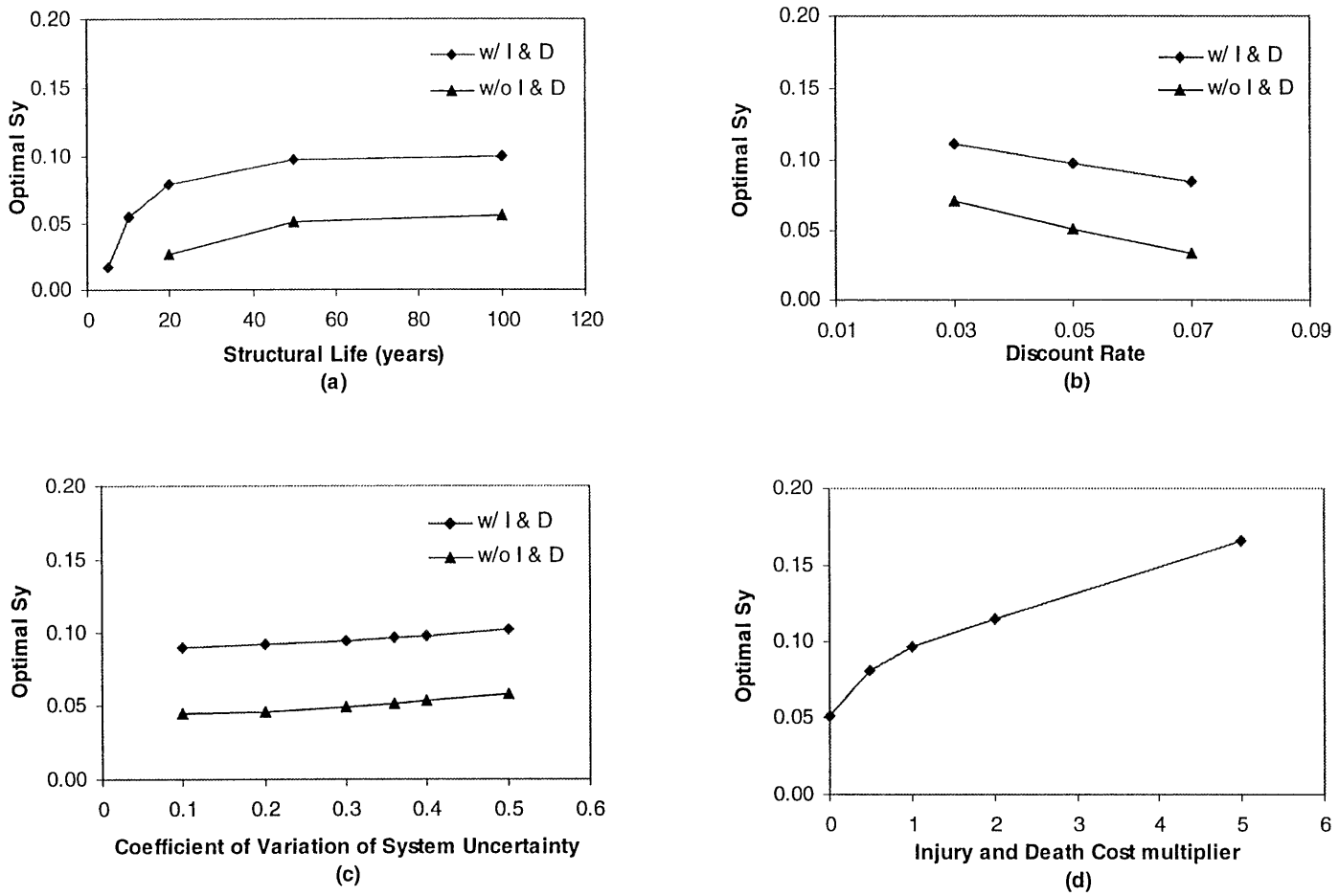

Figure 3.25 Sensitivity of optimal design to (a) life-time (b) discount rate (c) coefficient of variation of system uncertainty (d) injury and death cost at Charleston.

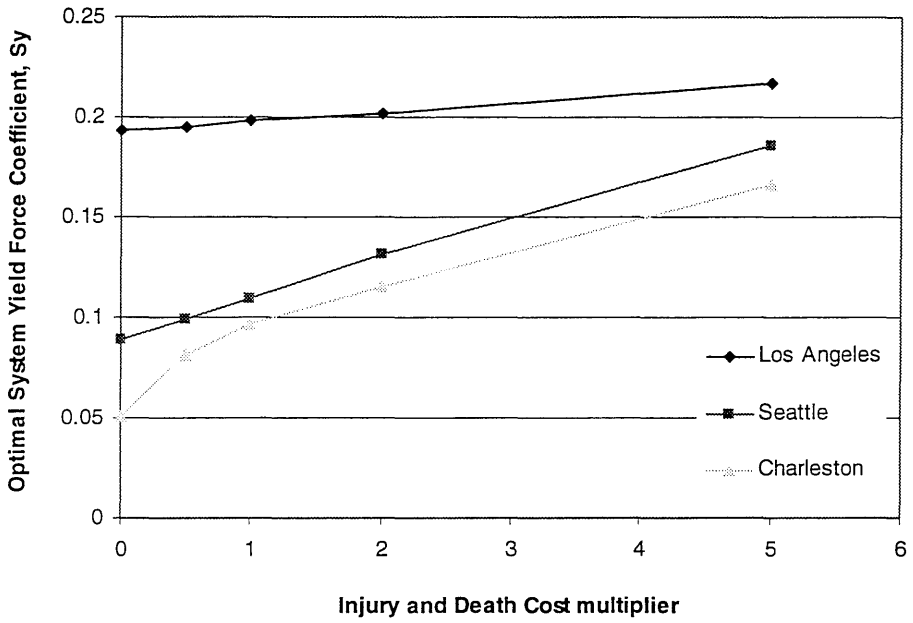

Figure 3.26 Comparison of optimal system yield force coefficient (S_y) as function of injury and death cost at three cities.

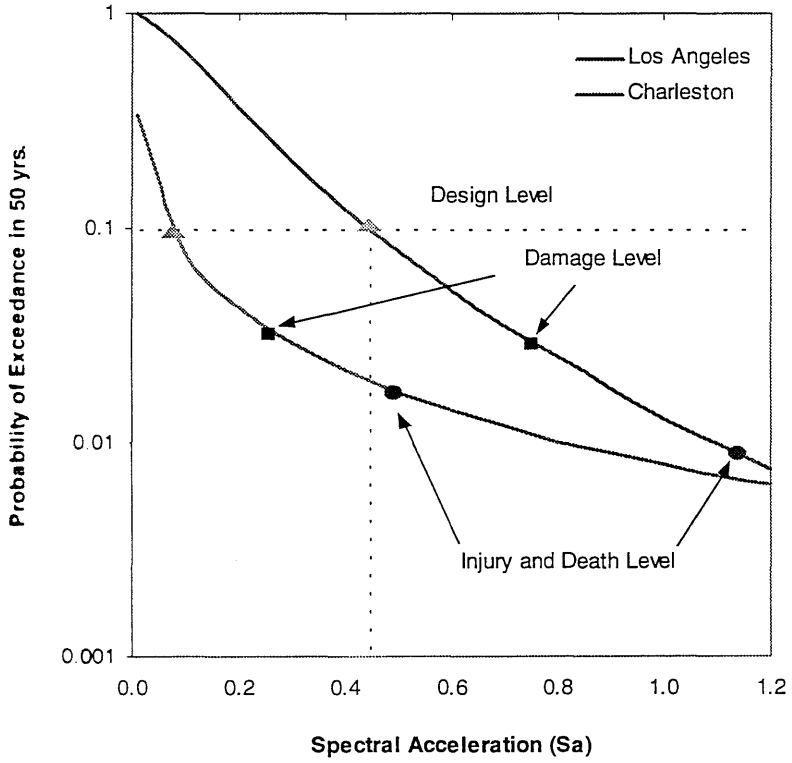

Figure 3.27 Different characteristics of the seismic hazards at Los Angeles and Charleston.

CHAPTER 4

APPLICATION TO WIND DESIGN

4.1 Introduction

Data of damage and economic losses caused by natural disasters in last few decades show that wind damages dominate. Therefore, the determination of design wind load is an important issue. According to Barton and Nishenko (1997), economic losses from natural disasters on global scale have tripled since the 1960s. They also showed that while property losses increased, loss of life due to hurricanes in the continental U.S. decreased in the last few decades.

Daneshvaran et al. (1997) estimated the catastrophic losses in the United States during 1986 through 1993 to be $47.13 billion dollars based on the report of the Property Claim Services (NCPI, 1993). The catastrophic losses related to wind comprise 87 % of the total loss. The damage due to hurricanes and associated hazards such as tornadoes has an increasing trend due to the increasing number of events as compared to a relatively quiet period from 1970 to 1990, and the increasing population in hurricane prone regions.

U.S. Department of Housing and Urban Development (1993) reported the estimated dollar cost of damage for Hurricane Hugo of 1989, Hurricanes Andrew and Iniki of 1992 to be 4 billion, $20-25 billion and $1.2-1.4 billion, respectively. The report by Texas Department Insurance (1992) concluded that the property loss experienced from hurricanes strongly demonstrated the need for some mitigating measures to reduce losses.

According to Metha et al. (1992), the Property Claim Services (PCS) in the U.S. records an event as a catastrophe when there are numerous claims for property loss and the total claim amount exceeds 5 million dollars. Dollar losses to the insurance industry caused by these catastrophes are shown in Figure 4.3 for years 1986 through 1992. Figure

4.4 shows dollar loss by catastrophe type. These figures clearly indicate that wind is a major factor in causing property losses. Close to 90 percent of property losses are due to hurricanes, tornadoes and other windstorm catastrophes.

After Hurricane Andrew in 1992, several researchers, e.g., Dye (1993), Levitan et al (1993), Marshall (1993) and McDonald and Mehnert (1993), pointed out that widespread damage to manufactured homes was caused by Hurricane Andrew winds exceeding the current U.S. Department of Housing and Urban Development (HUD) structural design standards. They proposed that manufactured home wind load should be upgraded accordingly. In addition to these proposals, Walter (1993) suggested that a benefit-cost analysis should be taken into consideration for upgrading the current wind standards, and asked for a cost-effective wind safety standard for low-rise residential structures, including special requirements for manufactured homes constructed.

Recently, there have been many proposals, e.g., U.S. Geological survey, (1997) and Daneshvaran et al. (1997), for determination of the relationship between wind damage and economic losses. As shown above, even though the damage and economic losses by wind are very large, no rational methods based on economic evaluation have been applied to design wind load. Return period and probability of exceedance are often used based on experience, judgement, and consensus. Loss/Cost has not been included into consideration. Therefore, a more rational method based on minimum life-cycle cost is needed also for design against wind.

In this chapter, the methodology for minimum life-cycle cost design criteria is applied to wind load. The limit states of a building under wind can be described in terms of structural limit state such as large deflection and failure of the building envelope, i.e., glass or cladding failure caused by the wind pressure and missile debris. Hence, in the case of wind load, the design wind intensity for buildings needs to be considered separately; one related to structural limit state, and the other related to failure of the building envelope.

The response of structural frames to the wind load is calculated by using the method proposed in ASCE 7-98. The limit state and cost function are the same as those for earthquake loads.

To determine the design intensity for the building envelope, twelve glass types according to glass thickness are considered. Failure probabilities by the wind pressure and windborne missile debris effects are calculated. The optimal design intensity for wind load is determined by minimizing the expected life-cycle cost. Sensitivity analysis of the optimal design to lifetime, discount ratio and missile amount and existence factor also is carried out.

4.2 Application to Design of Structural Frame

4.2.1 Structural Response Analysis

Wind hazard at a given location is described by the basic wind speed with mean recurrence interval (MRI) of 50 years in ASCE 7-98. From ASCE 7-98, basic wind speeds can be obtained as 130 mph for Charleston, 110 mph for Boston and 85 mph for Los Angeles and Seattle. Since the basic wind speeds for Los Angeles and Seattle are the same, indicating similar wind environments, only Los Angeles is considered. By using proper conversion factors, wind speed with different mean recurrence intervals (MRI) can be obtained as shown in Table 4.2. Since all buildings are assumed to be in downtown, exposure categories for each city are assumed as Exposure The annual and 50 years exceedance probability of wind speed are shown in Figure 4.5 and 4.6.

Ten 9-story buildings from S1 to S10, the same as in Chapter 3, are used. In order to determine the probability of structural response in terms of drift ratio, the procedure for calculating maximum along-wind displacement in ASCE 7-98 is used. Details are given in Appendix D.

Table 4.2 shows the result of drift ratio of ten structures at Charleston, Boston, and Los Angeles (or Seattle). Figures 4.4 to 4.6 show the annual and 50 years probability of

exceedance of drift ratio for three structures, i.e. S1, S6, and S10, at Charleston, Boston, and Los Angeles, respectively.

4.2.2 Calculations of Total Expected Life-Cycle Cost

The Weibull distribution is used to fit the drift ratio.

$$F_{z_1}(z) = 1 - \exp\left[-\left(\frac{z-\varepsilon}{w_1-\varepsilon}\right)^k\right] \tag{4.1}$$

in which k is the shape parameter and w_1 is the characteristic value. The Weibull distribution of the drift ratio for S4 at three cities are shown in Figure 4.7. The fits are all very good.

The calculation of the total expected life-cycle cost for wind load again follows Equation (2.4). The cost vector includes damage cost, loss of contents, relocation cost, economic loss and the cost of injury and human fatality, same as in previous Chapter. The central damage factors adopted FEMA 227 (1992) is used. Tables 4.3, 4.4, and 4.5 show limit state failure probability at Charleston, Boston, and Los Angeles, respectively.

The total expected life-cycle cost for a lifetime of 50 years and a discount ratio (λ) of 0.05 at Charleston, Boston, and Los Angeles are shown in Tables 4.6 to 4.8 and Figures 4. 8 to 4.10, respectively. The optimal system yield force coefficients and corresponding life-cycle costs for each city are summarized in Table 4.9.

It is seen that optimal limit state probability at Charleston is between those of S4 (S_y = 0.115) and S5 (S_y = 0.140) in Table 4.6. The optimal limit state probabilities at Boston between those of S3 (S_y = 0.093) and S4 (S_y = 0.115), and between S2 (S_y = 0.061) and S3 (S_y = 0.093) at Los Angeles. There is virtually no difference in the optimal design intensity whether or not injury and death cost are considered, because the probability of such occurrence in wind is extremely small.

The current design according to ASCE 7-98 and Ambore (1993) is close to between S2 (S_y = 0.061) and S3 (S_y = 0.093) at Charleston and Boston, and between S1 (S_y = 0.033) and S2 (S_y = 0.061) at Los Angeles.

4.2.3 Sensitivity Analysis

An analysis of the sensitivity of optimal design is carried to changes in design lifetime, discount rate, and injury and death cost. The results of sensitivity analysis are shown in Figure 4.11 to 4.13. As expected, the optimal design intensity is not sensitive at all to assumption of death and injury cost. The design in moderately dependent upon the discount rate for long life and also on the change in design life. At Charleston, the optimal design system yield coefficient increases from 0.092 for T = 5 years to 0.121 for T = 100 years. At Boston and Los Angeles, the increases are from 0.072 to 0.106 and from 0.063 to 0.073, respectively.

4.2.4 Summary

The methodology of minimum life-cycle design is applied to wind load. Wind hazard and calculation of structural response follow provisions given in ASCE 7-98. Definition of limit state, calculation of limit state probability, and calculation of total expected life-cycle cost, e. t. c. are the same as in the previous Chapter and a sensitivity analysis is also carried out.

The following conclusions can be drawn from the results:

1. Optimal design building strengths in terms of system yield force coefficient to wind load are 0.121 at Charleston, while 0.106 at Boston and 0.073 at Los Angeles. All these design intensities are larger than those based on the current design according to ASCE 7-98 and Ambrose (1993).
2. There is virtually no difference whether injury and death cost is considered due to the extremely small probability of such occurrence.
3. The optimal design intensity moderately depends on discount rate and design life change.

4.3 Application to Building Envelope Design

4.3.1 Background of Building Envelope Failure

According to Beason et al. (1984), there are two primary mechanisms that cause window glass breakage in windstorms: lateral pressure and missile impact. The missile impact dominates the window glass breakage if there are windborne missiles, since winds tend to lift and sustain missiles at windspeeds considerably less than windspeeds required to cause critical lateral pressure. Similar conclusions were reached by Reed (1970) based on wind damage at Lubbock, Texas: (1) missiles caused the most damage at low heights and (2) 80 percent of window damage to large buildings were probably caused by windborne missiles. His final observation was that designs based only on wind force alone were inadequate.

The importance of addressing the envelope failure, i.e., the failure of glass in tall buildings, became evident after Hurricane Alicia hit the central business district of Houston, Texas, in 1983, resulting in extensive glass breakage and glass particle fallout. According to Kareem and Stevens (1984), 80% of the broken glass was caused by windborne debris based on a survey by a glass companies (Neunlist, 1983). Beason et al. (1984) also concluded that the principal source of the missiles in downtown Houston was rooftops in the center of the business district. King (1974) reported that small rocks from gravel surfaced roofs, including single-ply membrane roofs with ballast, could become airborne at wind speeds as low as 40-45 mph, and Minor et al. (1978) also proposed that windborne debris had the potential of impacting glass in taller buildings. In fact, according to Vild (1984), the wind velocities that occurred in downtown Houston during hurricane Alicia (80-85 mph) were below those required for the designs by the Houston building code, i.e., normally 90 mph. All these observations and facts strongly suggest that small missile impacts should be a consideration in the design of window glass in hurricane-prone areas (Pantelides et al. 1993).

According to Minor and Behr (1992), damage to architectural glazing systems caused by Hurricane Andrew on August 24, 1992 was extensive. About 20 buildings in Miami were examined with respect to architectural glazing performance. Most building occupants were forced to move out and conduct business elsewhere for time periods that, in some cases, approached a year.

In recent years, however, failures of building subcomponents, especially failures of windows during windstorms, have become more serious. Entire contents of multistory buildings have been destroyed because of window failures during windstorms. Furthermore, building contents have become so valuable in modern times that their replacement costs approach or exceed the values of the buildings themselves.

As Devlin mentioned (1997), the property damage to the Burger King headquarters in Miami during Hurricane Andrew, for instance, came mostly from lost business and destroyed interiors rather than structural damage to the building. According to Minor, "the building's structural engineer did an excellent job, but from the owner's perspective it was total loss-loss of contents, loss of business, relocation costs and the like." The windows in the six-story headquarters building withstood the 175 mph wind speeds, but the window frames were bent from the force, allowing rain to seep into the structure. The internal property damage was estimated at $25 to $30 million.

Therefore, small missile impacts should be considered in the design of window glass in hurricane-prone areas as pointed out by Pantelides et al. (1993). The overall procedure to determine optimal window glass thickness based on minimum total expected life-cycle cost for wind load is shown in Figure 4.14.

4.3.2 Envelope System Modeling

According to ASCE 7-98, building envelope is defined as cladding, roofing, exterior walls, glazing, door assembles, window assembles, skylight assembles, and other components enclosing the building.

In this study, the building has curtain walls composed of stone panels and window glass as shown in Figure 4.15. Stone panels and window glass are connected to steel

frame by steel grid strut and aluminum support. In glass panel, the aspect ratio is 1.2, and unit glass area is 30 sq ft and total glass area is 21,600 sq ft, while total cladding area of stone panel is 26,000 sq ft. Total window area is 46.2 % of the wall.

According to Building Construction Cost Data (BCCD) (1998), different openings require different type of glass. The three most common types are float, tempered, and insulating glasses. Most exterior windows are glazed with insulating glass. Entrance doors and window walls, where the glass is less than 18" from the floor, generally are glazed with tempered glass. Interior windows are glazed with float glass.

Laminated glass units are used in a variety of products to resist a wide range of loadings and environmental conditions. Included are architectural glazing products such as insulating glass, overhead glazing, and safety glazing. Laminated flat glass is a popular architectural glazing product. Laminated glass consists of two monolithic layers of glass joined with an elastomeric interlayer to form a unit as shown in Figure 4.16. The glass units are composed of two layers of glass connected by a thin interlayer of polyvinyl butyral.

Despite its increased use as a cladding material, its structural properties of glass were not well known before Behr, et al (1985, 1986) studied the behavior of laminated glass. Behr et al. (1985, 1986) showed when the interlayer is effective in transferring shear between the glass plates (e.g., at room temperature) the laminated glass unit behaves as if it were a monolithic glass plate. Minor and Reznik(1990) confirmed the conclusion by Behr, et al., (1985, 1986) through the destructive tests of a large number of laminated glass specimens. Test results reveal that failure strengths of annealed laminated glass specimens are equal to failure strengths of annealed monolithic glass specimens of the same nominal thickness at room temperature, and decrease to about 75% of monolithic glass strength at 170°F (77°C).

Based on the above information, in this study, with a thickness larger than a quarter of an inch, all glasses are assumed as laminated glass. In order to determine the optimal glass thickness based on minimum life-cycle cost, glasses are modeled according to thickness from 1/8 inch to 1.5 inches as shown in Table 4.11.

According to the Indiana Limestone Handbook (1997), the properties of cladding stone panels are as follows: The panel acts as a simple beam with uniformly distributed wind load if the panel is anchored at top and bottom only. The maximum allowable bending stress is 125 psi., representing a 8 to 1 safety factor using a modulus with a rupture value of 1000 psi. Panel is vertical, therefore panel weight causes no bending moments.

According to that handbook, the required minimum stone thickness for wind load can be obtained by using the equation

$$t = h\sqrt{0.006WL} \tag{4.2}$$

where WL is wind load (lb/sq ft), t is panel thickness (in.), and h is wind load span (ft.). From this equation, wind load can be calculated if t and h are given. If h is 5 ft, and t is 3 ft, the wind load that the panel can endure is 60.0 psf, while the wind load is 106.7 psf when h is 5 ft, and t is 4 ft. In order to avoid the panel failure in calculation of failure probability in the envelope, all panels are assumed as 4 inches.

4.3.3 Calculation of Initial Cost

Initial cost is composed of glass cost, cladding cost, and aluminum frame cost. In calculation of glass cost, the cost of glass is not in proportion to its thickness, so interpolation is sometimes necessary. Unit costs are based on BCCD (1998), and cladding cost is $23.5 per sqft for a limestone sugarcube finish. Aluminum frame is assumed at $7.80 per ft.

Table 4.11 shows these three costs for each envelope system, and Figure 4.17 shows the glass thickness and total initial cost. In order to calculate initial cost at each city, the initial cost must be multiplied by city cost index. The city cost index for Charleston is 77.6, and those of Boston and Los Angeles are 116.7 and 111.2, respectively.

4.3.4 Definition of Wind Hazard Level and Wind Hazard Level Probability

In envelope system, nine hazard levels according to mean recurrence interval (MRI) from 1 year to 500 years. Wind hazard level probability given the occurrence can be obtained according to Appendix B. Table 4.12 shows mean recurrence interval (MRI) and corresponding wind hazard level probability, and Table 4.13 shows the wind speeds corresponding to each wind hazard level at each city.

4.3.5 Analysis of Envelope System and Calculation of Failure Probability

In general, envelope failure due to wind load comes from window glass failure and failure of cladding. In this study, since cladding thickness is assumed to be 4 inches and maximum wind load is 106.7 psf. It is sufficient to resist wind load. Hence, only window glass failure is considered in calculating the failure probability of envelope.

Kareem and Stevens (1984) summarized the glass breakage mechanisms by surveying Houston's Central Business District (CBD) after hurricane Alicia. According to their reports, the glass breakage and cladding damage during hurricane Alicia could be attributed to one or more of the following mechanisms: (1) Wind pressure exceeding design values; wind speed exceeding design values, underestimation of surface pressure coefficients, internal building pressure, local wind channelization, and improper modeling of hurricane wind fields. (2) Missile impact from windborne debris: roof gravel, loose sheet metal, construction debris, broken glass, and rooftop appurtenances, (3) Performance of glass: strength degradation, load duration, stress induced by structural displacements, and improper installation.

Based on the above failure mechanisms, window glass failure is divided into two categories: wind pressure and windborne debris. Hence, the probability of envelope failure, P_f, can be estimated by

$$P_f = P_{wp} + P_{wm} - P_{(wp \cap wm)} \tag{4.3}$$

in which P_{wp} is envelope failure probability by wind pressure, and P_{wm} is envelope failure probability by windborne missile. If two events are statistically independent, envelope failure probability can be expressed by

$$P_f = P_{wp} + P_{wm} - P_{wp}P_{wm} \tag{4.4}$$

The procedure to obtain both probabilities is as follows:

4.3.5.1 Window Failure by Wind Pressure

Wind pressures for each wind hazard level are calculated from wind speed as shown in Table 4.15. ASCE 7-98 suggested wind pressure for flexible building as

$$p = qG_f C_p - q_i(GC_{pi}) \quad (lb/sq\ ft) \tag{4.5}$$

in which q is velocity pressure, G_f is gust effect factor, C_p is external pressure coefficient, q_i is velocity pressure at h and GC_{pi} is internal pressure coefficient. Since wind pressure to window glass is considered, the second term in equation is neglected. Gust effect factor, G_f, depends on wind speed and characteristics of building, and the value of G_f for S2 at Charleston wind speed with 50 years MRI, 0.85, is assumed for all envelope systems. From tables and figures in ASCE 7-98, 0.8 is used as C_p, and velocity pressure q is calculated by

$$q_z = 0.00256 K_z K_{zt} K_d V^2 I \quad (lb/sq\ ft) \tag{4.6}$$

in which K_d is the wind directionality factor, K_z is the velocity pressure exposure coefficient, and K_{zt} is the topographic factor defined as

$$K_{zt} = (1 + K_1 K_2 K_3)^2 \tag{4.7}$$

According to tables and figures in ASCE 7-98 K_d is 0.85, I is 1, and K_{zt} is neglected here. K_z depends on building height, the value at 119 ft, 0.73, is used. Therefore, wind pressure is calculated by the following equation:

$$\begin{aligned} p &= (0.00256)(0.85)(0.73)V^2(1)(0.85)(0.8) \\ &= 0.00108V^2 \end{aligned} \tag{4.8}$$

In general, glass design charts made by major glass manufacturers, e.g., PPG chart, are used in glass design. However, there are significant differences in the glass strength information provided in those charts due to different judgements and simplified assumptions.

In order to provide more rational means to restore continuity to the glass design process, Beason and Morgan (1984) proposed a glass failure prediction model. They adopted the suggestions by Weibull (1939) for this model. Weibull proposed that the probability of failure, P_f, for materials with variable strength can be expressed by

$$P_f = 1 - e^{-B} \tag{4.9}$$

in which B is a function which reflects the risk of failure. According to Beason and Morgan (1984), the strength of glass depends on the magnitude and duration of the surface tensile stresses in the plate, the surface area of the plate exposed to tensile stress, and the geometries and orientations of the surface flaws. Since all significant glass strength variations depend on these factors, the risk function must include each of these factors. For the application of failure-prediction model to typical rectangular glass plates exposed to constant uniform lateral loads, Beason and Morgan (1984) also suggested a simplified methodology as follows:

If the duration of lateral load is t_d, the tensile stresses induced in the plate remain constant for the same time duration, t_d. Therefore, the equivalent stress transformation can be accomplished as

$$\tilde{\sigma}_{60}(q,x,y) = \sigma(q,x,y)(\frac{t_d}{60})^{1/16} \tag{4.10}$$

in which $\tilde{\sigma}_{60}(q,x,y)$ is the equivalent stress, and $\sigma(q,x,y)$ is the actual stress. By using these equations, risk function is expressed as

$$B = k(\frac{t_d}{60})^{m/16} \int_0^a \int_0^b [c(x,y)\sigma_{\max}(q,x,y)]^m dydx \tag{4.11}$$

where a and b are the rectangular dimensions of the plate, k and m are parameters which reflect the character of glass plate surface flaws, and $\sigma_{max}(q,x,y)$ is the magnitude of the nontransformed maximum principal tensile stress.

The magnitude of a uniform lateral load applied to a rectangular glass plate can be nondimensionalized using the following equation:

$$\tilde{q} = \frac{q(ab)^2}{Eh^4} \tag{4.12}$$

in which $\tilde{q}$ is the nondimensionalized lateral load, q is the magnitude of the actual lateral load, a and b are the rectangular plate dimensions, h is the plate thickness, and E is the modulus of elasticity of glass.

The magnitude of the stresses in a rectangular plate can be nondimensionalized as

$$\hat{\sigma}(\hat{q},x,y) = \frac{\sigma(q,x,y)ab}{Eh^2} \tag{4.13}$$

in which $\hat{\sigma}(\hat{q},x,y)$ is the nondimensionalized stress, and $\sigma(q,x,y)$ is the actual stress. By combining Equation (4.11) and (4.12) with Equation (4.10), generalized risk functions can be obtained as:

$$B = k(ab)^{1-m}(Eh^2)^m(\frac{t_d}{60})^{m/16}(ab)^{-1}\int_0^a\int_0^b\left[c(x,y)\hat{\sigma}(\hat{q},x,y)\right]^m dydx \tag{4.14}$$

The risk function can be written as

$$B = k(ab)^{1-m}(Eh^2)^m(\frac{t_d}{60})^{m/16}R(m,\hat{q},\frac{a}{b}) \tag{4.15}$$

in which the risk factor $R(m,\hat{q},a/b)$ is defined as

$$R(m,\hat{q},\frac{a}{b}) = (ab)^{-1}\int_0^a\int_0^b\left[c(x,y)\hat{\sigma}(\hat{q},x,y)\right]^m dydx \tag{4.16}$$

As shown in the above equation, the magnitude of the risk factor is a function of m, the nondimensionalized load $\hat{q}$, and the plate aspect ratio, a/b.

For more simplification, Equation (4.31) can be written as

$$B = \kappa R(m, \hat{q}, \frac{a}{b}) \tag{4.17}$$

in which κ is defined as follows:

$$\kappa = k(ab)^{1-m}(Eh^2)^m(\frac{t_d}{60})^{m/16} \tag{4.18}$$

for the specific plate geometry, load duration, and set of surface-flaw parameters the magnitude of κ is constant.

Probability of failure of a typical rectangular glass plate in terms of the risk factor $R(m, \hat{q}, a/b)$ and κ is

$$P_f = 1 - e^{-\kappa R(m,\hat{q},a/b)} \tag{4.19}$$

For small probabilities of failure ($P_f \leq 0.10$), the following approximate relationship is sufficiently accurate:

$$P_f \approx \kappa R(m, \hat{q}, \frac{a}{b}) \tag{4.20}$$

In order to calculate failure probability by using Equation (4.20), the values of m and k are needed, but currently, it is not possible to directly measure the magnitude of m and k. Hence, values of m and k must be estimated from results of carefully controlled glass plate tests of failure. Table 4.15 shows surface-flaw parameters for different glass samples by Beason and Morgan (1984). In this study, surface-flaw parameters m and k are assumed for a 9 and 3.02×10^{-38}, respectively.

Beason and Morgan (1984) compared the failure loads for square glass plates, and concluded that the strength of old and in-service glass plates is significantly less than the strength of new glass plates. Two more facts are found from that comparison, i.e., the strength of old and in-service glass plates tends to be relatively independent of the type of exposure and the strength of new glass plate depend on the glass area.

In order to determine tensile stresses in glass plate, a finite element analysis is carried out using the ABAQUS program (Hibbitt, Karlsson and Sorensen, 1995). An element is modeled by using shell elements, i.e., S8R5 model with 10^6 psi as Young's

modulus and 0.22 as Poisson ratio. Figure 4.18 shows the model of a shell element used in FEM analysis and its boundary conditions. Figure 4.19 shows lateral pressure and central deflection by the result of FEM analysis for rectangular glass plate 96" × 60" × 0.225". Cumulative probability of failure and lateral load for glass plates is shown in Figure 4.20. Figure 4.21 shows wind pressure and failure pressure and failure probability for each structure.

By using the failure prediction model, failure probability is obtained according to wind pressure at each wind hazard level as shown in Table 4.14. Table 4.16 shows failure probability of window glass by wind force for each wind hazard level at Charleston. This failure probability is used in the calculation of expected failure cost.

4.3.5.2 Availability of Roof Gravel

According to Minor (1974), roof gravel is the principal cause, among other potential missiles, e.g., facia material, sheet metal panels, and decorative exterior trim, of damage to glass windows in multistory buildings.

Minor (1974) examined the existence of gravel-surface roofs in areas adjacent to structures which have experienced window breakage during windstorms and to typical urban and suburban multistory buildings which, as yet, have not experienced window breakage during windstorms. As for sample structures, buildings in Lubbock were used served for the first analysis, and buildings in San Antonio, Texas, are included for the second analysis. In the first survey, a total of 54 buildings located within tow blocks of the Great Plains Life (GPL) building were found to have gravel-surfaced roofs, and loose gravel was found to exist on each of them. The field evaluation conducted in Lubbock revealed unexpectedly large amounts of loose gravel on roofs located in close proximity to glass walls of multistory buildings. The second survey result showed that twenty-seven buildings in the area possessed gravel roofs, and the character of gravel on these roofs was found to be very similar to those on the roofs in downtown Lubbock.

4.3.5.3 Loading Zones for Cladding on Multistory Buildings

In regrads to the cladding failure in urban areas, Minor et al. (1978) suggested that a given multistory building may be divided into three loading zones as shown in Figure 4.22. The lowest floors of a multistory building, e.g., the first to third floors, experience turbulent winds that have been "channeled" along streets. Cladding on these floors is also susceptible to impact from windborne debris that originates in the environment near the ground. The substance of this debris can include roof gravel, sheet metal, architectural treatments, roofing material, and broken glass. From about the third floor to an elevation equal to the highest adjacent rooftop, a building may be susceptible to impacts from windborne roof gravel and pieces of broken glass. Such impact will occur at windspeeds associated with code specified pressure. Above an elevation equal to the highest adjacent rooftop, a building may receive occasional missile impacts or experience impacts from broken windows on floors above, but the cladding will experience essentially pure wind pressures.

Table 4.17 summarizes the general requirements for cladding design for the three zones defined above. In each zone there are design requirements for wind and for missile impact. In zone 1 missile impact requirements will probably govern, as impacts from relatively large missiles can be expected in urban environments when the design windspeed occurs. Zone 2 has proven to be the most critical area for cladding as missile impacts are known to occur, and channelization and wake effects may produce large pressure excursions. Missile impacts in this zone are mostly roof gravel; therefore, design requirements are based upon a common roof gravel size that is capable of braking window glass. Zone 3 contains no missile impact requirement and wind pressures are calculated through established methodologies specified in codes and standards.

In Zone 1 missile sizes tend to be large and undefined (Garbage cans, pieces of roofing material, sheet metal and roof gravel), and in Zone 2, missiles are smaller and more easily defined. Zone 3 has no missile design requirement.

Since the model building is assumed to be located downtown in this study, Zone 3 is not considered, but only Zone 1 and Zone 2 are considered.

4.3.5.4 Missile Size

The results of the analysis of variance strongly implicate missile size as being the primary factor involved in window glass breakage due to missile impact. (Minor and Beason 1976). Therefore, an assessment of missile characteristics is important to analyze window damage by missile. The best way to determine missile size, is sampling loose gravel on the roofs in typical urban environments. Minor (1974) took fifty-four samples and twenty-seven samples in Lubbock and San Antonio, respectively. Figure 4.23 shows the result of sampling. From the statistical evaluations of roof gravel samples, two facts were found. There is a large variation between samples taken from individual roofs, both in Lubbock and in San Antonio and a high degree of similarity between the population of roof gravel from both cities. From these facts, two samples are combined for the average of missile characteristics. The statistical mean rock size for the combined sample was 0.61 gm. The large rock that represents an extreme upper limit of actual roof gravel rock sizes, was determined to be 5.55 gm. The first one can be used as average gravel size for Zone 2, and the last one can be used for an average missile size for Zone 1.

4.3.5.5 Injection Mechanism and Wind Propelled Missiles

There are three typical injection mechanisms for becoming airborne during windstorms (General Electric Company, 1970), i.e., explosive injection, aerodynamic injection, and ramp injection as shown in Figure 4.24. According to Minor (1974), explosive injection, in the case of roof gravel, involves failure of a roof structure in a manner that propels debris upward into the airstream. Wind damage experience indicates that this is a common type of injection mechanism. Aerodynamic injection related to objects have an airfoil-like configuration which produces lift in a horizontally flowing airstream. This mechanism is not common in the roof gravel situation as individual rocks tend to be more of a spherical shape than a flattened shape. Ramp injection involves

situations where an object is accelerated horizontally and is then deflected upward by an obstruction to the flow of air. Deflection can be achieved if the object encounters a ramp or if it bounces off of anchored objects. This injection mechanism is also a relatively common phenomenon with respect to gravel in windstorms.

Based on the above mechanism, two wind velocities need be determined, the velocity to accelerate, lift, and propel gravel, and that to break a window. The basic equation to determine the vertical wind velocity required to sustain a rock in the windstream is

$$W = \frac{1}{2}\rho V_v^2 C_D A \tag{4.21}$$

where W is the weight of the rock, ρ is the mass density of air, V_v is the vertical wind component, C_D is the appropriate drag coefficient, and A is the projected area of the rock. The vertical wind velocity to lift the gravel is as follows:

$$V_v = \left[\frac{2W}{\rho C_D A}\right]^{1/2} \tag{4.22}$$

If a rock is spherical and has a specific gravity of 2.7, the vertical wind velocity can be calculated. In this case, ρ is 2.376×10^{-3} slug/ft^3 for air. Table 4.18 shows the vertical velocity to sustain rocks of the sizes shown as airborne objects. This results show that nominal vertical wind velocities can sustain roof gravel as airborne objects.

In order to find out the velocity that can break window after the gravel becomes airborne and is sustained in an airborne state, the relationship between wind speed and airborne speed is needed. According to Minor (1974), governing equation for a dynamic relationship can be expressed as follows:

$$\frac{1}{2}\rho V^2 C_D A = \frac{W}{g}\ddot{x} \tag{4.23}$$

where, V is velocity of wind acting on the spherical rock, W is the weight of the spherical rock, x, $\dot{x}$, $\ddot{x}$ are displacement, velocity, and acceleration of the spherical rock, ρ is the mass density of air, C_D is a drag coefficient for a small sphere in an airstream and A is the

projected area of the spherical rock. Substituting $V = V_h - \dot{x}$ into equation (4.23), that equation becomes a differential equation as follows:

$$\frac{2W}{\rho C_D A}\ddot{x} - \dot{x}^2 + 2V_h\dot{x} = V_h^2 \tag{4.24}$$

The solution of this differential equation can be expressed in terms of velocity or displacement as follows:

$$\dot{x} = \frac{V_h^2}{V_h + \dfrac{2W}{\rho C_D A g t}} \tag{4.25}$$

$$x = V_h t + \frac{2W}{\rho C_D A g t}\ln\left[\frac{\dfrac{2W}{\rho C_D A g t}}{\dfrac{2W}{\rho C_D A g t} + V_h t}\right] \tag{4.26}$$

$$1 + \frac{2W}{\rho C_D A g t}x = \frac{V_h}{V_h - \dot{x}} - \ln\left[\frac{V_h}{V_h - \dot{x}}\right] \tag{4.27}$$

By using the specific gravity of gravel of 2.7, and C_D of 0.4, and the mass density of air as 2.376×10^{-3} slug/ft^3, the curves can be obtained for the velocity attained and for the distance traveled as function of time. Figure 4.25 shows velocity and distance traveled. Table 4.19 shows the gravel velocity for each limit state and each city when distance is 100 feet.

4.3.5.6 Resistance of Glass to Impact

In order to complete the calculation of mean damage function, the data on the resistance of glass to small missile impact are required. Table 4.20 shows the resistance of glass to the impact of 0.0122 lbf (=5.55 gm) missile according to Minor et al. (1978), Minor and Beason (1974) and by Harris (1978). In the case of highly tempered glass, additional thickness does not provide additional small missile impact resistance. Hence, this data can not be used. In case of annealed glass, by using linear regression, mean

minimum breaking threshold velocity (MMBT) corresponding to glass thickness can be obtained.

However, the glass used in this study is laminated glass. Since there is no data provide the glass thickness and mean minimum breaking threshold velocity (MMBT) or mean minimum damage threshold velocity (MMDT), the relationship between MMBT of annealed glass and MMBT of laminated glass is needed. Pantelides et al. (1993) provided missiles impact test results after a full-scale experimental investigation. They suggested the MMBT and MMDT for laminated glass, but only in case of 2.03 g as missile size with thickness as 3/16 in. (0.1875 in.). Hence a conversion factor from annealed glass to laminated glass can be obtained by comparing both velocities when missile size is 2.03g. Table 4.21 shows MMBT and MMDT for laminated glass at each city.

According to Minor et al. (1978), previous experience with large size panels (Minor, 1974) indicated that the variation in specimen surface area had little effect on the mean minimum breaking velocity, apparently because of the local character of missile-induced failures. Hence the data in Table 4.21 can be used without conversion for adjusted glass area.

4.3.5.7 Glass Failure Probability

Glass failure probability (P_g) consists of failure probability by wind pressure and by windborne missile as follows:

$$P_g = P_f(wind\ pressrue \bigcup windborne\ missile) \tag{4.28}$$

Let P_f^p be the probability of failure by wind pressure and P_f^m be probability of failure by windborne missile, then Equation (4.28) becomes

$$P_g = P_f^p + P_f^m - P_f^p \cdot P_f^m \tag{4.29}$$

in which, P_f^p can be obtained by using the glass failure prediction model proposed by Beason and Morgan (1984), and an independence assumption is used. Probability of failure by windborne missile, P_f^m, depends on windborne missile, e.g., missile

availability, its velocity, direction of missile, missile size, and loading zone. P_f^m, in this study, is considered as

$$P_f^m = P_m \times P_a \tag{4.30}$$

where P_m is the probability of failure when the missile strikes the envelope with a given wind speed and P_a is probability of missile availability. P_m can be obtained by using the First Order Reliability Method (FORM) with windborne missile speed and resistance speed of glass, both assumed to have normal distributions. The probability of missile availability, P_a, is a function of missile amount and existence ratio, the possibility of a missile flying, and the ratio of the missile striking glass area to the total area. Hence, the probability of missile availability, P_a, is expressed as

$$P_a = f(F_a, F_e, F_f, F_r, F_s, F_t) \tag{4.31}$$

where F_a is the missile amount ratio factor, F_e is the missile existence ratio factor, F_f is the missile flying factor, F_r is the missile arriving ratio factor, F_s is the missile size factor, and F_t is the velocity threshold factor. The missile flying factor, F_f, determines whether wind can lift and sustain the missile or not. Therefore if wind speed is less than the velocities in Table 4.19, this factor will be zero, otherwise it will be one. The damage ratio factor, F_r, is the ratio of missile arrived area to the total area. It depends on wind speed. The missile size factor, F_s, depends on the zone mentioned in the previous section. If Zone 1 is considered, the velocity of a large missile size (5.55g) is used, and the case of mean missile size (0.61g) is used if Zone 2 is considered. The velocity threshold factor, F_t, depends on the failure status. In case of glass breakage, mean minimum breaking threshold velocity (MMBT) is used, but if only glass damage is considered, mean minimum damage threshold velocity (MMDT) is used.

4.3.6 Cost Function and Calculation of Failure Cost

Since there is a very small probability of injury and death due to the envelope failure, cost of injury and death is neglected. Therefore the cost function can be expressed by

$$C = C^{dam} + C^{con} + C^{rel} + C^{eco} + C^{env} \tag{4.32}$$

in which C^{dam} is the damage/repair cost function, C^{con} is the loss of contents, C^{rel} is the relocation cost, C^{eco} is the economic loss caused by a structural damage and C^{env} is the cost of damage of envelope system. The equation of each cost function and basic costs are summarized in Table 4.22, where all basic costs except damage cost are the same as in previous Chapter. Total damage costs are determined as shown in Table 4.23. Historical index and city indexes are used to determine total damage cost.

4.3.7 Total Expected Life-Cycle Cost and Optimal Glass Thickness

Total expected life-cycle cost for envelope system can be calculated using glass damage probability and cost functions,. When the lifetime is 50 years, the discount rate (λ) is 0.05, and the missile existence factor, F_e, is assumed to be 0.3, the total expected life-cycle cost at Charleston, Boston, and Los Angeles are shown in Figure 4.26 to 4.28. By using a numerical polynomial fit, the optimal glass thickness for each city can be obtained. They are 0.806 in, 0.687 in, and 0.528 in, for Charleston, Boston, and Los Angeles, respectively. These results can be compared with 5/16"(0.313"), 1/4" (0.250") and 3/16" (0.188"), common used glass thickness based on PPG glass design chart for Charleston, Boston and Los Angeles, respectively. Also, 1/2" glass is used in John Hancock building in Boston after window failure and two 1/4 " glasses with 1/2" air space in Chicago.

4.3.8 Sensitivity Analysis

A sensitivity analysis of the optimal thickness is carried out to change in design lifetime, discount rate, and possibility of missile availability and amount. The results are shown in Figures 4.29 to 4.32. It is seen that the optimal glass thickness depends on discount rate moderately and on design life change, while it is very sensitive to the factors of missile availability and amount. For example, at Charleston, the optimal thickness increases from 0.278 in for F_a (missile amount factor) = 10 % to 1.138 in for F_a

= 100 %. The same is true at in Boston and Los Angeles, respectively. As for design lifetime, at Charleston, the optimal thickness increases from 0.515 in in for T = 10 years to 0.830 in for T = 100 years, from 0.254 in to 0.707 in at Boston, from 0.240 in to 0.546 in at and Los Angeles. Tables 4.24 to 4.27 show the results of analysis of sensitivity to lifetime, discount rate, and missile amount and existence factor.

4.3.9 Summary

The proposed methodology is applied to design of a building envelope system under wind load. Twelve envelope systems of different glass are studied. Currently available glass failure prediction model is adopted and a FEM analysis is carried out to evaluate the failure probability of each system by wind pressure. Failure probability of envelope systems by windborne missiles is evaluated as a function of glass type, missile size, loading zone, injection mechanism, vertical velocity to sustain missile, mean minimum breaking threshold velocity (MMBT) and minimum damage threshold velocity (MMDT).

The following conclusions can be drawn from the results:

1. The optimal glass thickness under wind load is found to be 0.794" at Charleston, 0.687" at Boston and 0.528" at Los Angeles (Seattle). These optimal glass thicknesses are larger than that based on current PPG glass chart and 1/2" used in buildings at Boston and Chicago.
2. The building envelope failure probability is primarily due to the windborne missiles. Wind pressure contribution is very small.
3. The optimal glass thickness depends moderately on discount rate for long life span and on design life change. Optimal glass thickness is more sensitive to the availability and amount of wind borne missiles. These two factors become very important in the design decision on glass thickness. These findings are in agreement with the conclusions by Reed (1970) and by Minor (1974) which indicates that the building envelope damage was largely due to windborne missiles even when wind speeds are low.

Table 4.1 Basic wind speed corresponding to different Mean Recurrence Interval (MRI).

Cities		Charleston		Boston		Los Angeles & Seattle	
V* (mph)		130		110		85	
MRI	Annual Pb of Exc.	Conversion Factor	V (mph)	Conversion Factor	V (mph)	Conversion Factor	V (mph)
500	0.002	1.23	159.9	1.23	135.3	1.23	104.6
200	0.005	1.14	148.2	1.14	125.4	1.14	96.9
100	0.01	1.07	139.1	1.07	117.7	1.07	91.0
50	0.02	1.00	130.0	1.00	110.0	1.00	85.0
25	0.04	0.88	114.4	0.88	96.8	0.93	79.1
10	0.1	0.74	96.2	0.74	81.4	0.84	71.4
5	0.2	0.66	85.8	0.66	72.6	0.78	66.3

V* is 3 second gust wind speed at 33 ft(10m) above ground for exposure category C.

Table 4.2 Drift ratio (%) and annual probability of exceedance.

City	Annual Prob. Of Exceedance	S1	S2	S3	S4	S5	S6	S7	S8	S9	S10
Charleston	0.002	1.454	0.709	0.437	0.357	0.275	0.225	0.197	0.171	0.151	0.136
	0.005	1.222	0.600	0.371	0.304	0.234	0.192	0.168	0.146	0.129	0.116
	0.01	1.058	0.522	0.324	0.265	0.205	0.168	0.147	0.128	0.113	0.102
	0.02	0.909	0.450	0.281	0.230	0.178	0.146	0.128	0.112	0.099	0.089
	0.04	0.684	0.342	0.214	0.176	0.137	0.112	0.099	0.086	0.076	0.069
	0.1	0.468	0.237	0.150	0.123	0.096	0.079	0.069	0.060	0.053	0.048
	0.2	0.366	0.187	0.118	0.097	0.076	0.063	0.055	0.048	0.042	0.038
Boston	0.002	0.994	0.491	0.305	0.250	0.194	0.159	0.139	0.121	0.107	0.096
	0.005	0.838	0.417	0.260	0.213	0.165	0.136	0.119	0.104	0.092	0.083
	0.01	0.728	0.364	0.228	0.187	0.145	0.119	0.104	0.091	0.080	0.073
	0.02	0.627	0.315	0.198	0.162	0.126	0.104	0.091	0.079	0.070	0.063
	0.04	0.474	0.240	0.152	0.125	0.097	0.080	0.070	0.061	0.054	0.049
	0.1	0.327	0.167	0.106	0.088	0.068	0.056	0.049	0.043	0.038	0.034
	0.2	0.257	0.132	0.084	0.069	0.054	0.045	0.039	0.034	0.030	0.027
Los Angeles & Seattle	0.002	0.561	0.283	0.178	0.146	0.114	0.094	0.082	0.072	0.063	0.057
	0.005	0.475	0.241	0.152	0.125	0.097	0.080	0.070	0.061	0.054	0.049
	0.01	0.415	0.211	0.133	0.110	0.085	0.070	0.062	0.054	0.048	0.043
	0.02	0.359	0.183	0.116	0.096	0.074	0.061	0.054	0.047	0.042	0.038
	0.04	0.307	0.158	0.100	0.082	0.064	0.053	0.047	0.041	0.036	0.032
	0.1	0.248	0.128	0.081	0.067	0.052	0.043	0.038	0.033	0.029	0.026
	0.2	0.212	0.110	0.070	0.058	0.045	0.037	0.033	0.029	0.025	0.023

Table 4.3 Probability of limit state given wind storm occurrence at Charleston.

Structure	I	II	III	IV	V	VI	VII
S1	0.7645142	0.1416225	0.0544074	0.0380753	0.0013803	0.0000004	0.0000000
S2	0.8769128	0.1103748	0.0107318	0.0019806	0.0000000	0.0000000	0.0000000
S3	0.9498106	0.0496981	0.0004900	0.0000013	0.0000000	0.0000000	0.0000000
S4	0.9706936	0.0292822	0.0000242	0.0000000	0.0000000	0.0000000	0.0000000
S5	0.9880774	0.0119226	0.0000000	0.0000000	0.0000000	0.0000000	0.0000000
S6	0.9956929	0.0043071	0.0000000	0.0000000	0.0000000	0.0000000	0.0000000
S7	0.9984365	0.0015635	0.0000000	0.0000000	0.0000000	0.0000000	0.0000000
S8	0.9996738	0.0003262	0.0000000	0.0000000	0.0000000	0.0000000	0.0000000
S9	0.9999462	0.0000538	0.0000000	0.0000000	0.0000000	0.0000000	0.0000000
S10	0.9999948	0.0000052	0.0000000	0.0000000	0.0000000	0.0000000	0.0000000

Table 4.4 Probability of limit state given wind storm occurrence at Boston.

Structure	I	II	III	IV	V	VI	VII
S1	0.8201437	0.1433863	0.0239348	0.0125277	0.0000074	0.0000000	0.0000000
S2	0.9327318	0.0657304	0.0015192	0.0000186	0.0000000	0.0000000	0.0000000
S3	0.9820998	0.0178997	0.0000005	0.0000000	0.0000000	0.0000000	0.0000000
S4	0.9923011	0.0076989	0.0000000	0.0000000	0.0000000	0.0000000	0.0000000
S5	0.9985969	0.0014031	0.0000000	0.0000000	0.0000000	0.0000000	0.0000000
S6	0.9998716	0.0001284	0.0000000	0.0000000	0.0000000	0.0000000	0.0000000
S7	0.9999867	0.0000133	0.0000000	0.0000000	0.0000000	0.0000000	0.0000000
S8	0.9999995	0.0000005	0.0000000	0.0000000	0.0000000	0.0000000	0.0000000
S9	1.0000000	0.0000000	0.0000000	0.0000000	0.0000000	0.0000000	0.0000000
S10	1.0000000	0.0000000	0.0000000	0.0000000	0.0000000	0.0000000	0.0000000

Table 4.5 Probability of limit state given wind storm occurrence at Los Angeles and Seattle.

Structure	I	II	III	IV	V	VI	VII
S1	0.7908973	0.2052310	0.0035922	0.0002795	0.0000000	0.0000000	0.0000000
S2	0.9866154	0.0133829	0.0000017	0.0000000	0.0000000	0.0000000	0.0000000
S3	0.9993258	0.0006742	0.0000000	0.0000000	0.0000000	0.0000000	0.0000000
S4	0.9998905	0.0001095	0.0000000	0.0000000	0.0000000	0.0000000	0.0000000
S5	0.9999979	0.0000021	0.0000000	0.0000000	0.0000000	0.0000000	0.0000000
S6	1.0000000	0.0000000	0.0000000	0.0000000	0.0000000	0.0000000	0.0000000
S7	1.0000000	0.0000000	0.0000000	0.0000000	0.0000000	0.0000000	0.0000000
S8	1.0000000	0.0000000	0.0000000	0.0000000	0.0000000	0.0000000	0.0000000
S9	1.0000000	0.0000000	0.0000000	0.0000000	0.0000000	0.0000000	0.0000000
S10	1.0000000	0.0000000	0.0000000	0.0000000	0.0000000	0.0000000	0.0000000

Table 4.6 Total expected life-cycle cost, expected damage cost, and initial cost at Charleston. (w/) and (w/o) denote with and without consideration of costs of injury and death.

Structure	Sy	E[C(t)] (w/)	E[C(t)](w/o)	IC	EFC (w/)	EFC (w/o)
S1	0.033	5,945,961	5,891,340	1,182,217	4,763,744	4,709,123
S2	0.061	1,993,919	1,990,055	1,247,258	746,662	742,798
S3	0.093	1,503,213	1,502,704	1,321,040	182,173	181,664
S4	0.115	1,490,910	1,490,635	1,388,844	102,066	101,792
S5	0.140	1,492,494	1,492,383	1,451,130	41,364	41,253
S6	0.169	1,531,177	1,531,136	1,516,234	14,943	14,903
S7	0.188	1,587,728	1,587,714	1,582,304	5,424	5,410
S8	0.213	1,648,644	1,648,641	1,647,512	1,132	1,129
S9	0.230	1,723,995	1,723,994	1,723,808	187	186
S10	0.245	1,798,803	1,798,803	1,798,785	18	18

Table 4.7 Total expected life-cycle cost, expected damage cost, and initial cost at Boston. (w/) and (w/o) denote with and without consideration of costs of injury and death.

Structure	Sy	E[C(t)] (w/)	E[C(t)](w/o)	IC	EFC (w/)	EFC (w/o)
S1	0.033	4,678,421	4,663,152	1,777,895	2,900,525	2,885,256
S2	0.061	2,265,425	2,264,655	1,875,708	389,716	388,947
S3	0.093	2,079,988	2,079,822	1,986,667	93,321	93,155
S4	0.115	2,128,767	2,128,696	2,088,635	40,132	40,061
S5	0.140	2,189,619	2,189,606	2,182,306	7,314	7,301
S6	0.169	2,280,882	2,280,881	2,280,213	669	668
S7	0.188	2,379,642	2,379,642	2,379,573	70	69
S8	0.213	2,477,640	2,477,640	2,477,638	2	2
S9	0.230	2,592,377	2,592,377	2,592,377	0	0
S10	0.245	2,705,132	2,705,132	2,705,132	0	0

Table 4.8 Total expected life-cycle cost, expected damage cost, and initial cost at Los Angeles and Seattle. (w/) and (w/o) denote with and without consideration of costs of injury and death.

Structure	Sy	E[C(t)] (w/)	E[C(t)](w/o)	IC	EFC (w/)	EFC (w/o)
S1	0.033	2,845,540	2,843,039	1,694,104	1,151,436	1,148,935
S2	0.061	1,853,836	1,853,711	1,787,307	66,528	66,404
S3	0.093	1,896,386	1,896,379	1,893,037	3,349	3,343
S4	0.115	1,990,742	1,990,741	1,990,199	544	543
S5	0.140	2,079,465	2,079,465	2,079,455	10	10
S6	0.169	2,172,748	2,172,748	2,172,747	0	0
S7	0.188	2,267,425	2,267,425	2,267,425	0	0
S8	0.213	2,360,868	2,360,868	2,360,868	0	0
S9	0.230	2,470,200	2,470,200	2,470,200	0	0
S10	0.245	2,577,641	2,577,641	2,577,641	0	0

Table 4.9 Optimal design system yield force coefficient for wind load.

Case	Optimal Value	Charleston	Boston	Los Angeles
With injury and Death	S_y	0.121	0.106	0.073
	Cost ($)	1,489,000	2,108,000	1,788,000
Without injury and Death	S_y	0.121	0.106	0.073
	Cost ($)	1,489,000	2,108,000	1,788,000

Table 4.10 Envelope system glass thickness.

Envelope System	Thickness (in.)	
E1	1/8	0.125
E2	5/32	0.15625
E3	3/16	0.1875
E4	1/4	0.25
E5	5/16	0.3125
E6	3/8	0.375
E7	1/2	0.5
E8	5/8	0.625
E9	3/4	0.75
E10	1	1
E11	1-1/4	1.25
E12	1-1/2	1.5

Table 4.11 Initial cost of envelope system.

Envelope System	Thickness (in.)	Unit Glass Cost	Glass Cost	Frame Cost	Cladding Cost	Total Initial Cost
E1	1/8"	7.45	160,920	62,057	611,000	833,977
E2	5/32"	7.80	168,480	62,057	611,000	841,537
E3	3/16"	8.15	176,040	62,057	611,000	849,097
E4	1/4"	12.64	273,000	62,057	611,000	946,057
E5	5/16"	16.64	359,328	62,057	611,000	1,032,384
E6	3/8"	20.63	445,655	62,057	611,000	1,118,712
E7	1/2"	29.10	628,639	62,057	611,000	1,301,696
E8	5/8"	37.58	811,623	62,057	611,000	1,484,680
E9	3/4"	48.51	1,047,731	62,057	611,000	1,720,788
E10	1"	69.00	1,490,435	62,057	611,000	2,163,491
E11	1-1/4"	91.21	1,970,030	62,057	611,000	2,643,087
E12	1-1/2"	115.12	2,486,517	62,057	611,000	3,159,574

Table 4.12 Nine wind hazard levels according to mean recurrence interval (MRI) and wind hazard level probability.

Wind hazard Level	MRI (T)	Wind Hazard Level Probability
I	$T < 1$	0.1945349
II	$1 < T < 5$	0.1823216
III	$5 < T < 10$	0.1177830
IV	$10 < T < 25$	0.0645385
V	$25 < T < 50$	0.0206193
VI	$50 < T < 100$	0.0101524
VII	$100 < T < 200$	0.0050378
VIII	$200 < T < 500$	0.0030105
IX	$500 < T$	0.0020020

Table 4.13 Wind speeds for each wind hazard level at each city.

Wind hazard Level	Wind Speed (mph)		
	Charleston	Boston	Los Angeles
I	31.2	27.5	25.9
II	74.1	63.8	59.1
III	91.0	77.0	68.9
IV	105.3	89.1	75.2
V	122.2	103.4	82.0
VI	134.6	113.9	88.0
VII	143.7	121.6	93.9
VIII	154.1	130.4	100.7
IX	164.5	139.2	107.5

Table 4.14 Wind pressures for wind hazard level at each city.

Wind Hazard Level	Wind Pressure (psf)		
	Charleston	Boston	Los Angeles
I	1.1	0.8	0.7
II	5.9	4.4	3.8
III	8.9	6.4	5.1
IV	12.0	8.6	6.1
V	16.1	11.5	7.3
VI	19.6	14.0	8.4
VII	22.3	16.0	9.5
VIII	25.6	18.4	11.0
IX	29.2	20.9	12.5

Table 4.15 Surface-flaw parameters for different glass samples by Beason and Morgan (1984).

Source of Glass	Size (in×in×in)	Mean(psf)	St.d.(psf)	Parameters
GPL(20yrs)	28.5×60.5×0.2188	79	18.4	m =6, k =4.40×10^{-25}
	28.5×28.5×0.2188	168	37.5	
Dallas(20yrs)	16.25×19.75×0.125	229	61.9	m =6, k =2.09×10^{-25}
Anton(25yrs)	14×36.25×0.25	134.3	33.7	m =5, k=9.67×10^{-22}
PPG(new)	16.25×19.75×0.125	427.7	77.4	m =9, k=3.02×10^{-38}

Table 4.16 Failure probability of window glass by wind pressure at Charleston.

	I	II	III	IV	V	VI	VII	VIII	IX
E1	0.00000	0.00000	0.00000	0.000004	0.000029	0.000114	0.000283	0.000721	0.001737
E2	0.00000	0.00000	0.00000	0.000000	0.000003	0.000012	0.000030	0.000076	0.000191
E3	0.00000	0.00000	0.00000	0.000000	0.000001	0.000003	0.000006	0.000015	0.000035
E4	0.00000	0.00000	0.00000	0.000000	0.000000	0.000001	0.000001	0.000003	0.000006
E5	0.00000	0.00000	0.00000	0.000000	0.000000	0.000000	0.000000	0.000001	0.000001
E6	0.00000	0.00000	0.00000	0.000000	0.000000	0.000000	0.000000	0.000000	0.000000
E7	0.00000	0.00000	0.00000	0.000000	0.000000	0.000000	0.000000	0.000000	0.000000
E8	0.00000	0.00000	0.00000	0.000000	0.000000	0.000000	0.000000	0.000000	0.000000
E9	0.00000	0.00000	0.00000	0.000000	0.000000	0.000000	0.000000	0.000000	0.000000
E10	0.00000	0.00000	0.00000	0.000000	0.000000	0.000000	0.000000	0.000000	0.000000
E11	0.00000	0.00000	0.00000	0.000000	0.000000	0.000000	0.000000	0.000000	0.000000
E12	0.00000	0.00000	0.00000	0.000000	0.000000	0.000000	0.000000	0.000000	0.000000

Table 4.17 Design requirements of cladding in urban area (Minor et al. 1978).

Zone	Description	Wind effects	Missile Impact
1	Lowest three floors	Wind pressures brought about through channelization	Environmental debris near street level: roofing material, broken glass, architectural treatments (awnings, facia), sheet metal
2	Next three floors up to elevation of tallest adjacent building	Wind pressure brought about through channelization and wake effect	Debris blow-off from adjacent roofs: principally roof gravel but including roofing material.
3	Above elevation of tallest adjacent building	Wind pressures derived from modern code or standard specified procedures (power-law relationships between windspeed and elevation)	None

Table 4.18 Vertical wind velocities required to sustain spherical roof gravel as airborne objects (Minor, 1974).

Roof Gravel	Weight	V_v
Mean Roof Gravel	0.61 gm	77.4 fts (52 mph)
Large Roof Gravel	5.55 gm	108.1 fps (74 mph)

Table 4.19 Missile velocities corresponding to wind speed for each limit state and each city.

Wind Hazard Level		I	II	III	IV	V	VI	VII	VIII	IX
Wind Speed (mph)	Charleston	31.2	74.1	91.0	105.3	122.2	134.6	143.7	154.1	164.5
	Boston	27.5	63.8	77.0	89.1	103.4	113.9	121.6	130.4	139.2
	Los Angeles	25.9	59.1	68.9	75.2	82.0	88.0	93.9	100.7	107.5
Missile Speed (fps) (0.61gm)	Charleston	18.6	44.2	54.3	62.8	72.9	80.3	85.7	91.9	98.1
	Boston	16.4	38.0	45.9	53.1	61.6	67.9	72.6	77.7	83.0
	Los Angeles	15.4	35.2	41.1	44.8	48.9	52.5	56.0	60.0	64.1
Missile Speed (fps) (5.55gm)	Charleston	14.9	35.3	43.4	50.2	58.2	64.1	68.4	73.4	78.4
	Boston	13.1	30.4	36.7	42.5	49.3	54.3	58.0	62.1	66.3
	Los Angeles	12.3	28.2	32.8	35.8	39.1	41.9	44.8	48.0	51.2

Table 4.20 Resistance of glass to impact from 0.0122 lbf missile (Minor et al., 1978).

Glass Thickness	Annealed Glass		Highly Tempered Glass	
	MMBT	COV	MMBT	COV
3/16	33.4	7.1	66.5	6.1
1/4	31.3	5.1	-	-
5/16	28.3	4.4	64.4	8.3
3/8	35.8	11.2	62.0	12.0
1/2	38.7	7.0	50.0	9.8
3/4	56.8	15.6	54.6	19.7

Table 4.21 Mean minimum breaking threshold velocity (MMBT) and mean minimum damage threshold velocity (MMDT) for laminated glass.

System	Glass Thickness	MMBT		MMDT	
		0.61g	5.55g	0.61g	5.55g
E1	0.125	53.61	33.51	29.49	18.43
E2	0.1563	56.68	35.42	31.17	19.48
E3	0.1875	59.74	37.34	32.86	20.53
E4	0.25	65.86	41.16	36.22	22.64
E5	0.3125	71.99	44.99	39.59	24.74
E6	0.375	78.11	48.82	42.96	26.85
E7	0.5	90.36	56.47	49.70	31.06
E8	0.625	102.60	64.13	56.43	35.27
E9	0.75	114.85	71.78	63.17	39.48
E10	1	139.35	87.09	76.64	47.90
E11	1.25	163.84	102.40	90.11	56.32
E12	1.5	188.34	117.71	103.59	64.74

Table 4.22 Cost functions due to wind damage.

Function	Cost	Equations	Basic Cost
C^{dam}	Damage/ Repair	Replacement Cost × Floor Area × Glass Breakage Probability	\$39.8/sqft for replacement cost
C^{con}	Loss of contents	Unit Contents Cost × Floor Area × Glass Breakage Probability	\$28.9/sqft for unit contents cost
C^{rel}	Relocation	Relocation Cost × Gross Leasable Area × Loss of Time	\$1.5/month/sqft
C^{eco}	Economic Loss	Rental Cost(C^{ren}) + Income Cost(C^{inc})	
C^{ren}	Rental	Rental Rate × Gross Leasable Area × Loss of Function	\$0.6/month/sqft
C^{inc}	Income	Rental Rate × Gross Leasable Area × Out of Business	\$100/year/sqft
C^{env}	Envelope	Initial Cost × Glass Damage Probability	

Table 4.23 Total damage cost for each cost function with adjustment for location.

Cost Function	C(dam)	C(con)	C(rel)	C(ren)	C(inc)
Charleston	4,314,193	3,136,254	162,781	66,198	10,852,088
Boston	6,487,969	4,716,505	244,801	99,553	16,320,087
Los Angeles	6,182,195	4,494,219	233,264	94,861	15,550,931

Table 4.24 Sensitivity of optimal design glass thickness (inch) to lifetime.

t	5	10	20	50	100
Charleston	-	0.520	0.685	0.794	0.816
Boston	0.254	0.437	0.576	0.687	0.707
LA & Seattle	0.240	0.343	0.425	0.528	0.546

Table 4.25 Sensitivity of optimal design glass thickness (inch) to discount rate.

λ	0.03	0.05	0.07
Charleston	0.885	0.794	0.713
Boston	0.772	0.687	0.610
LA & Seattle	0.596	0.528	0.471

Table 4.26 Sensitivity of optimal design glass thickness (inch) to missile amount factor, F_a, when F_e is 0.25.

F_a (%)	10	20	30	40	50
Charleston	0.278	0.616	0.794	0.886	0.940
Boston	0.229	0.506	0.687	0.781	0.840
LA & Seattle	0.160	0.401	0.528	0.619	0.680

F_a (%)	60	70	80	90	100
Charleston	1.012	1.053	1.090	1.116	1.138
Boston	0.874	0.902	0.924	0.942	0.956
LA & Seattle	0.721	0.750	0.773	0.792	0.807

Table 4.27 Sensitivity of optimal design glass thickness (inch) to missile existence factor, F_e, when F_a is 0.3.

F_e (%)	10	25	50	75	100
Charleston	-	0.806	1.012	1.116	1.176
Boston	0.264	0.687	0.874	0.942	0.978
LA & Seattle	0.271	0.528	0.721	0.792	0.830

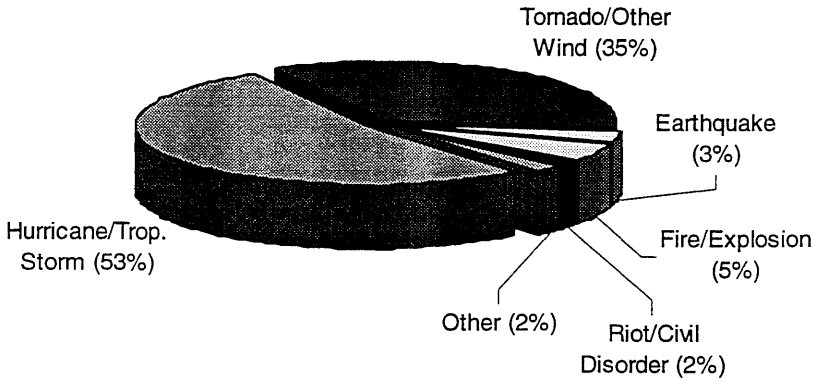

Figure 4.1 Percentage of property damage by type of designated catastrophes during 1986-1992 (by National Committee on Property Insurance, 1993).

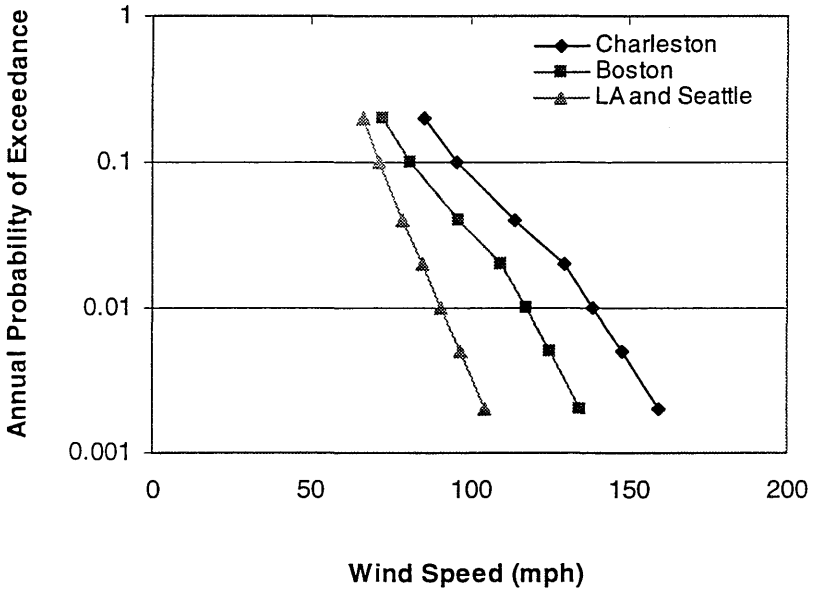

Figure 4.2 Annual probability of exceedance of wind speed for 4 cities.

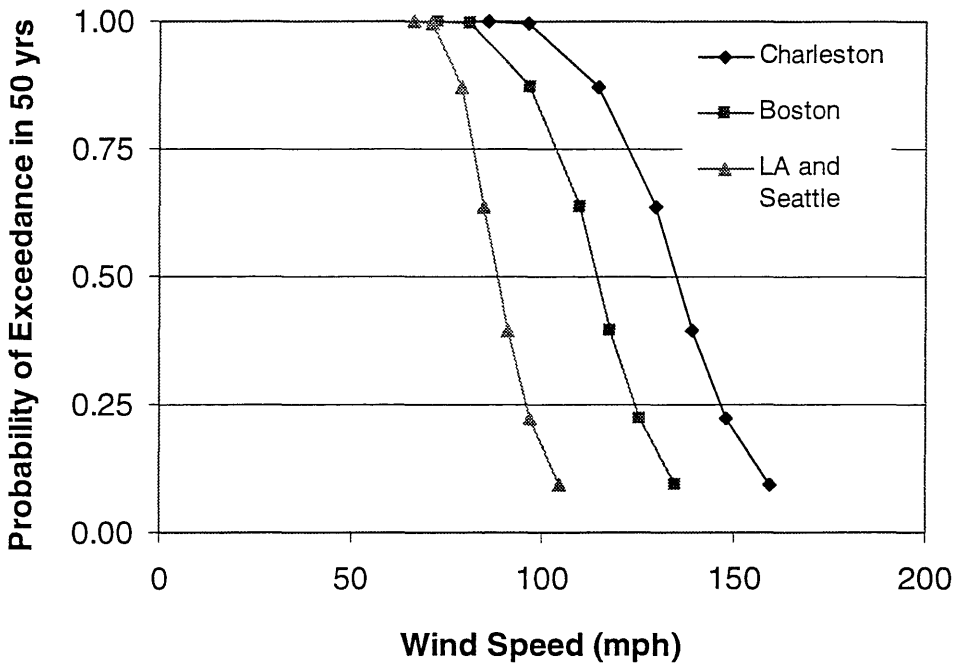

Figure 4.3 Probability of exceedance of wind speed in 50 years for 4 cities.

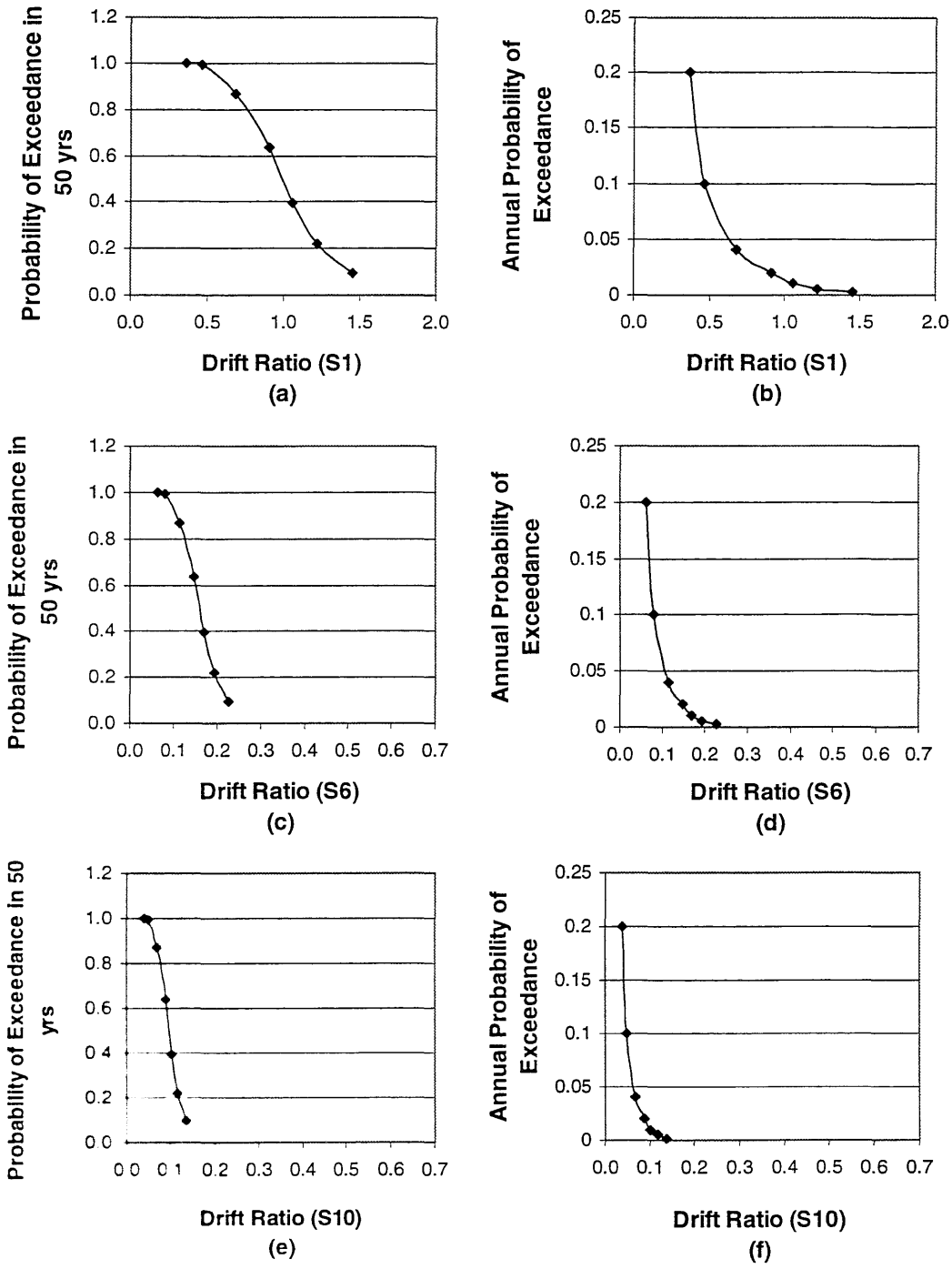

Figure 4.4 Annual and 50 years probability of drift ratio exceedance for S1 (a and b), S6 (c and d), and S10 (e and f) at Charleston.

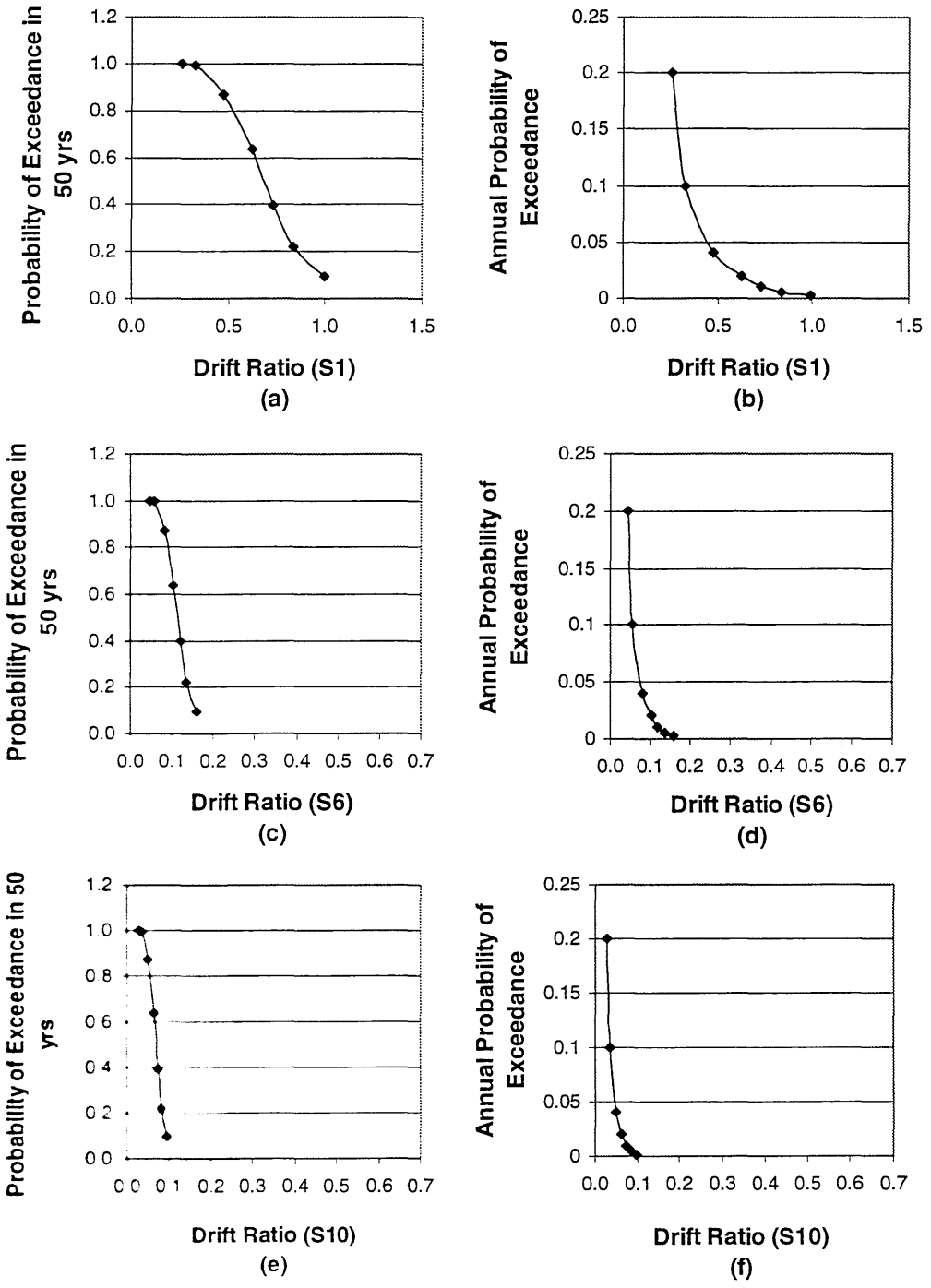

Figure 4.5 Annual and 50 years probability of drift ratio exceedance for S1 (a and b), S6 (c and d), and S10 (e and f) at Boston.

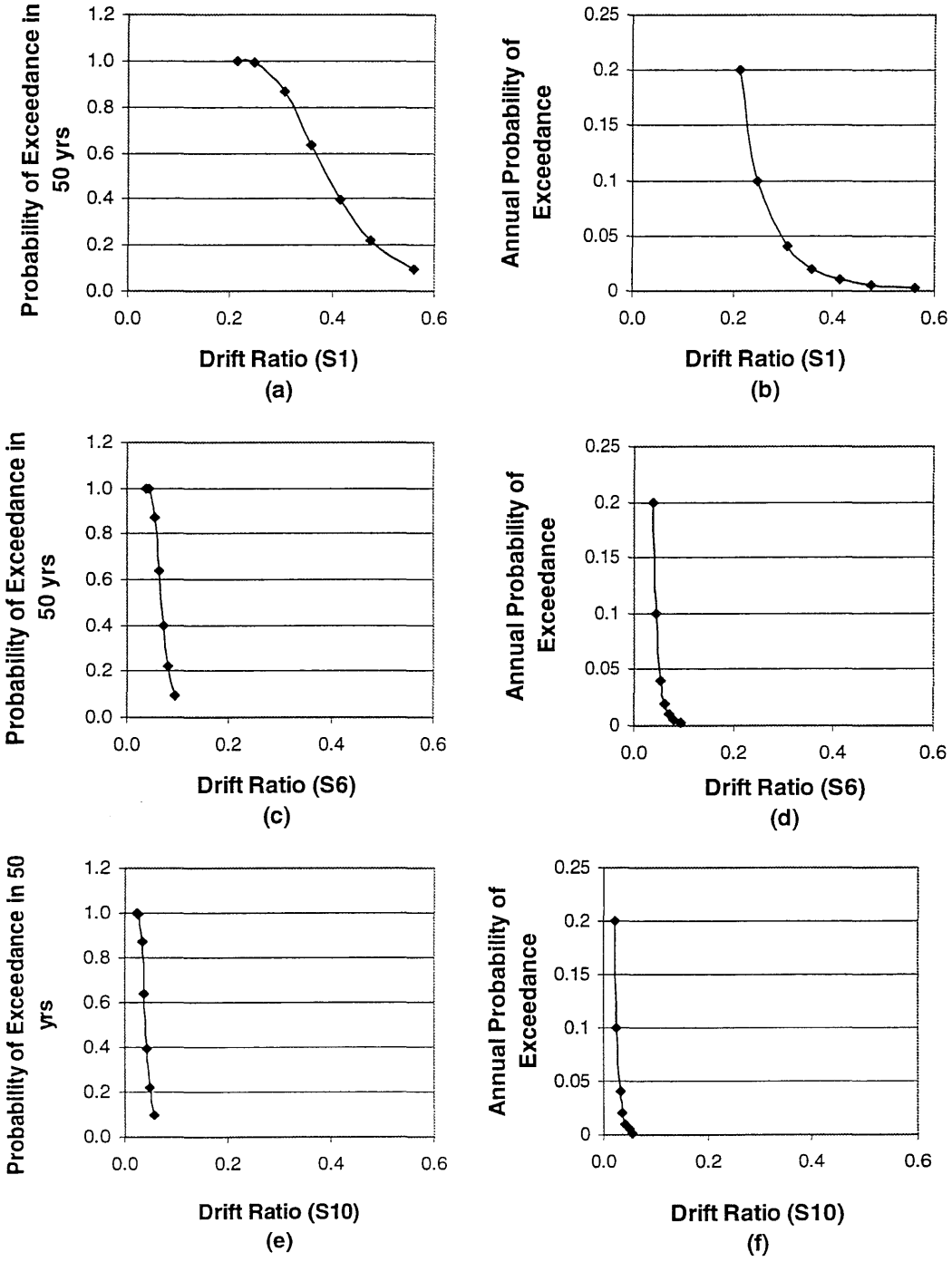

Figure 4.6 Annual and 50 years probability of drift ratio exceedance for S1 (a and b), S6 (c and d), and S10 (e and f) at Los Angeles.

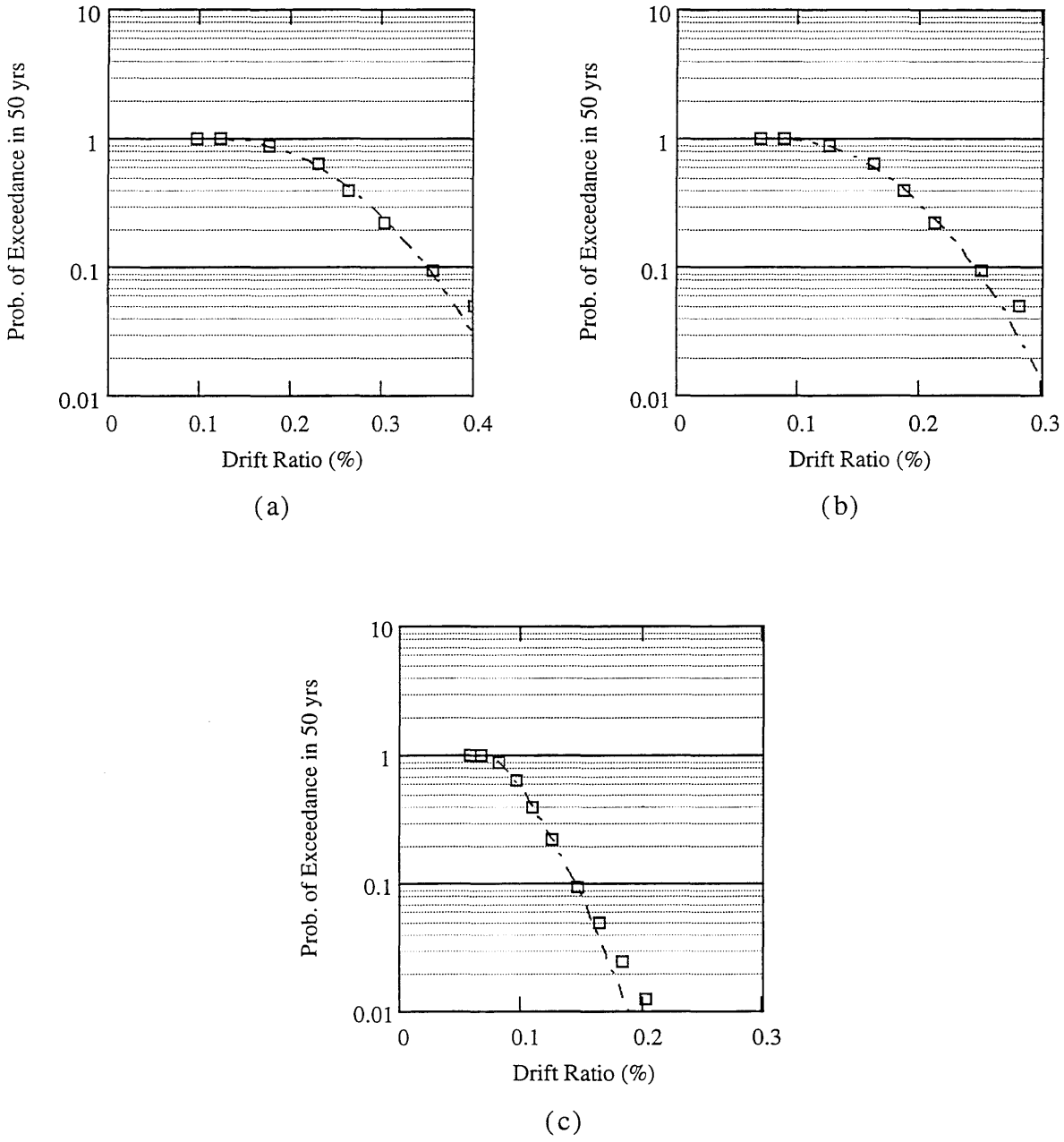

Figure 4.7 Fitting drift ratio and probability of exceedance in 50 years for S4 at (a) Charleston, (b) Boston, and (c) Los Angeles and Seattle.

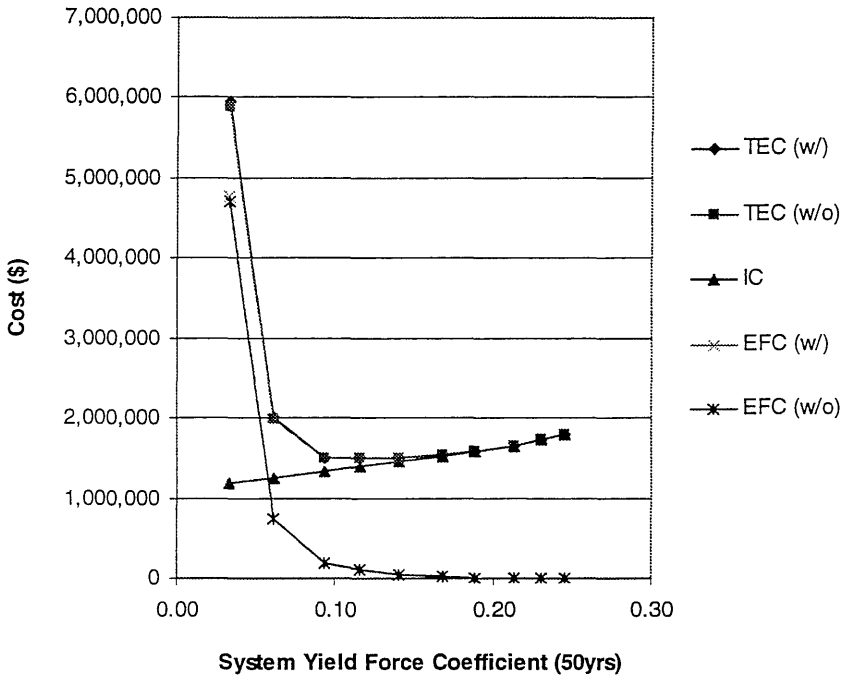

Figure 4.8 Total expected life-cycle cost as a function of system yield force coefficient at Charleston for t = 50 years and $\lambda = 0.05$.

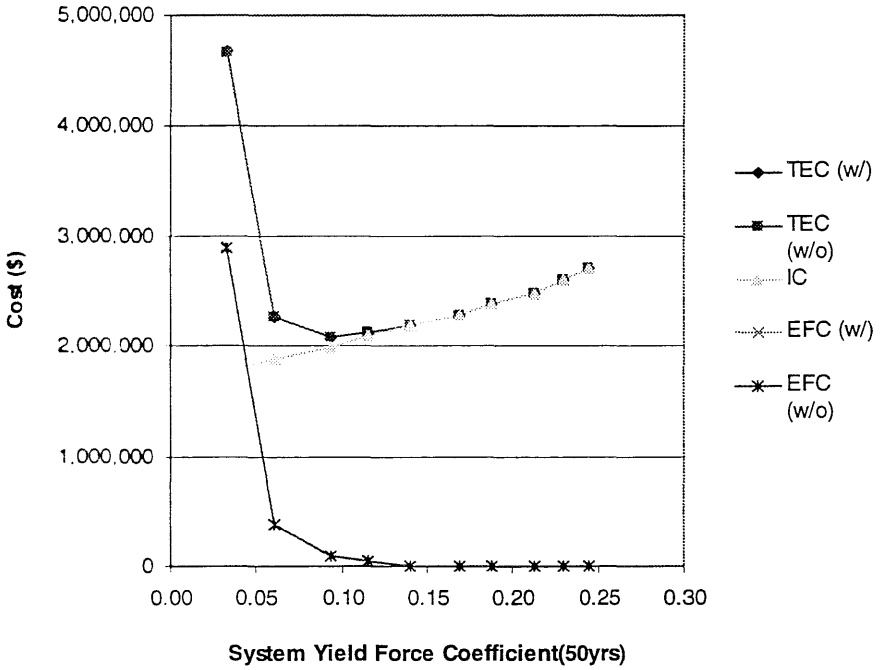

Figure 4.9 Total expected life-cycle cost as a function of system yield force coefficient at Boston for t = 50 years and $\lambda = 0.05$.

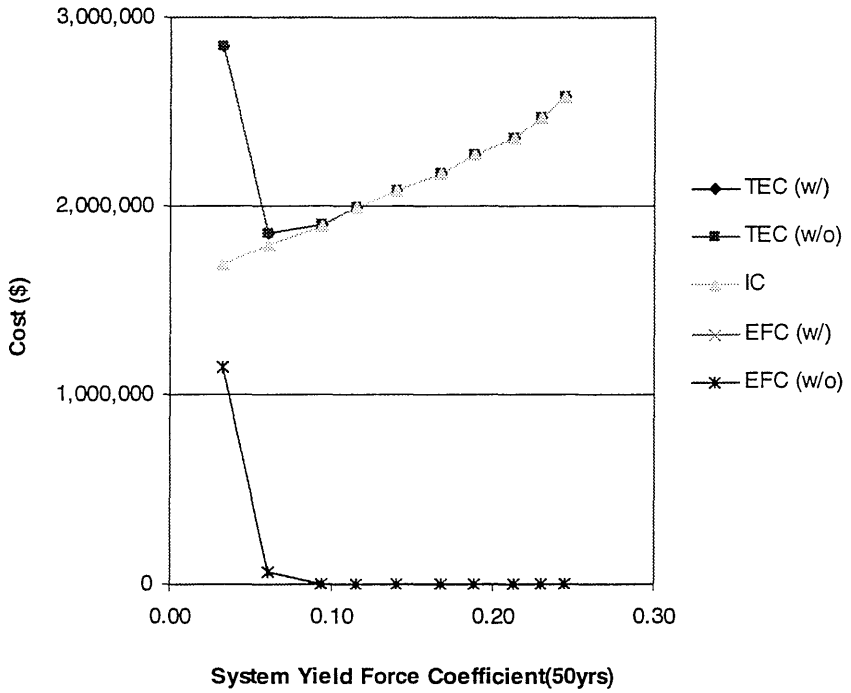

Figure 4.10 Total expected life-cycle cost as a function of system yield force coefficient at Los Angeles and Seattle for t = 50 years and λ = 0.05.

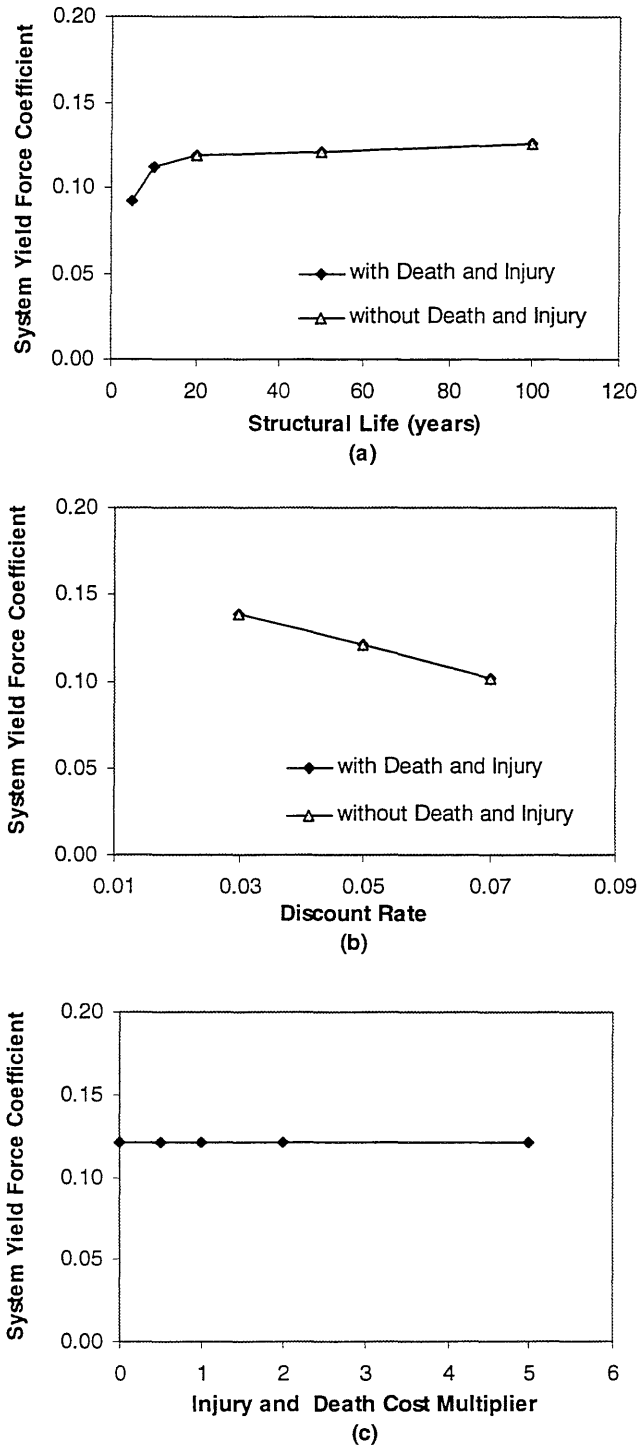

Figure 4.11 Sensitivity of optimal design to (a) lifetime, (b) discount rate, and (c) injury and death cost at Charleston.

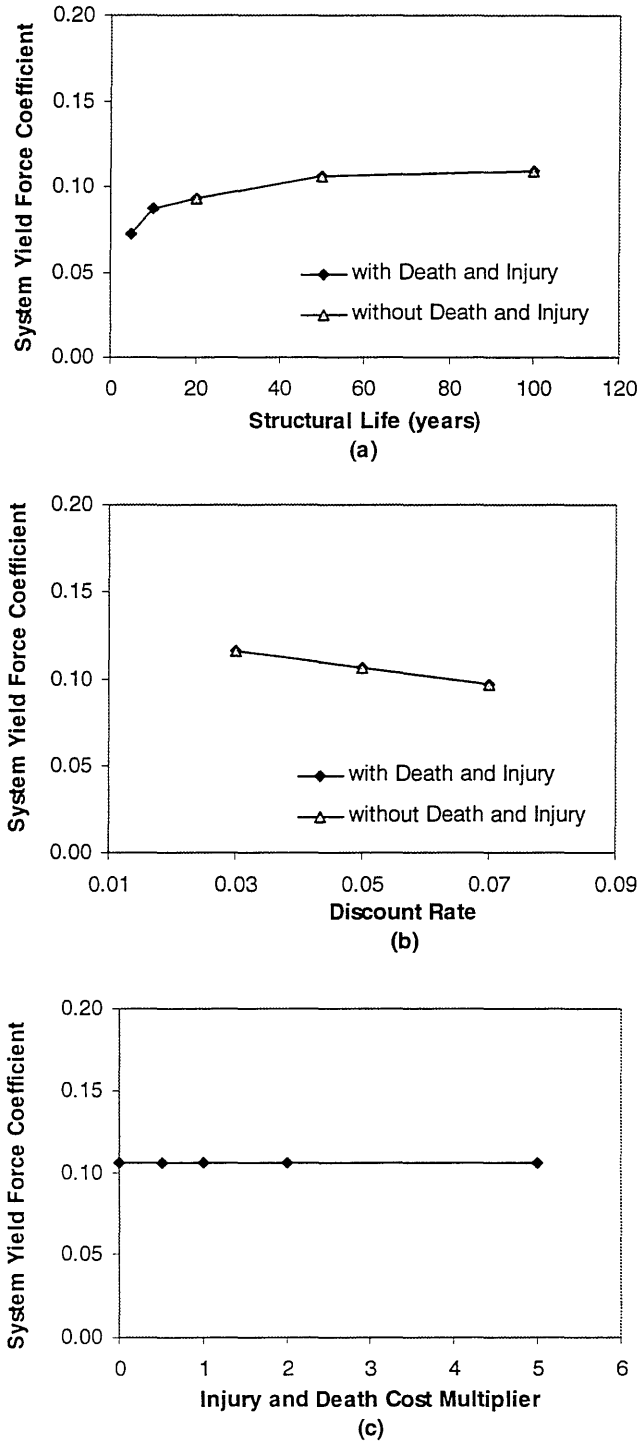

Figure 4.12 Sensitivity of optimal design to (a) lifetime, (b) discount rate, and (c) injury and death cost at Boston.

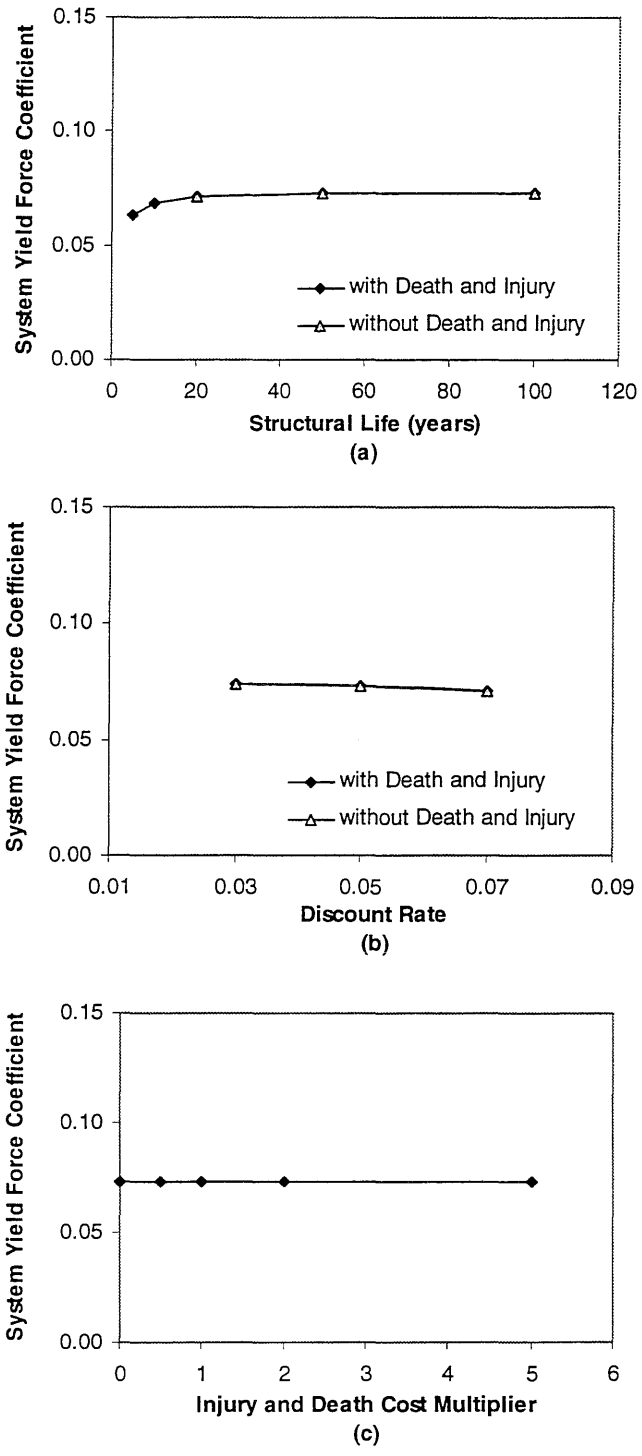

Figure 4.13 Sensitivity of optimal design to (a) lifetime, (b) discount rate, and (c) injury and death cost at Los Angeles and Seattle.

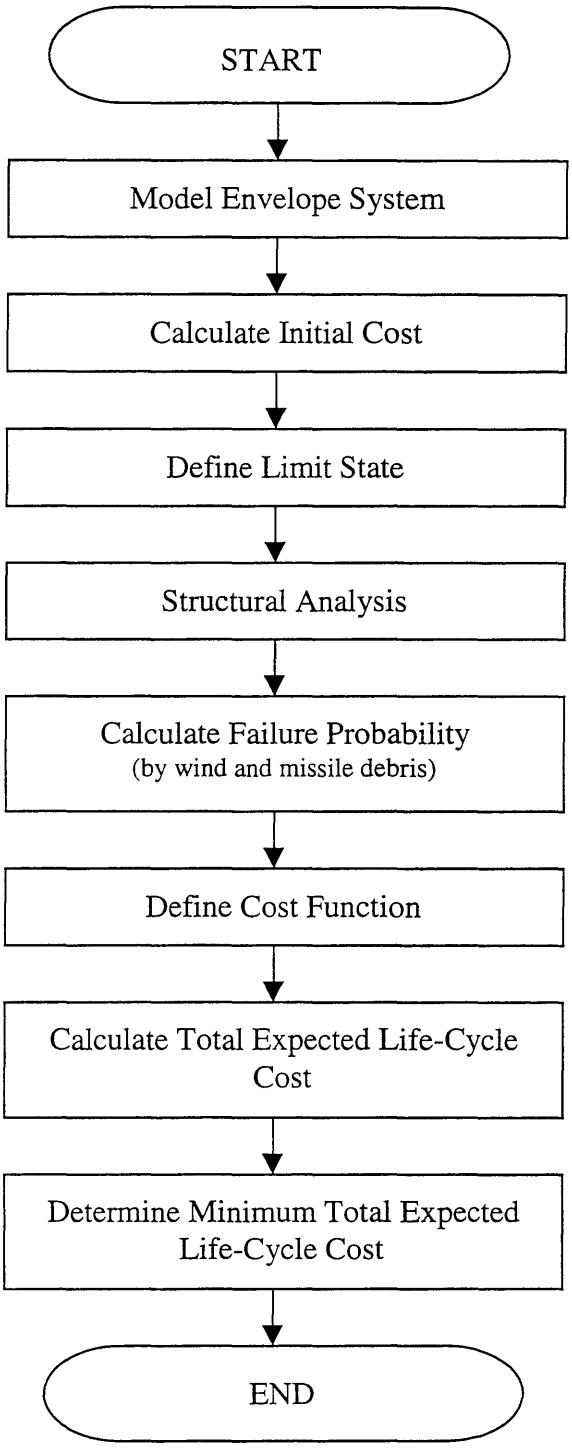

Figure 4.14 Procedure for determination of minimum total expected life-cycle cost of building envelope system due to wind load.

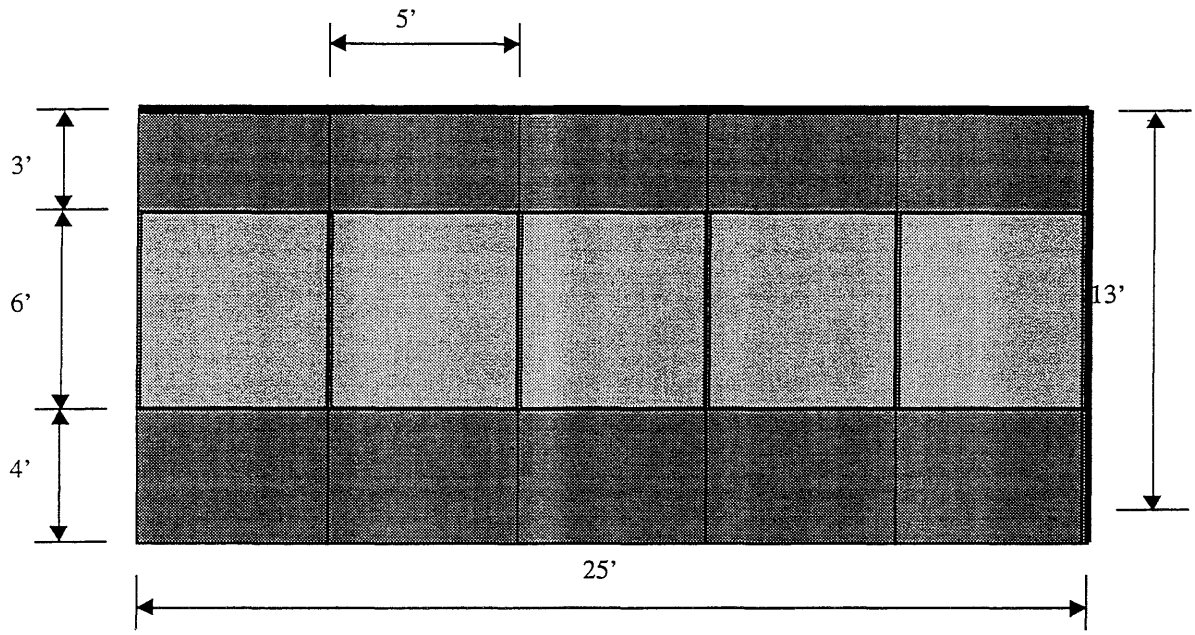

Figure 4.15 Typical envelope system with stone panels and window glass.

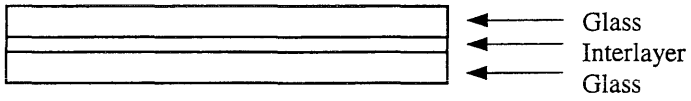

(a) Typical Laminated Glass Units

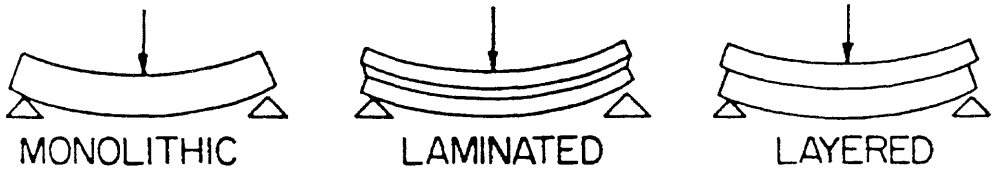

(b) Behavior of three types of glass

Figure 4.16 Glass plate system.

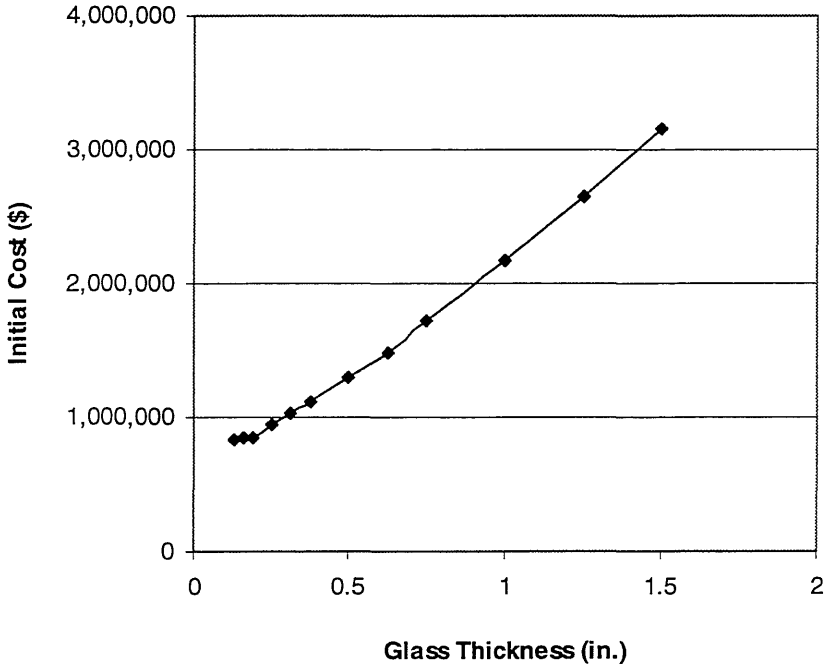

Figure 4.17 Initial cost as function of glass thickness.

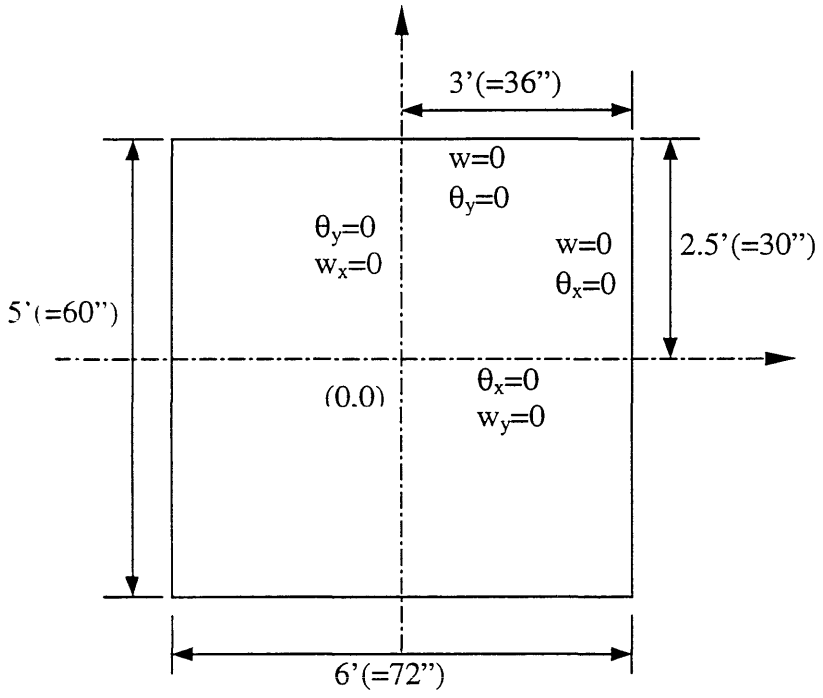

Figure 4.18 FEM model and boundary conditions for a rectangular glass plate.

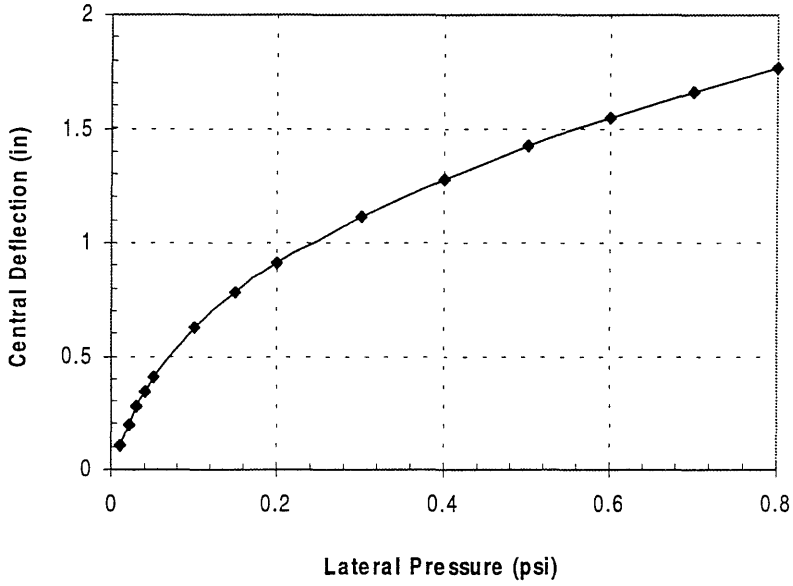

Figure 4.19 Central deflection as function of lateral pressure for a rectangular glass plate of 96"×60" ×0.225".

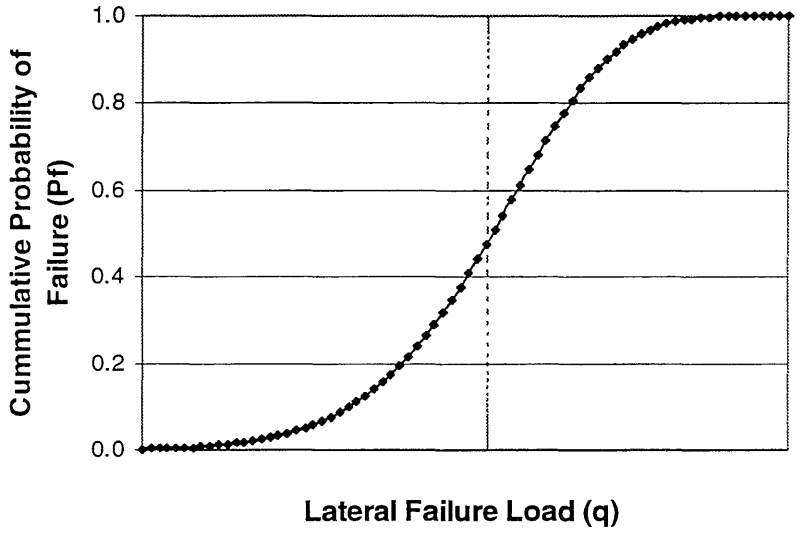

Figure 4.20 Cumulative probability of failure as function of lateral load for glass plate.

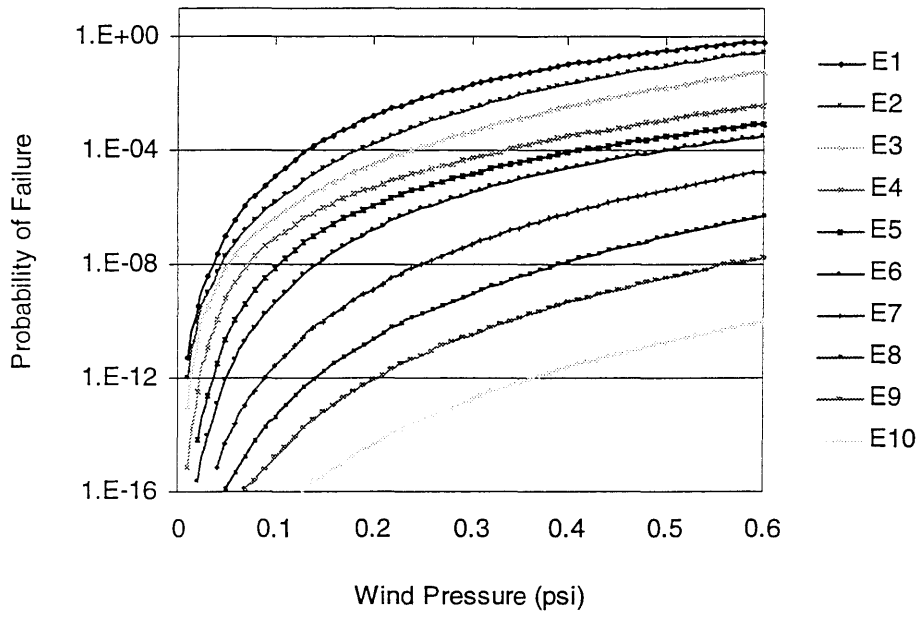

Figure 4.21 Probability of failure as function of wind pressure for each envelope system.

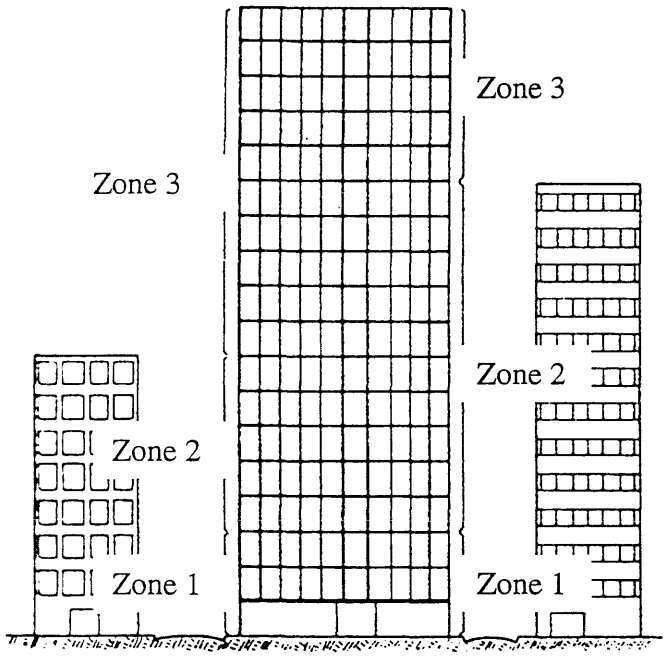

Figure 4.22 Suggested loading zones for cladding on multistory buildings (Minor et al., 1978)

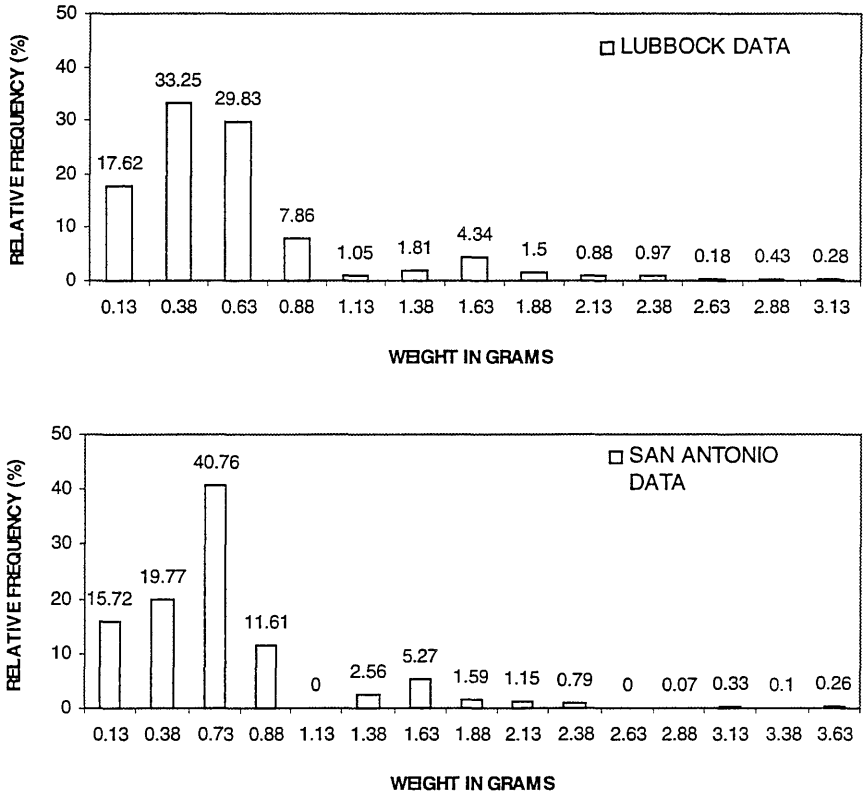

Figure 4.23 Characteristics of roof gravel; Lubbock and San Antonio Populations (Minor, 1974).

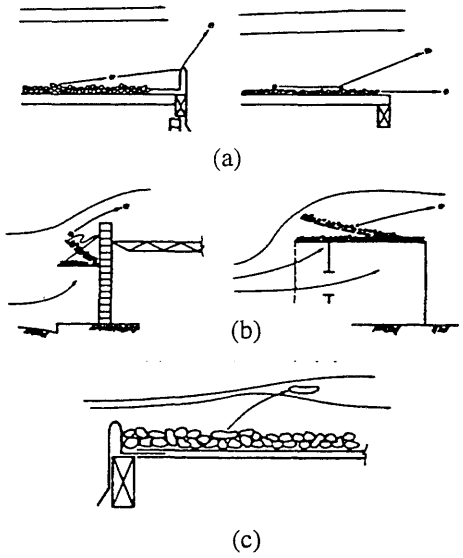

Figure 4.24 Missile injection mechanisms (a) ramp injections (b) explosion injections (c) aerodynamic injections (Minor and Beason, 1976).

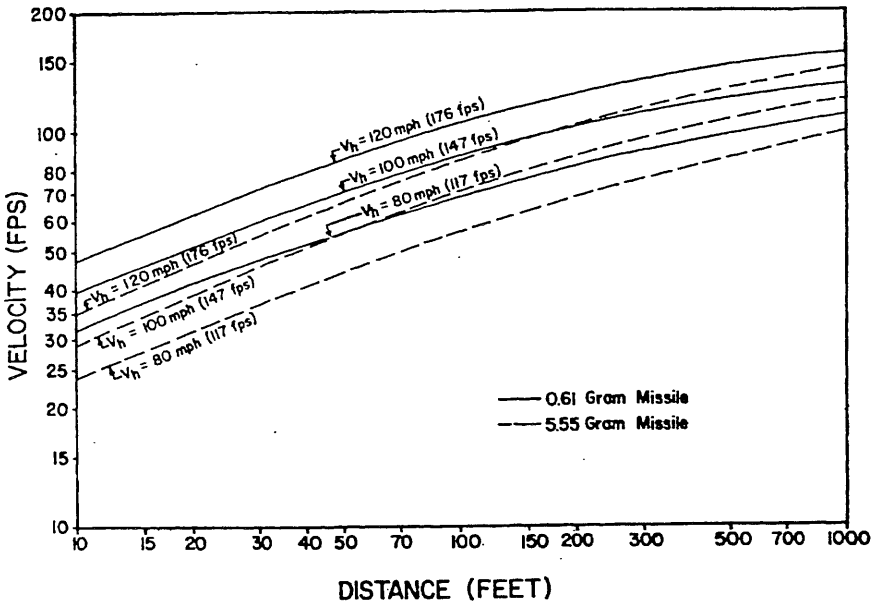

Figure 4.25 Missile velocities attained as a function of distance traveled for spherical missiles in horizontal airstreams (Minor, 1974).

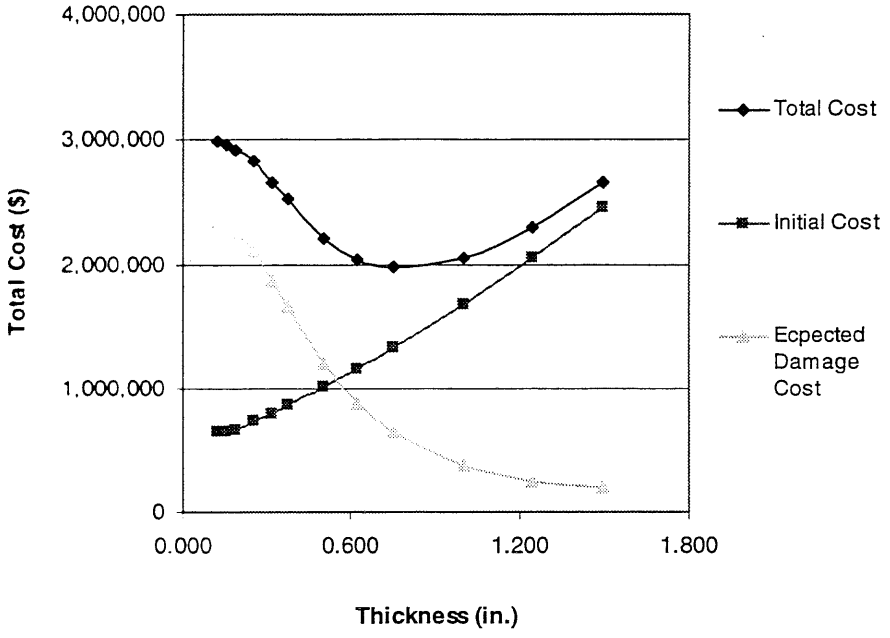

Figure 4.26 Total expected life-cycle cost at Charleston.

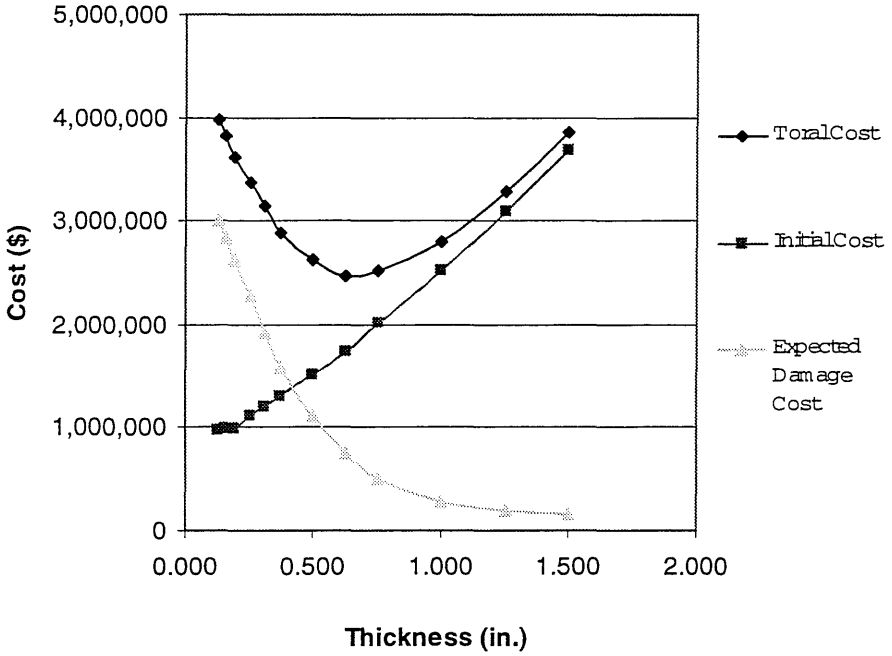

Figure 4.27 Total expected life-cycle cost at Boston.

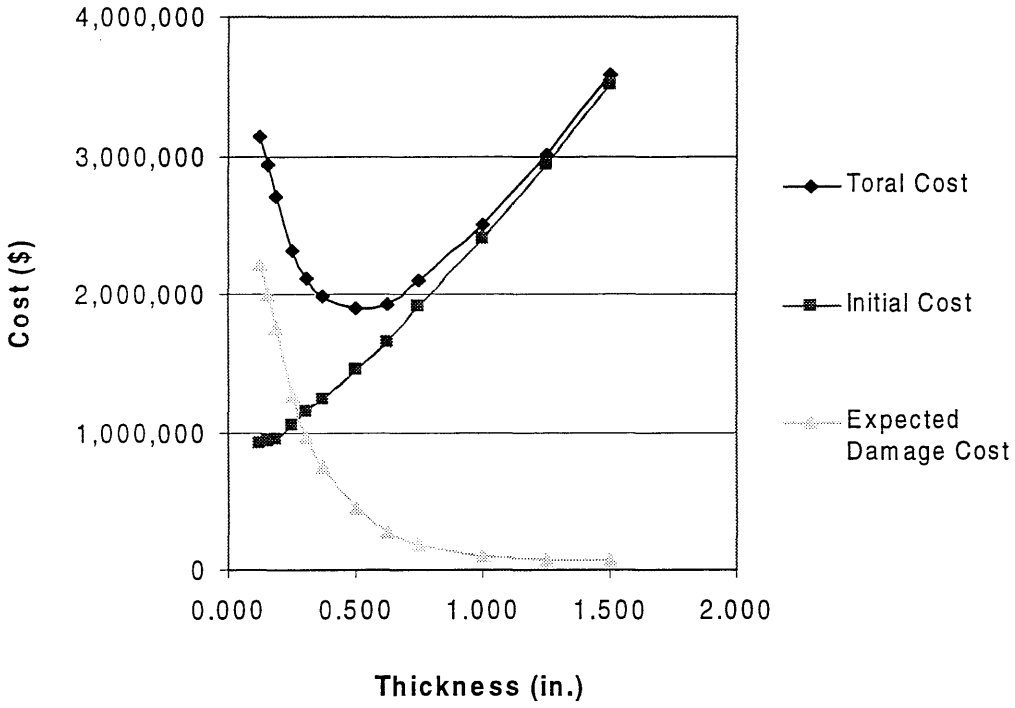

Figure 4.28 Total expected life-cycle cost at Los Angeles.

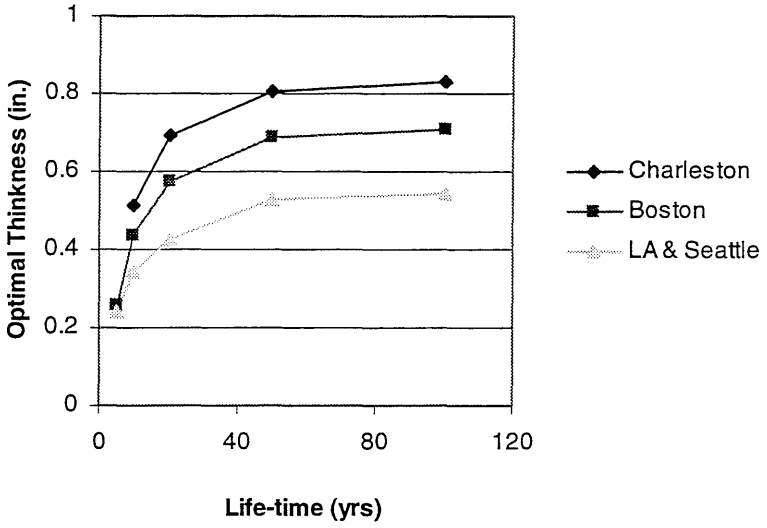

Figure 4.29 Sensitivity of optimal glass thickness to lifetime.

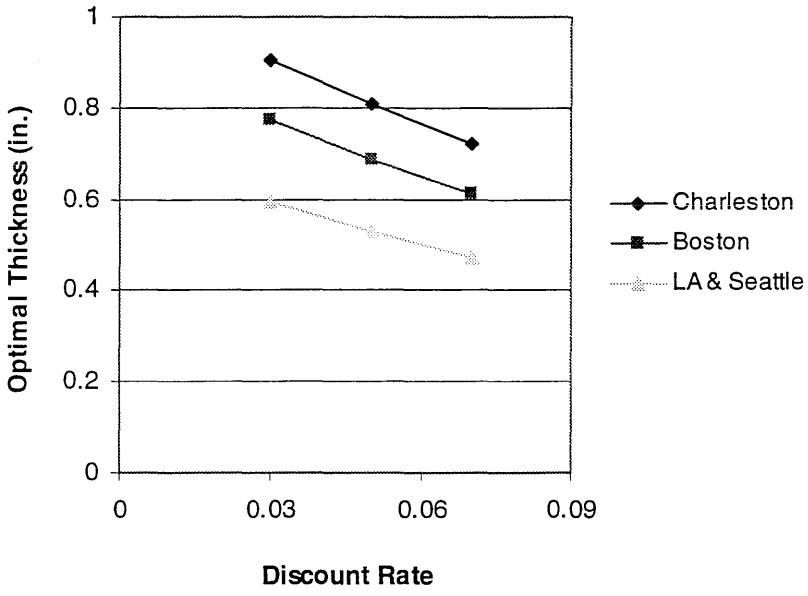

Figure 4.30 Sensitivity of optimal glass thickness to discount rate.

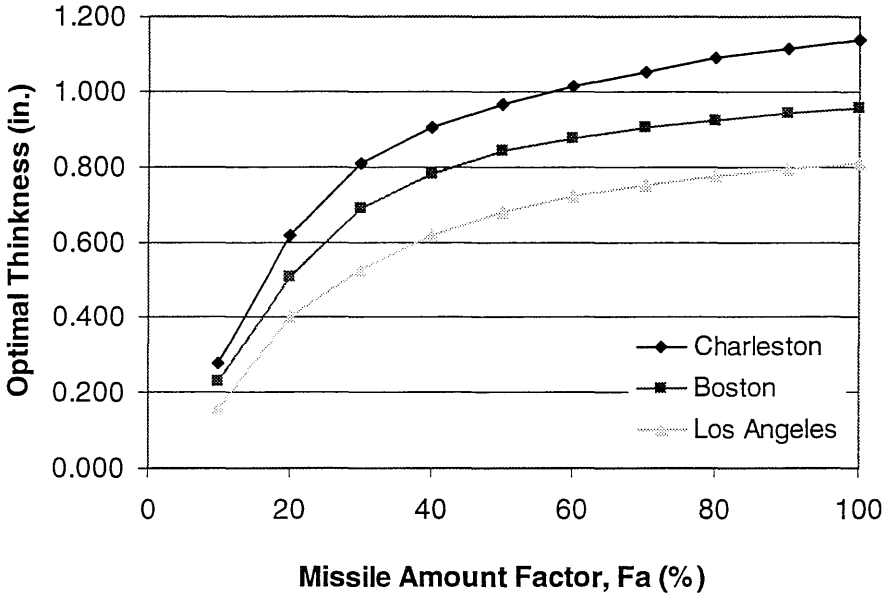

Figure 4.31 Sensitivity of optimal glass thickness to missile amount factor for Fe=0.5.

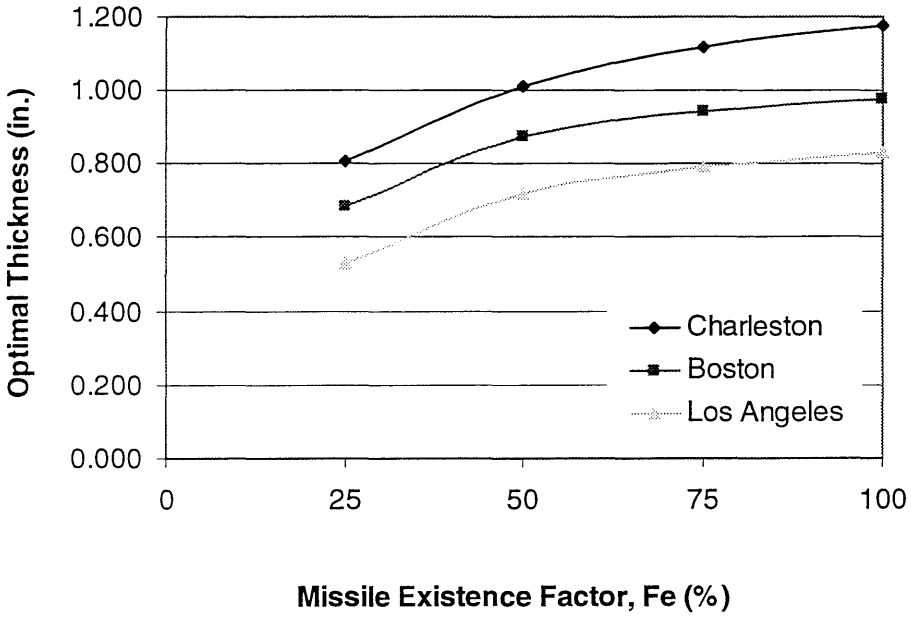

Figure 4.32 Sensitivity of optimal glass thickness to missile existence factor for Fa=0.3.

CHAPTER 5

APPLICATIONS TO MULTIPLE LOADS

5.1 Introduction

Most civil structural systems are subjected to multiple hazards during their life. The random occurrence in time of the loads and combinations of loads and load effects needs to be considered. As shown in Chapter 3 and Chapter 4, earthquakes and winds are major natural hazards and the effects of these two loads are important in structural design. In this chapter, both loads are considered in the minimum life-cycle cost based design.

The analytical formulation for multiple hazards in Chapter 2 is applied to a two-load design. Since the probability of simultaneous occurrence is generally very small, the coincident term in the equation can be neglected. Hence, the analytical formulation for two loads can be derived in terms of initial cost and the expected damage cost functions for each load.

The expected damage cost functions for earthquake and wind in the two previous Chapters are used herein again. Analysis of sensitivity is carried out to lifetimes, discount rate and injury and death cost.

5.2 Analytical Formulation

For two hazards and multi-limit states, Equation (2.5) in Chapter 2 can be rewritten as

$$E[C(t,X)] = C_0 + \sum_{l=1}^{k} C_l[\nu_1 P_l^1 + \nu_2 P_l^2 + \nu_{12} P_l^{12}] \cdot \frac{(1-e^{-\lambda t})}{\lambda} + \frac{C_m}{\lambda}(1-e^{-\lambda t}) \qquad (5.1)$$

where, ν_{12} is coincident rate of hazards 1 and 2; P_l^{12} is probability of limit-state l given the coincidence of hazards i and j; and μd_i is mean duration of hazard i.

Since ν_{12} is in general very small for wind and earthquake due to the extremely small probability of simultaneous occurrence of these two cases, the contribution of the coincidence term can be neglected.

As a result, the expected limit state cost can be calculated separately for each hazard. If there are k limit states under load 1 and l limit states under load 2, Equation (5.1) can be rewritten as

$$E[C(t,X)] = C_0 + (C_1P_1 + C_2P_2 + ... + C_kP_k)\frac{\nu_1}{\lambda}(1-e^{-\lambda t}) + (C_1P_1 + C_2P_2 + ... + C_lP_l)\frac{\nu_2}{\lambda}(1-e^{-\lambda t}) + \frac{C_m}{\lambda}(1-e^{-\lambda t}) \tag{5.2}$$

in which C_k is the k-th limit-state failure cost, P_k is the k-th limit state probability, C_l is the l-th limit-state failure cost, and P_l is the l-th limit state probability.

Denoting $EFC_{earthquake}[(t,X)]$ and $EFC_{wind}[(t,X)]$ as the expected failure costs for earthquake and wind loads, respectively, and neglecting maintenance cost, one can simplify Equation (5.2) as

$$E[C(t,X)] = C_0 + EFC_{earthquake}[(t,X)] + EFC_{wind}[(t,X)] \tag{5.3}$$

5.3 Optimal Design Under Seismic and Wind Loads

The optimal design and total expected life-cycle cost can be obtained by minimizing Equation (5.3) when both earthquake and wind loads are considered. The same twelve structures and limit states for earthquake and wind loads are considered. Since the focus here is optimal structural strength under both winds and earthquakes, building envelope is not considered.

The calculation results of the total expected lifecycle cost for each city are shown in Table 5.1 to 5.3 and Figure 5.1 to 5.3. Also included are also the initial cost, the expected

failure cost by earthquake and the expected failure cost by wind. Optimal system yield force coefficients are 0.198, 0.115 and 0.146 for Los Angeles, Seattle and Charleston, respectively. The optimal value at Charleston is larger than that at Seattle primaring due to the impact of hurricane winds.

Analysis of sensitivity is carried out to lifetimes, discount rate, and injury and death cost. The results are shown in Table 5.4 to 5.6 and Figure 5.4 to 5.6. It is seen that sensitivity varies according to location. While the optimal design at Los Angeles is sensitive to lifetimes, it is not sensitive to injury and death cost. It depends on discount rate moderately. At Seattle, optimal design is very sensitive to injury and death cost, sensitive to lifetime, moderately sensitive to discount rate. At Charleston, optimal design is sensitive to the injury and death cost function and to lifetimes, and moderately sensitive to discount rate.

Figures 5.7 to 5.9 show the comparison of sensitivity of optimal designs to various design parameters under earthquakes, winds, and both loads. It is seen that optimal designs at Los Angeles and Seattle are dominated by earthquake load, whereas they are dominated by wind load at Charleston.

5.4 Summary

In this chapter, the proposed minimum life-cycle cost based design method for multiple loads is applied to design for winds and earthquakes. The total expected life-cycle costs for earthquake and wind for four cities are obtained and sensitivity analyses to lifetime, discount rate, and injury and death cost are carried out.

Conclusions from the results can be summarized as follows:

1. The optimal design depends on the characteristics of the loads at each city. At Los Angeles, optimal design for two loads is almost the same as that for earthquakes. At Seattle and Charleston, both loads contribute. The affect of non-dominating load to the optimal design at Charleston is larger than at

Seattle. As a result, the optimal design at Charleston can be higher than that at Seattle.

2. The optimal design is sensitive to lifetime and it depends on discount rate moderately. It is not sensitive to injury and death cost at Los Angeles, but it is at Seattle and Charleston. The sensitivity to injury and death cost depend on the dominating load, i.e., earthquakes at Los Angeles and Seattle, and winds at Charleston.

Table 5.1 Total expected life-cycle cost for earthquake and wind loads at Los Angeles (t=50 years, λ=0.05).

Structure	Sy	IC	EQ (w/o)	EQ (w/)	Wind (w/o)	Wind (w/)	Total (w/o)	Total (w/)
S1	0.033	1,694,104	6,244,360	7,477,637	1,148,935	1,151,436	9,087,400	10,323,177
S2	0.061	1,787,307	3,611,544	4,115,719	66,404	66,528	5,465,256	5,969,555
S3	0.093	1,893,037	2,045,247	2,311,130	3,343	3,349	3,941,627	4,207,516
S4	0.115	1,990,199	1,540,588	1,787,155	543	544	3,531,330	3,777,898
S5	0.140	2,079,455	1,138,450	1,309,032	10	10	3,217,915	3,388,497
S6	0.169	2,172,747	863,962	993,825	0	0	3,036,709	3,166,573
S7	0.188	2,267,425	755,426	868,412	0	0	3,022,851	3,135,837
S8	0.213	2,360,868	677,131	788,188	0	0	3,037,999	3,149,057
S9	0.230	2,470,200	589,741	686,397	0	0	3,059,940	3,156,596
S10	0.245	2,577,641	534,875	617,953	0	0	3,112,515	3,195,594
S12	0.321	2,880,165	379,908	431,657	0	0	3,260,073	3,311,822
S15	0.408	3,234,728	303,657	346,379	0	0	3,538,385	3,581,107

Table 5.2 Total expected life-cycle cost for earthquake and wind loads at Seattle (t=50 years, λ=0.05).

Structure	Sy	IC	EQ (w/o)	EQ (w/)	Wind (w/o)	Wind (w/)	Total (w/o)	Total (w/)
S1	0.033	1,607,266	707,805	1,282,640	1,090,042	1,092,543	3,405,113	3,982,449
S2	0.061	1,695,692	448,402	802,684	63,000	63,125	2,207,094	2,561,500
S3	0.093	1,796,002	335,239	599,325	3,171	3,178	2,134,412	2,398,504
S4	0.115	1,888,183	295,511	533,069	515	516	2,184,209	2,421,768
S5	0.140	1,972,864	254,032	460,706	10	10	2,226,906	2,433,580
S6	0.169	2,061,375	226,142	408,050	0	0	2,287,517	2,469,425
S7	0.188	2,151,199	203,001	367,280	0	0	2,354,200	2,518,479
S8	0.213	2,239,853	179,736	321,809	0	0	2,419,589	2,561,662
S9	0.230	2,343,580	166,871	299,061	0	0	2,510,450	2,642,641
S10	0.245	2,445,514	158,646	284,086	0	0	2,604,160	2,729,600
S12	0.321	2,732,530	133,702	239,011	0	0	2,866,232	2,971,542
S15	0.408	3,068,919	119,318	213,310	0	0	3,188,237	3,282,229

Table 5.3 Total expected life-cycle cost for earthquake and wind loads at Charleston (t=50 years, λ=0.05).

Structure	Sy	IC	EQ (w/o)	EQ (w/)	Wind (w/o)	Wind (w/)	Total (w/o)	Total (w/)
S1	0.033	1,182,217	268,412	646,636	4,709,123	4,763,744	6,159,752	6,592,597
S2	0.061	1,247,258	186,881	445,312	742,798	746,662	2,176,937	2,439,232
S3	0.093	1,321,040	148,069	354,465	181,664	182,173	1,650,773	1,857,677
S4	0.115	1,388,844	127,328	302,980	101,792	102,066	1,617,963	1,793,890
S5	0.140	1,451,130	110,715	263,872	41,253	41,364	1,603,099	1,756,366
S6	0.169	1,516,234	102,237	243,650	14,903	14,943	1,633,374	1,774,826
S7	0.188	1,582,304	93,790	226,087	5,410	5,424	1,681,504	1,813,815
S8	0.213	1,647,512	87,200	208,299	1,129	1,132	1,735,841	1,856,943
S9	0.230	1,723,808	82,808	199,276	186	187	1,806,802	1,923,271
S10	0.245	1,798,785	78,962	188,748	18	18	1,877,766	1,987,551
S12	0.321	2,009,899	68,033	162,034	0	0	2,077,932	2,171,934
S15	0.408	2,257,328	62,495	149,526	0	0	2,319,823	2,406,854

Table 5.4 Sensitivity of optimal design to lifetime for each city.

City	Injury and Death	5yrs	10yrs	20yrs	50yrs	100yrs
Los Angeles	with I and D	0.139	0.167	0.181	0.198	0.202
	without I and D	0.131	0.161	0.178	0.193	0.197
Seattle	with I and D	0.085	0.097	0.105	0.115	0.124
	without I and D	0.079	0.092	0.093	0.094	0.099
Charleston	with I and D	0.101	0.120	0.127	0.146	0.151
	without I and D	0.095	0.115	0.123	0.134	0.138

Table 5.5 Sensitivity of optimal design to discount rate.

City	Injury and Death	0.03	0.05	0.07
Los Angeles	with I and D	0.213	0.198	0.187
	without I and D	0.208	0.193	0.182
Seattle	with I and D	0.130	0.115	0.102
	without I and D	0.109	0.094	0.081
Charleston	with I and D	0.161	0.146	0.135
	without I and D	0.150	0.134	0.117

Table 5.6 Sensitivity of optimal design to injury and death cost.

Cost Multiplier	0	0.5	1	2	5
Los Angeles	0.198	0.194	0.198	0.205	0.220
Seattle	0.094	0.106	0.115	0.130	0.205
Charleston	0.134	0.142	0.146	0.157	0.177

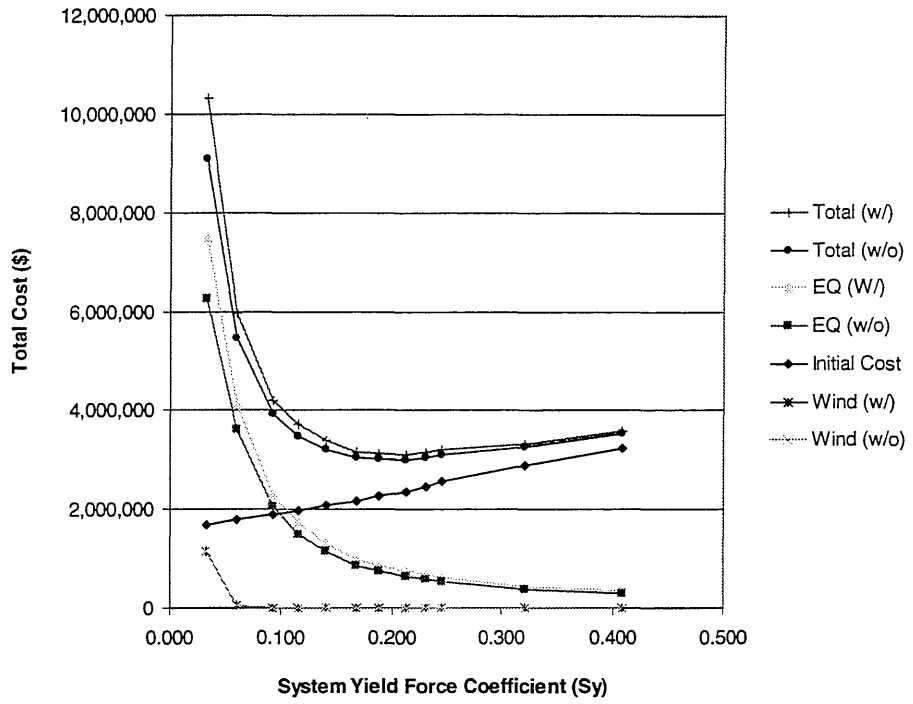

Figure 5.1 Total expected life-cycle cost as function of system yield force coefficient at Los Angeles (t=50 years, λ=0.05).

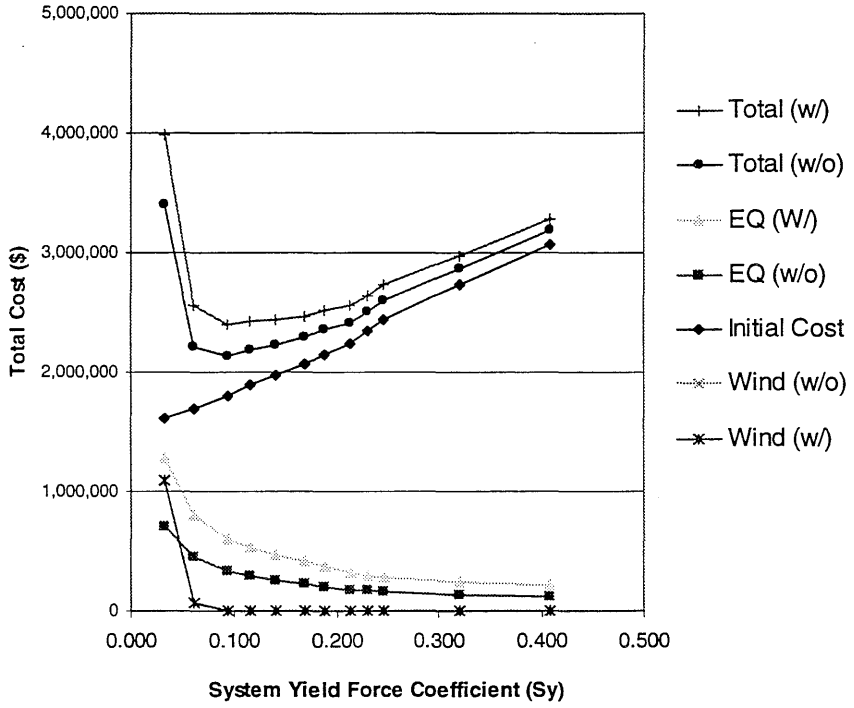

Figure 5.2 Total expected life-cycle cost as function of system yield force coefficient at Seattle (t=50 years, λ=0.05).

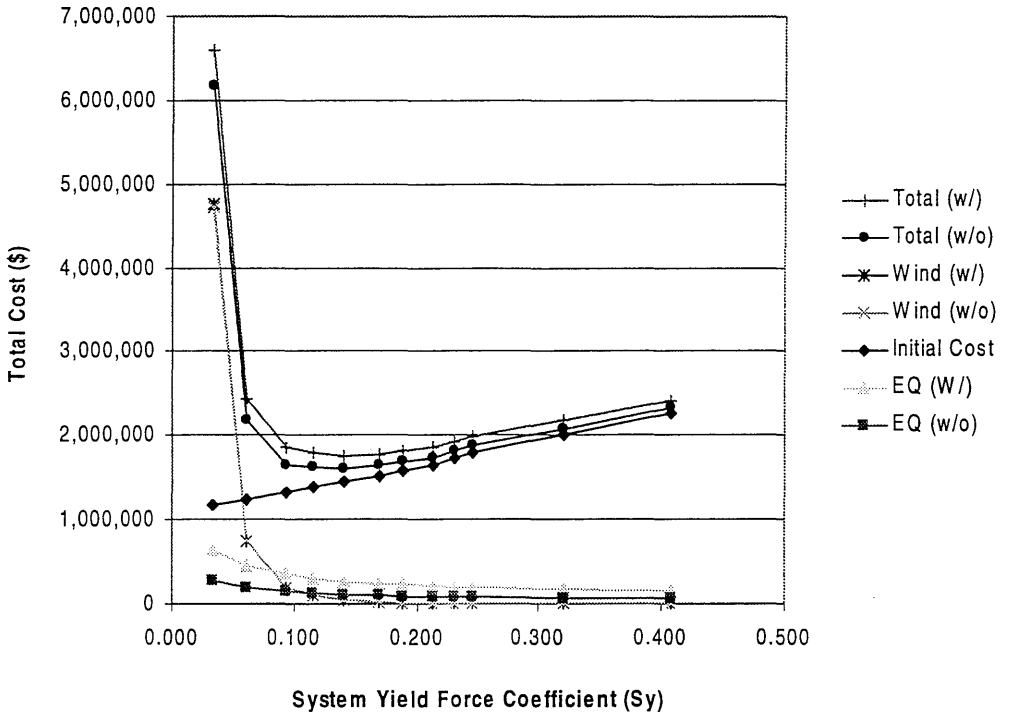

Figure 5.3 Total expected life-cycle cost as function of system yield force coefficient at Charleston (t=50 years, λ=0.05).

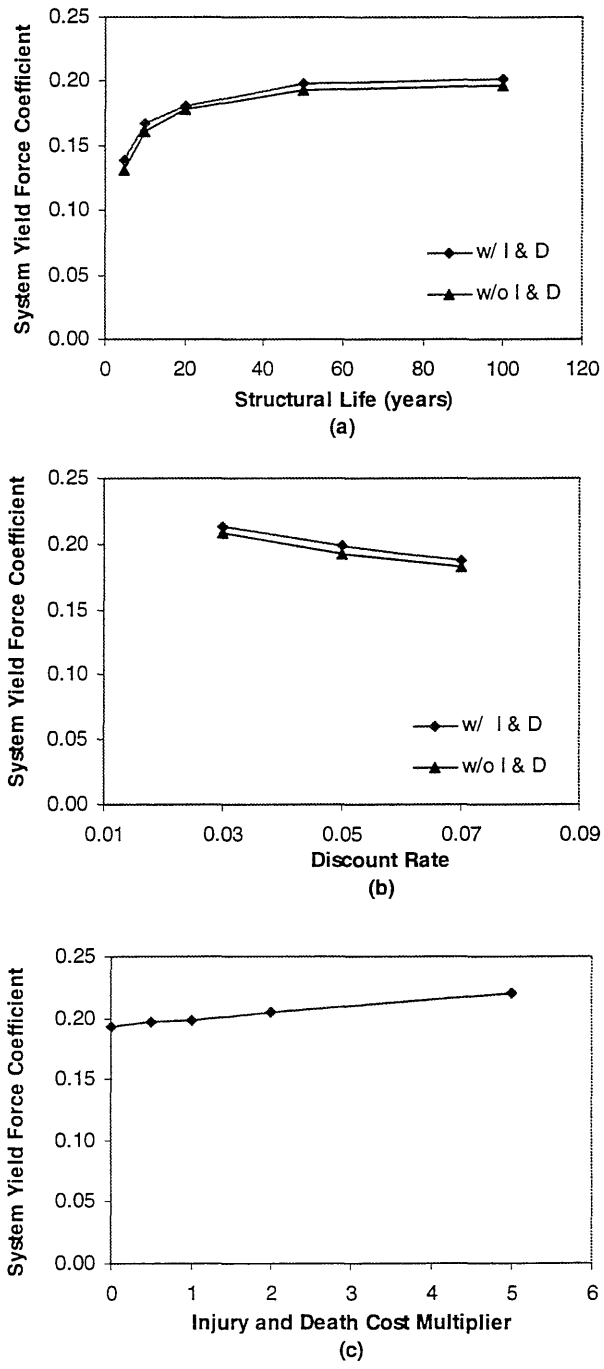

Figure 5.4 Sensitivity of optimal design to (a) lifetime, (b) discount rate and (c) injury and death cost at Los Angeles.

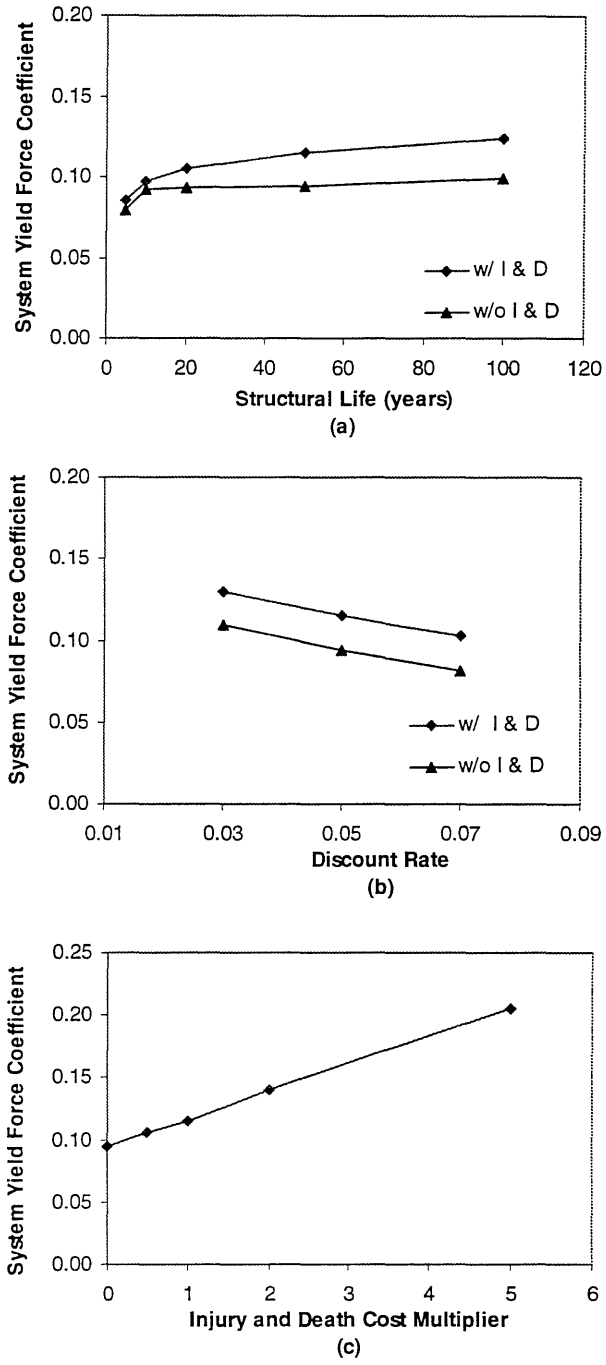

Figure 5.5 Sensitivity of optimal design to (a) lifetime, (b) discount rate and (c) injury and death cost at Seattle.

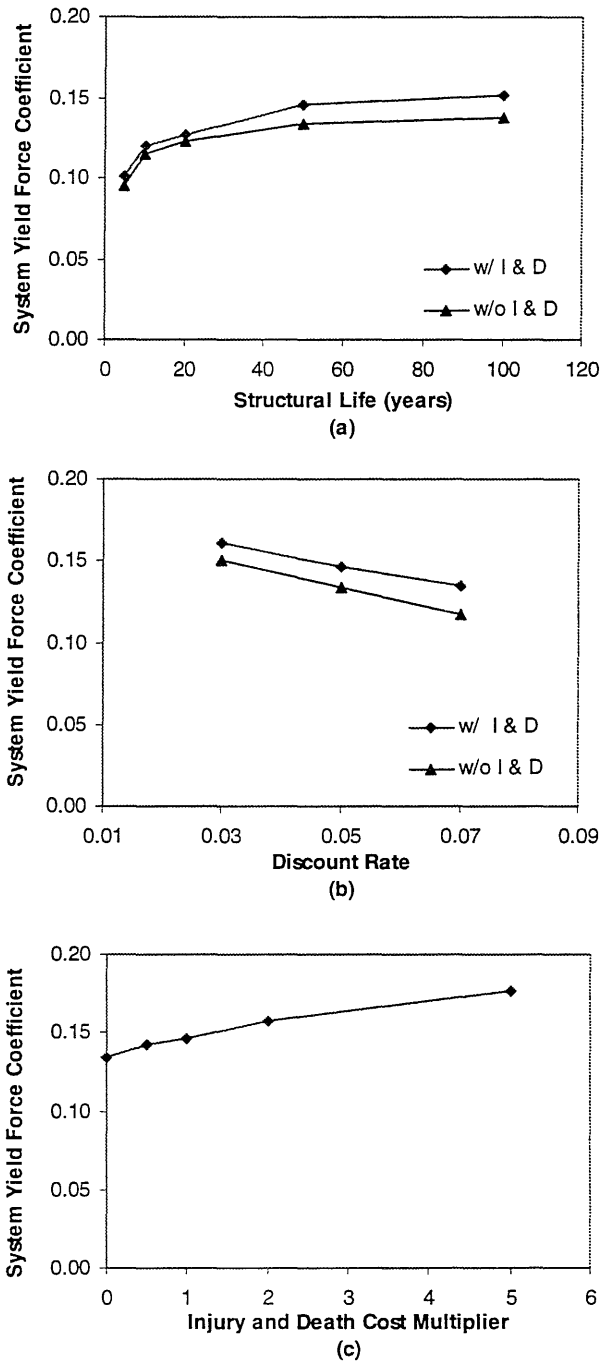

Figure 5.6 Sensitivity of optimal design to (a) lifetime, (b) discount rate and (c) injury and death cost at Charleston.

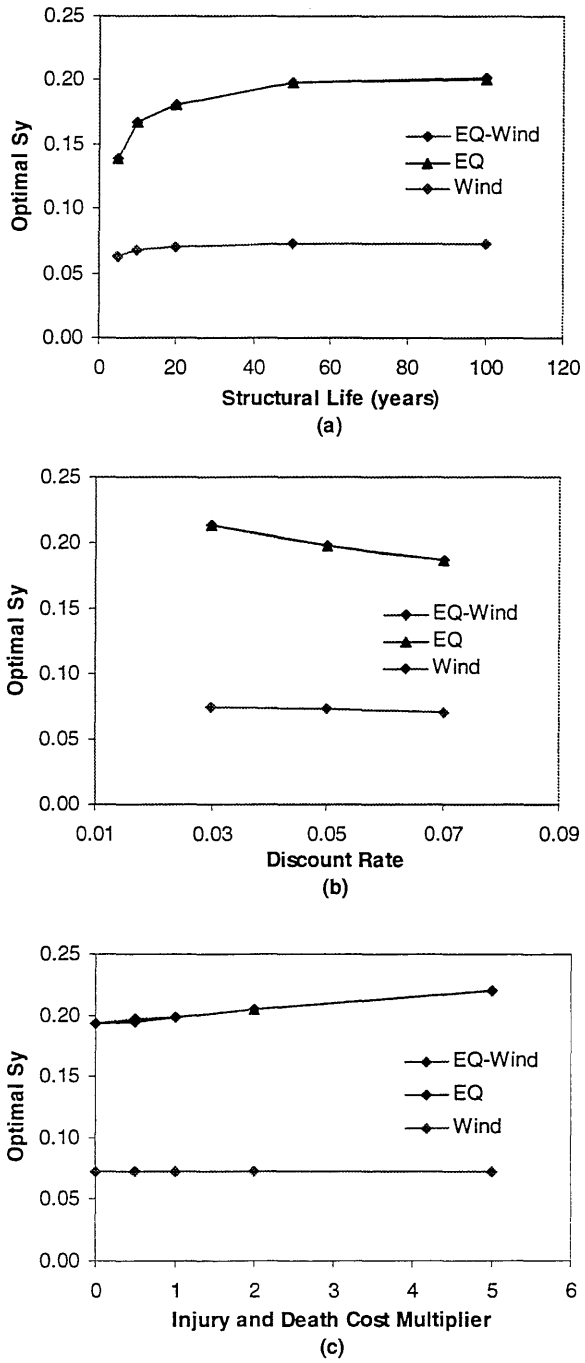

Figure 5.7 Comparison of sensitivity of optimal design for earthquake, wind and both earthquake and wind to (a) lifetime, (b) discount rate, and (c) injury and death cost at Los Angeles.

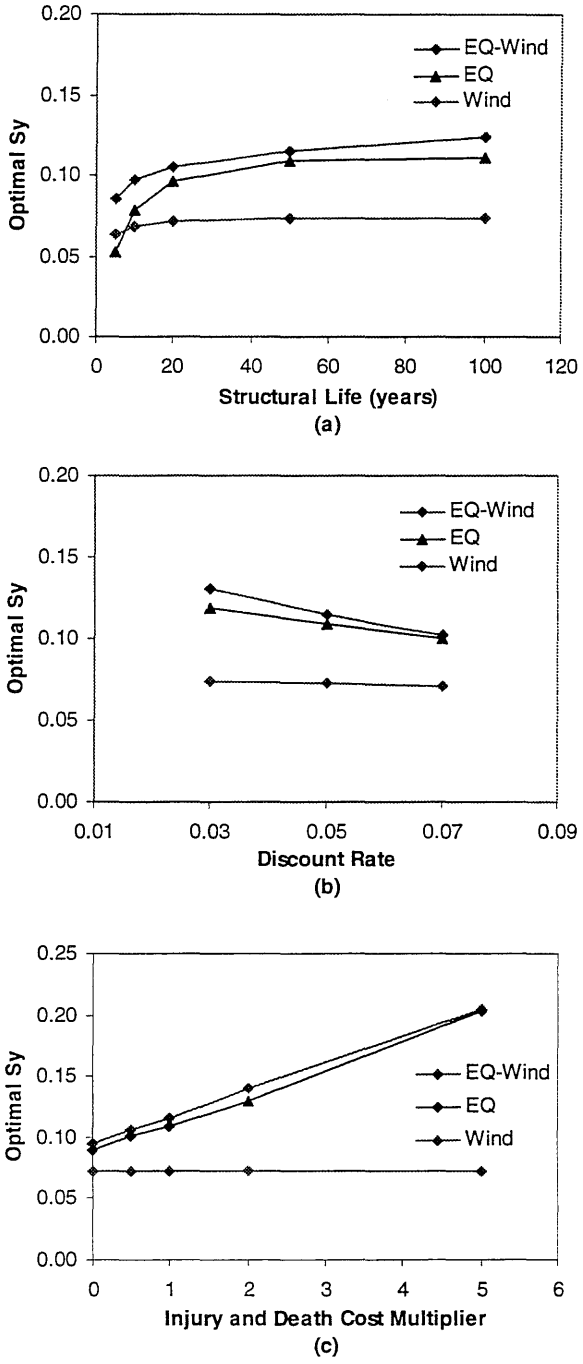

Figure 5.8 Comparison of sensitivity of optimal design for earthquake, wind and both earthquake and wind to (a) lifetime, (b) discount rate, and (c) injury and death cost at Seattle.

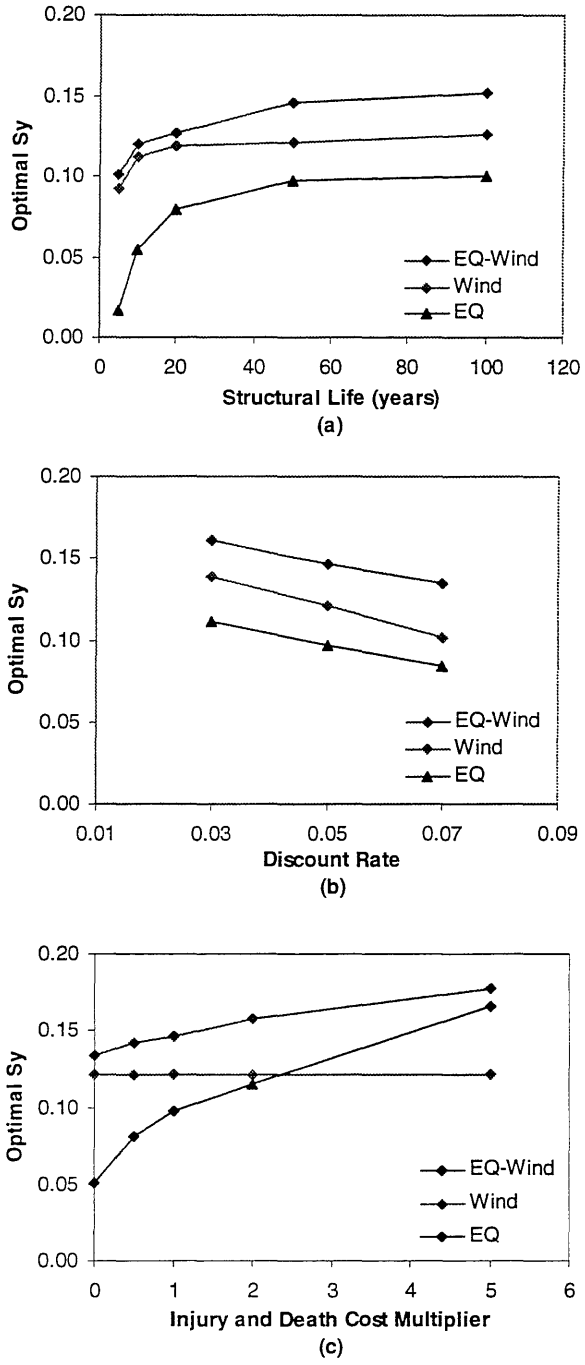

Figure 5.9 Comparison of sensitivity of optimal design for earthquake, wind and both earthquake and wind to (a) lifetime, (b) discount rate, and (c) injury and death cost at Charleston.

CHAPTER 6

SUMMARY, CONCLUSIONS, AND FUTURE WORK

6.1 Summary and Conclusions

A methodology is developed for the determination of design criteria for structures against natural hazards based on minimum expected life-cycle cost. Feasibility of application of the methodology to design for earthquakes and winds is also shown.

The optimization problem is formulated according to Wen and Ang (1991) and Wen and Shinozuka (1994) and extended to structures under multiple hazards. The emphasis is on proper modeling of the uncertainty of loads and load effects in the structural lifetime and treatment of the lifetime costs including initial cost, cost of structural limit state such as damage loss, loss of revenue and cost of death and injury. Discounting of cost over time is also considered. Parametric studies with respect to these parameters are carried out. Numerical results of design for the case of a simple limit state under earthquake and wind loads are obtained.

The methodology is then applied to the design of a 9-story office building under seismic loads in Los Angeles. Twelve designs of the structure according to a wide range of design intensity and the 1997 NEHRP provisions and multiple limit states are considered. The seismic hazard is evaluated based on USGS data and FEMA 273 provisions. The structural response (drift ratio) is calculated based on the equivalent SDOF method by Collins et al (1996) in which a nonlinear inelastic push-over analysis by DRAIN-2DX is carried out to establish the equivalent SDOF system parameters. The inelastic response spectra method and a structural capacity uncertainty correction factor are then used to evaluate the structural limit state probability. The initial cost of each structure is calculated according to the 1998 Building Construction Cost Data (BCCD).

Cost functions are developed to estimate the damage cost, relocation cost, content loss cost, economic loss cost and injury and death cost due to various structural limit states. The optimal design is obtained by minimizing the total expected life-cycle cost via a numerical procedure. A sensitivity analysis of the optimal design to change in design life, death and injury cost, structural capacity uncertainty and discount rate is carried out. The application is then extended to design in locations of different seismicity represented by Seattle, Charleston and Boston.

For design against winds, ten 9-story office buildings are considered. Design for optimal structural strength and optimal envelope strength are considered separately. The response of structural frame to the wind load is calculated using the provisions in ASCE 7-98. The same limit states and cost functions are used. Building envelope of twelve glass types according to thickness are considered. Probabilities of glass failure by wind pressure and missile debris are calculated using most recent data and information in the literature. The optimal design for wind loads is then obtained by minimizing the total expected life-cycle cost. Analysis of sensitivity of optimal design is carried out to change in lifetime, discount rate and missile availability. The application is then extended to design for both earthquake and wind loads.

The significant conclusions of this study are summarized below:

1. A methodology for the determination of design criteria based on minimum life-cycle cost is developed and the feasibility of application to earthquake and wind load is demonstrated.
2. The analytical formulation allows closed form solutions to the expected lifetime cost which also facilitates the analysis of sensitivity of optimal design to design parameters.
3. At Los Angeles, the optimal design intensity for earthquakes is higher than the intensity according to current design code (1997 NEHRP), while the differences are small at Seattle and Charleston.
4. The optimal design is not sensitive to structural capacity uncertainties, moderately sensitive to discount rate and design life change. The optimal

design for earthquakes is sensitive to the injury and death cost at Seattle and Charleston, but not at Los Angeles due to the different characteristics of seismic hazards in these regions.

5. The failure probability of the building envelope is dominated by the windborne missiles. Wind pressure-caused failure plays a minor role.
6. The optimal window glass thickness is larger than that based on current PPG glass chart. Optimal glass thickness depends moderately on discount rate for long life span and on design life changes. The optimal glass thickness is more sensitive to availability and amount of wind borne missiles.
7. The optimal design under two loads is generally controlled by the dominant load in terms of intensity and uncertainty. It is moderately sensitive to lifetime and discount rate. As in the one load case, it is sensitive to the injury and death cost at Seattle and Charleston, but not at Los Angeles.
8. The lifecycle cost based design method presented here is a useful tool for decision on design load intensity. The results have important implications in the development of future codes and design guide lines.

6.2 Suggestions for Future Research

The results of this study provide a basic framework for a minimum lifecycle cost design criteria. There are still many unresolved issues that need to be addressed before this procedure can be applied in the formulation design loads in future codes. Some of these issues are described below:

1. For definition of limit states, the relationship between measurable structural response (e.g., drift ratio) and damage status is needed. In this study, story drift ratio limits are based on Maison and Bonowitz (1998) and a cost function index follows that of FEMA 227 (1992). However, the drift ratio limit also depends on the definition of structural failure,

building story, year built, structural type and connection type (Yun and Foutch, 1998). Hence, further research to define the appropriate limit state is strongly encouraged.

2. The equivalent Single Degree of Freedom (SDOF) system method by Collins et al. (1996) and the DRAIN-2DX program used for calculating the drift ratio of the structure are two-dimensional analyses. For more accurate and realistic results, three-dimensional modeling and analysis under multi-dimensional ground motions are necessary.
3. In the cost functions, the cost indexes are used and evaluated based on the data in FEMA 227 and 228. The historic index and city index strongly depend on location and time. In order to apply the proposed methodology for more accurate results, it is necessary to use the current cost index that is used in the target area, e.g., the real property values based on living cost in a specific area.
4. In calculating the probability of envelope failure by missile impact, data are limited. In this study, many factors, e.g., resistance of laminated glass by the missile impact, are assumed based on current available data. More investigations are needed to calculate the glass properties according to its thickness, area and year manufactured. Therefore, in order to determine an accurate optimal design glass thickness based on minimum life-cycle cost, it is necessary to collect more data on old glass, new glass, glass type, strength of glass, and MMBT and MMDT of the glass.

APPENDIX A

DRIFT RATIO CALCULATION

In order to determine limit state probability and expected failure cost, structural response analyses are needed to determine the limit states according to drift ratio. For probabilistic response analysis of the system, an equivalent single-degree-of freedom (SDOF) system proposed by Collins et al. (1996) is used. In this appendix, in addition to equivalent SDOF method, the methods for determination of maximum interstory drift ratio, bias factors, elastic force coefficient, site soil factor, reduction factor and ductility factor are summarized.

A.1 Equivalent SDOF Model

Collins et al. (1996) proposed equivalent SDOF models of a MDOF structure by using an approximate analysis methodology that used the results of static push-over analysis. Equations and description for an equivalent SDOF model can be summarized as follows:

The equation of motion of a two-dimensional MDOF structure subjected to horizontal base motion can be written as

$$[M]\{\ddot{u}\}+[C]\{\dot{u}\}+\{R\}=-[M]\{1\}\ddot{u}_g \tag{A.1}$$

where *[M]* is the mass matrix, *{u}={u(t)}* is the vector of lateral displacements at each floor, *[C]* is the damping matrix, *{R}={R(t)}* is the restoring force vector, *{1}* is a vector with all components equal to unity, and $u_g=u_g(t)$ is the ground displacement.

To develop an equivalent SDOF model, assumptions are needed for the displacement vector *{u}* and the restoring force vector *{R}*. It is assumed that $\{\Psi_1\}$ represents an assumed lateral displacement profile of the structure which has been normalized such that the component of $\{\Psi_1\}$ corresponding to the top (roof) displacement

is unity and is assumed that this profile remains constant, i.e., $\{\Psi_1\}$ is not a function of time. It is assumed that $\{R\}$ can be represented by the same set of forces used in the push-over analysis, i.e., $\{R\}=V\{f\}$. Substituting for $\{R\}$ and $\{u\}$ the relations $V\{f\}$ and $\{\Psi_1\}D$, respectively, Equation (A.1) transforms to:

$$[M]\{\Psi_1\}\ddot{D}+[C]\{\Psi_1\}\dot{D}+V\{f\}=-[M]\{1\}\ddot{u}_g \tag{A.2}$$

During the push-over analysis, the variation of V and D can be monitored, and a plot of V versus D can be made. Figure A.1 shows a plot of V versus D for the 9-story building by a nonlinear push-over analysis. In general, the resulting V versus D curve can be represented mathematically as

$$V = KG(D) \tag{A.3}$$

where K is the slope of the initial portion of the curve and $G(D)$ is the scalar mathematical function describing the shape of the curve. If the relation between V and D is assumed to be a bilinear relation, then

$$\begin{aligned} G(D) &= D && for \quad D \le D_y \\ G(D) &= D_y + \alpha(D - D_y) && for \quad D > D_y \end{aligned} \tag{A.4}$$

where α is the post-to-preyield stiffness ratio and D_y is the global yield displacement. Substituting Equation (A.3) for Equation (A.4) gives

$$[M]\{\Psi_1\}\ddot{D}+[C]\{\Psi_1\}\dot{D}+KG(D)\{f\}=-[M]\{1\}\ddot{u}_g \tag{A.5}$$

By multiplying $\{\Psi_2\}^T$ on both sides, the vector equation can be reduced to a single equation,

$$\{\Psi_2\}^T[M]\{\Psi_1\}\ddot{D}+\{\Psi_2\}^T[C]\{\Psi_1\}\dot{D}+KG(D)\{\Psi_2\}^T\{f\}=-\{\Psi_2\}^T[M]\{1\}\ddot{u}_g \tag{A.6}$$

By definition of $M^*=\{\Psi_2\}^T[M]\{\Psi_1\}$, $C^*=\{\Psi_2\}^T[M]\{\Psi_1\}$, $K^*=K\Psi_2\}^T\{f\}$, $L^*=\{\Psi_2\}^T[M]\{1\}$, $P^*=L^*/M^*$, $(\omega^*)^2=K^*/M^*$, and $C^*/M^*=2\xi\omega^*$, Equation (A.6) becomes

$$M^*\ddot{D}+C^*\dot{D}+K^*G(D)=-L^*\ddot{u}_g \tag{A.7}$$

or after dividing through by M^*

$$\ddot{D}+2\xi\omega^{*}\dot{D}+(\omega^{*})^{2}G(D)=-P^{*}\ddot{u}_{g} \tag{A.8}$$

Table A.1 shows the parameters for equivalent SDOF models for the twelve 9-story building. These values are derived from the results of the nonlinear push-over analysis by DRAIN-2DX (Parkash et al., 1993).

A.2 Maximum Interstory Drift Ratio

By using the equivalent SDOF system described by Equation (A.8), maximum roof displacement, D_{max}, can be determined; then a global drift ratio can be defined as D_{max}/H where H is the total height of the structure. However, the drift ratio in each story is required to calculate limit state probabilities. Thus, it is necessary to relate the global drift ratio to the maximum interstory drift ratio.

The story drift ratio at any story i can be defined in terms of the displacements of floor i directly above the story and the floor i-1 directly below the story by

$$\Delta_{L}=\frac{u_{max,i}-u_{max,i-1}}{h_{i}}=\frac{D_{max}[\Psi_{1,i}-\Psi_{1,i-1}]}{h_{i}} \tag{A.9}$$

where Δ_L is the interstory drift ratio and h_i is the height of the story. The maximum interstory drift ratio can be calculated by

$$(\Delta_{L})_{\max}=D_{\max}\left\{\frac{[\Psi_{1,i}-\Psi_{1,i-1}]}{h_{i}}\right\}_{\max} \tag{A.10}$$

Also, the global drift ratio, Δ_G, is defined as

$$\Delta_{G}=\frac{D_{\max}}{H} \tag{A.11}$$

where H is the total height of the building. From Equation (A.10) and (A.11), the relationship between global drift ratio and maximum interstory drift ratio can be determined by using β_{LG}.

$$(\Delta_L)_{\max} = \frac{D_{\max}\left[\frac{\Psi_{1,i} - \Psi_{1,i-1}}{h_i}\right]_{\max}}{\frac{D_{\max}}{H}} \Delta_G = H\left[\frac{\Psi_{1,i} - \Psi_{1,i-1}}{h_i}\right]_{\max} \Delta_G = \beta_{LG}\Delta_G \quad \text{(A.12)}$$

A.3 Bias Factors

Based on response analysis under a set of ground motions consisting of 21 simulated records and 11 real records, Collins et al. compared the maximum roof displacement and maximum interstory drift ratio predicted by the linear and nonlinear equivalent system models and the MDOF model. They then summarized the results of the linear elastic and nonlinear inelastic responses of the MDOF system in terms of a bias factors for roof displacement and interstory drift ratio for each structure. The bias factor for a particular response quantity is the ratio of the response calculated using the MDOF model to the response calculated using the equivalent SDOF system model, i.e.,

$$bias\ factor = \frac{MDOF\ response}{Equivalent\ system\ response} \quad \text{(A.13)}$$

Bias factors for the 9-story building by Collins are summarized in Table A.2, N_s^{DISP} is bias factor for estimates of maximum roof displacement for linear elastic response, N_s^{DRIFT} is bias factor for estimates of maximum interstory drift ratio for linear elastic response, N_u^{DISP} is bias factor for estimates of maximum roof displacement for nonlinear inelastic response, and N_u^{DRIFT} is bias factor for estimates of maximum interstory drift ratio for nonlinear inelastic response. These bias factors are given as follows:

$$N_S^{DISP} = \frac{D_{MDOF}}{D_{Equivalent\ SDOF}}$$
$$N_S^{DRIFT} = \frac{\Delta_{MDOF}}{\Delta_{Equivalent\ SDOF}}$$
$$N_U^{DISP} = \frac{D_{MDOF}}{D_{Equivalent\ SDOF}} \qquad (A.14)$$
$$N_U^{DRIFT} = \frac{\Delta_{MDOF}}{\Delta_{Equivalent\ SDOF}}$$

The results showed that the equivalent system model based on $\{\Psi_2\}=\{\Psi_1\}$ (Virtual Work Formulation) predicts very well the maximum roof displacement for linear elastic response, while the equivalent system model based on $\{\Psi_2\}=\{1\}$ (Base Shear Formulation) overestimates roof displacement. On the other hand, the equivalent system model based on $\{\Psi_2\}=\{1\}$ (Base Shear Formulation) leads to a better (slightly conservative) estimates of maximum interstory drift ratio in most cases. For nonlinear inelastic response, the equivalent system model based on $\{\Psi_2\}=\{\Psi_1\}$ (Virtual Work Formulation) provides reasonably good predictions of roof displacement, and the equivalent system model based on $\{\Psi_2\}=\{1\}$ (Base Shear Formulation) provides better overall agreement with the MDOF results for computing maximum interstory drift ratio.

A.4 Elastic Force Coefficient

In the case of linear elastic response, the relative displacement to the ground can be determined by using the governing equation of motion for the SDOF system as follows:

$$\ddot{u} + 2\xi\omega\dot{u} + (\omega_n^2)u = -\ddot{x}_g \qquad (A.15)$$

where u is the relative displacement, x_g is the ground displacement, ω_n is the natural frequency, and ξ is the damping ratio. The maximum value of u at a given natural frequency under a given ground motion record can be used to determine the nondimensional maximum elastic force coefficient, *Ce*, defined as follows:

$$C_e = \frac{maximum \quad spring \quad force}{(mass) \quad (gravity)} \tag{A.16}$$

Ce can be expressed in terms of the parameters in Equation (A.15) and the maximum relative displacement, S_d.

$$C_e = (\omega_n)^2 \frac{S_d}{g} = (\frac{2\pi}{T_n})^2 \frac{S_d}{g} \tag{A.17}$$

where g is the acceleration of gravity expressed in appropriate units. Since C_e is equal to the spectral acceleration in terms of gravity, the uniform hazard response spectra in USGS and FEMA 273 can be used directly to calculate the C_e values.

Since uniform hazard spectra varies for different regions, Algermissen and Leyendecker (1992) proposed an approximate uniform hazard curve using the spectral ordinates at two periods: 0.3 second and 1.0 second.

$$C_e^p(T) = minimum\left[C_e^p(T=0.3), \frac{C_e^p(T=1.0)}{T^n} \right] \tag{A.18}$$

where p is the exceedance probability, n is an exponent depending on location and is equal to 0.924 for California and 1.300 for the central and eastern United States, and $C_e^p(T=0.3)$ and $C_e^p(T=1.0)$ are the mapped ordinates at periods of 0.3 and 1.0 second, respectively.

Table A.3 shows the elastic force coefficients for 12 structures at Los Angeles corresponding to an exceedance probability in 50 years.

A.5 Site Soil Factor

Borcherdt and others (1994) proposed regression curves after analyzing data recorded at 35 free-field sites. These regression curves describe horizontal spectral amplification factors as a function of mean shear wave velocity for two period ranges as follows:

Short-Period Range: $$F_a = (\frac{v_{ref}}{v_{site}})^{m_a} \quad \text{(A.19)}$$

Mid-Period Range: $$F_v = (\frac{v_{ref}}{v_{site}})^{m_v} \quad \text{(A.20)}$$

where F_a and F_v are the site soil factors, v_{ref} is the mean shear wave velocity for the reference soil conditions, v_{site} is the mean shear velocity for the soil profile at the site, and m_a and m_v are regression parameters. According to Collins et al. (1996), the short period range covers periods from 0.1 second up to about 0.4-0.5 second and the mid-period range includes periods between about 0.4 second and 2.0 seconds. Based on regression analyses of the data from the Loma Prieta Earthquake, the value of m_a and m_v are 0.35 and 0.65, respectively.

A.6 Reduction Factor and Ductility Factor

In the nonlinear response analysis for structure, a ductility reduction factor is often used to account for nonlinear inelastic behavior. Reduction factor can be determined using the method proposed by Collins et al. (1996) and Nassar and Krawinkler (1992).

Collins et al. (1996) defined the spectral reduction factor as the ratio of the elastic force coefficient, C_e, to the system yield force coefficient, C_y, at period T for a given target probability p, target ductility ratio μ, and strain-hardening ratio α, i.e.,

$$R(p,T,\mu,\alpha) \equiv \frac{C_e^p(T)}{C_y^p(T,\mu,\alpha)} \quad \text{(A.21)}$$

where nondimensional yield force coefficient, C_y, is defined as the ratio of the elastic force when $d=d_y$ to the weight of the structure, and can be expressed as

$$C_y = (\omega_n)^2 \frac{d_y}{g} \quad \text{(A.22)}$$

where d_y is the yield displacement of the SDOF structure.

Nassar and Krawinkler (1992) proposed the following empirical formula based on 15 records:

$$R_\mu = \left[c\,(\mu - 1) + 1\right]^{\frac{1}{c}} \tag{A.23}$$

in which R_μ is ductility reduction factor, μ is ductility ratio, and c is simple function of structural period and strain-hardening ratio. c is determined by

$$c = \frac{T^a}{T^a + 1} + \frac{b}{T} \tag{A.24}$$

where a and b are parameters which depend on the strain-hardening ratio α. Interpolating between the data provided by Nassar and Krawinkler for α=2 per cent and α=10 per cent, the values of a and b for α=5 per cent are 0.93 and 0.34, respectively.

Comparison between two reduction factors by Collins et al. (1996) showed that the difference is small and may be neglected in practical applications. Hence the ductility factor can be determined by using Equation (A.21) and (A.23), for given C_e, C_y, and c. The equation for the ductility factor can be established as follows:

$$\mu = 1 + \frac{1}{c}\left[\left(\frac{C_e}{C_y}\right)^c - 1\right] \tag{A.25}$$

where C_e, C_y, and c at $T = T^*$ are determined from Equation (A.18), (A.22), and (A.24), respectively. When C_y is calculated, soil factor f and equivalent system parameter P^* should be considered in Equation (A.22).

Table A.4 shows yield force coefficient, C_y, parameter, c, and ductility factor, μ, for each structure, in which a strain hardening ratio of 5% is assumed.

A.7 Calculation of Drift Ratio

According to Collins et al. (1996), maximum interstory drift ratio can be determined by using two different equations. One equation is for linear elastic response and the other is for nonlinear inelastic response.

The maximum interstory drift ratio predicted by equivalent system model for linear elastic response is given by

$$\Delta_{ES} = \frac{\beta_{LG}}{H} D_{ES} \tag{A.26}$$

where D_{ES} is maximum roof displacement predicted by the equivalent system model, β_{LG} is the equivalent system parameter, and H is the total structure height. Equation (A.26) can be rewritten in terms of spectral displacement, S_d, as follows:

$$\Delta_{ES} = \frac{\beta_{LG}}{H} P^* \cdot f \cdot S_d \tag{A.27}$$

where f is the site soil factor, and P^* is the excitation scale factor from the linear elastic equivalent SDOF model. Equation (A.27) can be rewritten in terms of the elastic force coefficient C_e in Equation (A.17) as

$$\Delta_{ES} = \frac{\beta_{LG}}{H} P^* \cdot f \cdot C_e \cdot \left[g \left(\frac{T^*}{2\pi} \right)^2 \right] \tag{A.28}$$

The maximum interstory drift ratio based on Equation (A.28) is approximate is then connected for bias by

$$\Delta_L = N_L^{DRIFT} \cdot \Delta_{ES} \tag{A.29}$$

Finally, maximum interstory drift ratio can be obtained by

$$\Delta = N_s^{DRIFT} \cdot \frac{\beta_{LG}}{H} \cdot P^* \cdot f \cdot C_e \cdot \left[g \left(\frac{T^*}{2\pi} \right)^2 \right] \tag{A.30}$$

where T^* is the parameter from the linear elastic equivalent SDOF model.

For nonlinear inelastic response, the estimated maximum interstory drift ratio from the equivalent system model, Δ_{ES}, is

$$\Delta_{ES} = \frac{\beta_{LG}}{H} D_{ES} \tag{A.31}$$

After correction for bias, one obtains

$$\begin{aligned}\Delta &= N_u^{DRIFT} \cdot \Delta_{ES} \\ &= N_u^{DRIFT} \cdot \frac{\beta_{LG}}{H} \cdot D_{ES} \\ &= N_u^{DRIFT} \cdot \frac{\beta_{LG}}{H} \cdot \mu \cdot D_y\end{aligned} \tag{A.32}$$

where $N_U{}^{DRIFT}$ is the value of the bias factor, μ is ductility factor, and D_y is global yield displacement.

Table A.1 Parameters for equivalent SDOF model.

		S1	S2	S3	S4	S5	S6	S7	S8	S9	S10	S11	S12
For Linear Elastic	L^*	13.06	13.17	13.30	13.41	13.52	13.63	13.75	13.86	13.97	14.08	14.42	14.83
	M^*	6.82	6.85	6.94	7.19	7.24	7.23	7.40	7.39	7.45	7.47	7.32	7.77
	P^*	1.915	1.922	1.915	1.866	1.867	1.885	1.857	1.876	1.876	1.886	1.971	1.908
	β_{LG}	1.127	1.109	1.098	1.076	1.063	1.072	1.047	1.047	1.046	1.053	1.009	1.051
	K^*	13.08	24.56	38.36	47.79	61.51	74.17	86.11	98.05	111.0	122.9	158.3	204.2
	W^*	1.38	1.89	2.35	2.58	2.91	3.20	3.41	3.64	3.86	4.06	4.65	5.13
	T^*	4.538	3.319	2.673	2.437	2.156	1.962	1.842	1.725	1.628	1.549	1.351	1.226
For Non-linear Inelastic	L^*	13.06	13.17	13.30	13.41	13.52	13.63	13.75	13.86	13.97	14.08	14.42	14.83
	M^*	6.46	6.72	7.05	7.48	7.72	7.71	7.90	7.89	7.98	8.01	8.33	8.58
	P^*	2.203	1.960	1.886	1.793	1.751	1.767	1.741	1.758	1.751	1.757	1.730	1.728
	β_{LG}	1.240	1.182	1.188	1.287	1.322	1.274	1.282	1.316	1.282	1.268	1.393	1.374
	K^*	12.61	24.23	38.26	47.81	61.50	74.61	86.37	98.87	111.9	124.7	162.9	162.9
	W^*	1.40	1.90	2.33	2.53	2.82	3.11	3.31	3.54	3.74	3.95	4.42	4.36
	T^*	4.496	3.309	2.697	2.485	2.226	2.020	1.900	1.774	1.678	1.593	1.421	1.442

Table A.2 Statistics for bias factors by Collins et al. (1996).

Bias Factors	$\{\Psi_2\}=\{1\}$ (Base Shear)		$\{\Psi_2\}=\{\Psi_1\}$ (Virtual Work)	
	Mean	Std. Dev.	Mean	Std. Dev.
N_s^{DISP}	0.73	0.041	0.98	0.051
N_s^{DRIFT}	0.96	0.27	1.29	0.35
N_u^{DISP}	0.79	0.18	0.92	0.17
N_u^{DRIFT}	0.90	0.19	1.06	0.20

Table A.3 Elastic force coefficient (C_e) for each structure at Los Angeles.

Structure	2%/50yrs	5%/50yrs	10%/50yrs	50%/50yrs	75%/50yrs
S1	0.214	0.151	0.110	0.048	0.036
S2	0.285	0.201	0.147	0.064	0.047
S3	0.344	0.243	0.177	0.078	0.057
S4	0.371	0.262	0.191	0.084	0.062
S5	0.410	0.290	0.212	0.093	0.068
S6	0.449	0.317	0.231	0.101	0.075
S7	0.475	0.336	0.245	0.107	0.079
S8	0.506	0.358	0.261	0.114	0.084
S9	0.533	0.377	0.275	0.120	0.089
S10	0.558	0.394	0.288	0.126	0.093
S11	0.619	0.437	0.319	0.140	0.103
S12	0.683	0.483	0.352	0.154	0.114

Table A.4 System yield force coefficient (C_y), parameter c and ductility factor (μ).

Structure	C_y	c	Ductility Factor μ in 50 years				
			2%	5%	10%	50%	75%
S1	0.052	0.877	3.825	2.784	2.076	linear	linear
S2	0.095	0.855	2.815	2.048	1.523	linear	linear
S3	0.146	0.842	2.259	1.639	1.213	linear	linear
S4	0.180	0.837	1.991	1.440	1.060	linear	linear
S5	0.219	0.831	1.824	1.316	linear	linear	linear
S6	0.263	0.826	1.670	1.201	linear	linear	linear
S7	0.294	0.824	1.589	1.140	linear	linear	linear
S8	0.332	0.822	1.503	1.076	linear	linear	linear
S9	0.359	0.821	1.466	1.048	linear	linear	linear
S10	0.383	0.820	1.443	1.031	linear	linear	linear
S11	0.502	0.820	1.229	linear	linear	linear	linear
S12	0.638	0.823	1.072	linear	linear	linear	linear

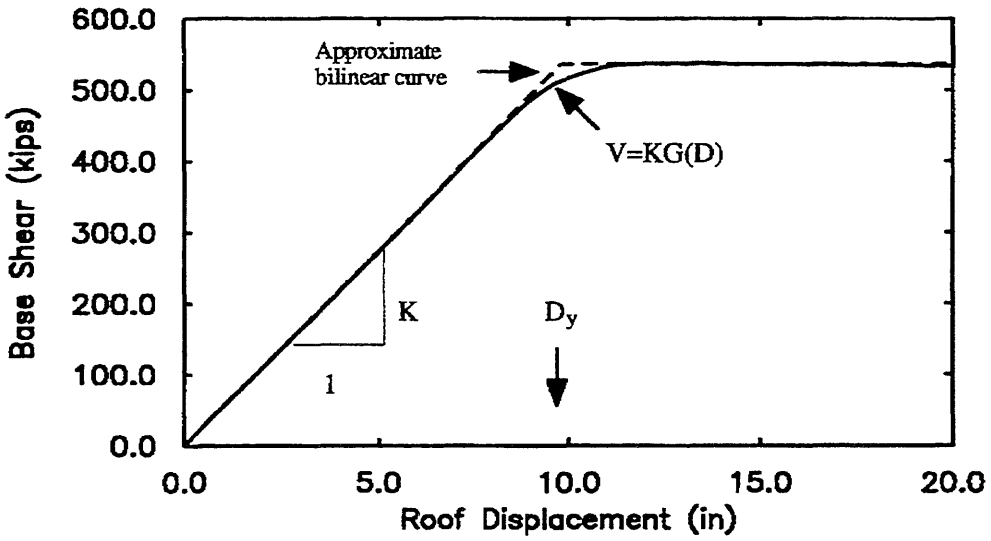

Figure A.1 Plot of base shear (V) and roof displacement (D) by Collins (1995).

APPENDIX B

CONVERSION OF LIFETIME LIMIT STATE PROBABILITY TO LIMIT STATE PROBABILITY GIVEN THE OCCURRENCE OF A HAZARD

If maintenance cost, C_m, is not considered, Equation (2.4) can be rewritten as

$$E[C(t,X)] = C_0 + (C_1P_1 + C_2P_2 + \ldots\ldots + C_kP_k)\frac{\nu}{\lambda}(1-e^{-\lambda t}) \tag{B.1}$$

However, in this equation, P_k is not a probability of exceedance but a k^{th} limit state probability. Thus, the relationship between probability of exceedance and limit state probability is needed.

If $P_t\ (\Delta>\Delta_a)$ is the probability that Δ is larger than Δ_a in t years, and if hazard occurrences can be modeled by a Poisson Process with occurrence rate of ν per year, the probability, $P_t\ (\Delta>\Delta_a)$, can be expressed by limit state probability, P_l, and occurrence rate, ν, as follows:

$$P_t(\Delta > \Delta_a) = 1 - e^{-\nu \cdot P_l(\Delta>\Delta_a)\cdot t} \tag{B.2}$$

where $P_l\ (\Delta>\Delta_a)$ is limit state probability that Δ is larger than Δ_a. From this equation, limit state probability is derived as:

$$P_l(\Delta > \Delta_a) = -\frac{1}{\nu \cdot t}\left[\ln(1 - P_t(\Delta > \Delta_a)\right] \tag{B.3}$$

If there are seven limit states, then there are 6 limit drift ratios as shown in Figure B.1. Based on Equation (B.3), each limit state probability can be expressed in terms of limit drift ratio as follows:

$$\begin{aligned} P_I &= P_l(\Delta < \Delta_I) = 1 - P_l(\Delta > \Delta_I) \\ &= 1 - \left\{-\frac{1}{\nu \cdot t}\left[\ln(1 - P_t(\Delta > \Delta_I)\right]\right\} \end{aligned} \tag{B.4}$$

$$
\begin{aligned}
P_i &= P_t(\Delta > \Delta_{i-1}) - P_t(\Delta > \Delta_i) \\
&= -\frac{1}{\nu \cdot t}\{\ln[1 - P_t(\Delta > \Delta_{i-1})\} - (-\frac{1}{\nu \cdot t})\{\ln[1 - P_t(\Delta > \Delta_i)\} \\
&= \frac{1}{\nu \cdot t}\{\ln[1 - P_t(\Delta > \Delta_i) - \ln[1 - P_t(\Delta > \Delta_{i-1})\}
\end{aligned} \tag{B.5}
$$

$$
\begin{aligned}
P_{VII} &= P_t(\Delta > \Delta_{VI}) \\
&= \frac{1}{\nu \cdot t}\{-\ln[1 - P_t(\Delta > \Delta_{VI})]\}
\end{aligned} \tag{B.6}
$$

where i is from II to VI. If $G_t(\Delta_i) = \ln [1\text{-}P_t (\Delta > \Delta_i)]$, Equation (B.4), (B.5), and (B.6) can be rewritten as

$$P_I = 1 + \frac{1}{\nu \cdot t} G_t(\Delta_I) \tag{B.7}$$

$$P_i = \frac{1}{\nu \cdot t}\{G_t(\Delta_i) - G_t(\Delta_{i-1})\} \tag{B.8}$$

$$P_{VII} = \frac{1}{\nu \cdot t}[-G_t(\Delta_{VI})] \tag{B.9}$$

If annual probability of exceedance is used, Equation (B.4), (B.5), and (B.6) can be changed as follows:

$$P_I = 1 - \left\{-\frac{1}{\nu}\left[\ln(1 - P_a(\Delta > \Delta_I)\right]\right\} \tag{B.10}$$

$$P_i = \frac{1}{\nu}\{\ln[1 - P_a(\Delta > \Delta_i) - \ln[1 - P_a(\Delta > \Delta_{i-1})\} \tag{B.11}$$

$$P_{VII} = \frac{1}{\nu}\{-\ln[1 - P_a(\Delta > \Delta_{VI})]\} \tag{B.12}$$

where i is from II to VI, and P_a is annual probability of exceedance. If $G_a(\Delta_i) = ln\ [1\text{-}P_a\ (\Delta > \Delta_i)]$, Equation (B.10), (B.11), and (B.12) are also rewritten as follows:

$$P_I = 1 + \frac{1}{\nu} G_a(\Delta_I) \tag{B.13}$$

$$P_i = \frac{1}{\nu}\{G_t(\Delta_i) - G_a(\Delta_{i-1})\} \tag{B.14}$$

$$P_{VII} = \frac{1}{\nu}[-G_a(\Delta_{VI})] \tag{B.15}$$

Therefore, by using Equation (B.7), (B.8), and (B.9), Equation (B.1) can be expressed in terms of probability of exceedance in t years as follows:

$$E[C(t,X)] = C_0 + \left\{ C_I \cdot [1 + \frac{1}{\nu \cdot t} G_t(\Delta_I)] + C_{II} \cdot \frac{1}{\nu \cdot t}[G_t(\Delta_{II}) - G_t(\Delta_I)] \right.$$
$$\left. + \ldots\ldots + C_{VII} \cdot \frac{1}{\nu \cdot t}[-G_t(\Delta_{VI})] \right\} \cdot \frac{\nu}{\lambda}(1 - e^{-\lambda t}) \tag{B.16}$$

If occurrence rate ν in Equation (B.16) cancels each other, occurrence rate ν remains only in a first limit state term as follows:

$$E[C(t,X)] = C_0 + \left\{ C_I \cdot [\nu + \frac{1}{t} G_t(\Delta_I)] + C_{II} \cdot \frac{1}{t}[G_t(\Delta_{II}) - G_t(\Delta_I)] \right.$$
$$\left. + \ldots\ldots + C_{VII} \cdot \frac{1}{t}[-G_t(\Delta_{VI})] \right\} \cdot \frac{1}{\lambda}(1 - e^{-\lambda t}) \tag{B.17}$$

Therefore, if C_I is zero in Equation (B.16), the total expected cost can be calculated without occurrence rate ν.

If annual probability of exceedance is used, Equation (B.17) can be rewritten as follows:

$$E[C(t,X)] = C_0 + \left\{ C_I \cdot [\nu + G_t(\Delta_I)] + C_{II} \cdot [G_t(\Delta_{II}) - G_t(\Delta_I)] \right.$$
$$\left. + \ldots\ldots + C_{VII} \cdot [-G_t(\Delta_{VI})] \right\} \cdot \frac{1}{\lambda}(1 - e^{-\lambda t}) \tag{B.18}$$

In this case, total expected cost can also be obtained without occurrence rate ν if C_I is zero. If the modified limit state probability is defined as

$$MP_I = \nu + G_a(\Delta_I) \tag{B.19}$$

$$MP_i = G_t(\Delta_i) - G_a(\Delta_{i-1}) \tag{B.20}$$

$$MP_{VII} = -G_a(\Delta_{VI}) \tag{B.21}$$

where i is from II to VI, Equation (B.18) can be further simplified as follows:

$$E[C(t,X)] = C_0 + \{C_I \cdot MP_I + C_{II} \cdot MP_{II} + ... + C_{VII} \cdot MP_{VII}\} \cdot \frac{1}{\lambda}(1 - e^{-\lambda t}) \quad \text{(B.22)}$$

Limit state probability can be obtained by using Equation (B.22).

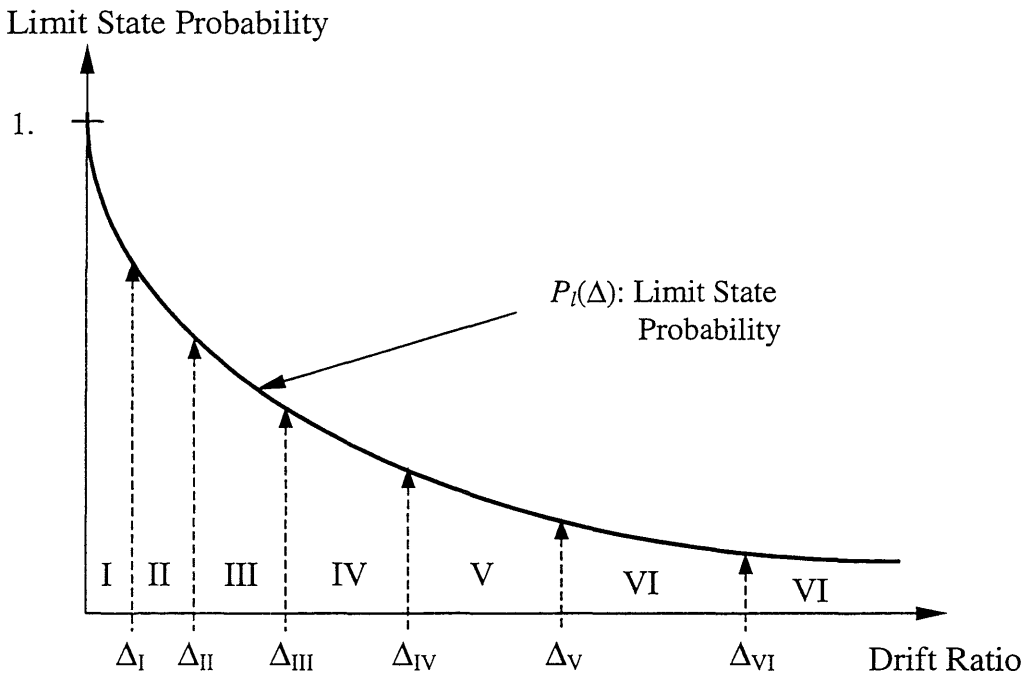

Figure B.1 Limit state probability (P_l)

APPENDIX C

INITIAL COST CALCULATION

As mentioned in Chapter 3, in general, initial cost is proportional to design intensity. In this study, system yield force coefficient, S_y, is used as design intensity, and 12 structures are designed according to different design response spectral accelerations; therefore, the initial cost will be different according to system yield force coefficient for each structure.

Since it is assumed that nonstructural items are same for all structures, there is no affection in determination of the optimal design intensity due to increasing the initial cost by nonstructural component cost. As shown in Figure C.1, the increase of initial cost by the nonstructural items cost only adjust the total expected life-cycle cost accordingly, and there is no change in optimal design intensity. Therefore, in this study, nonstructural items are not considered in calculating initial cost; initial cost is composed of only the cost of structural frame.

The items for initial cost are steel, shear connectors, metal decking, welded wire fabric, concrete (light weight), beam fireproofing and column fireproofing. Steel costs are calculated according to 1998 Building Construction Cost Data (BCCD), and other costs are calculated according to 1996 Means BCCD by Georgetown Laboratory Cost Estimate as shown in Table C.3.

For the calculation of steel cost, bare cost is the sum of material, installation (labor and equipment) cost. As adjustments for building story \$70 for bare cost and by \$100 for total cost, respectively, are used to general average cost per ton. Total cost includes size extra, specification extra, quantity extra and overhead and profit (Q&P). All these extra costs are based on 1998 Means BCCD. For calculation of shear connectors, metal decking, welded wire fabric, concrete (light weight), beam fireproofing and column fireproofing, the unit cost according to 1996 Means BCCD by Georgetown Laboratory

Cost Estimate are used. $ 1.75 is unit cost for each shear connector. The other unit costs are $1.86 for metal decking per square foot, $37 for welded wire fabric per 100 square feet, $1.63 for concrete (light weight) per square foot, $1.14 for beam fireproofing per square foot, $1.46 for column fireproofing per square foot, respectively. Beam fireproofing area and column fireproofing area can be calculated by:

$$\begin{aligned} Beam\,Fireproofing\ Area &= (2\times d + 3\times b_f - 4\times k_1)\times length \\ Column\,Fireproofing\ Area &= (2\times d + 4\times b_f - 4\times k_1)\times length \end{aligned} \tag{C.1}$$

in which d, b_f and k_1 are depth, flange width, and distance, respectively, as shown in Figure C.2.

For the calculation of initial cost, location factor is needed to adjust from national average to selected site. As a city cost index, 111.2, 105.5, 77.6, and 116.7 are used according to 98 BCCD. To convert 1996 Means BCCD to 1998 costs, historical cost index is needed. As a historical index, 1.038 is used. Table C.1 shows the whole initial cost calculation for structure S4. Table C.2 shows the initial costs adjusted by city cost index for four cities.

Table C.1 Calculation of initial cost for S4.

Floor	9	8	7	6	5	4	3	2	1	SUM
Beam 1	W18 x 35	W18 x 40	W18 x 40	W18 x 40	W18 x 40	W18 x 40	W18 x 40	W18 x 40	W18 x 40	
length(ft)	1225	1225	1225	1225	1225	1225	1225	1225	1225	
lb/ft	35	40	40	40	40	40	40	40	40	
lb	42875	49000	49000	49000	49000	49000	49000	49000	49000	434875
ton	19.4	22.2	22.2	22.2	22.2	22.2	22.2	22.2	22.2	197.3
d	17.70	17.90	17.90	17.90	17.90	17.90	17.90	17.90	17.90	
bf	6.000	6.015	6.015	6.015	6.015	6.015	6.015	6.015	6.015	
k1	0.75	0.81	0.81	0.81	0.81	0.81	0.81	0.81	0.81	
Area	5145.0	5164.9	5164.9	5164.9	5164.9	5164.9	5164.9	5164.9	5164.9	46464.3

Floor	9	8	7	6	5	4	3	2	1	SUM
Beam 2	W21 x 44	W21 x 57	W24 x 84	W27 x 84	W30 x 99	W30 x 99	W30 x 99	W30 x 108	W30 x 108	
length(ft)	350	350	350	350	350	350	350	350	350	
lb/ft	44	57	84	84	99	99	99	108	108	
lb	15400	19950	29400	29400	34650	34650	34650	37800	37800	273700
ton	7.0	9.0	13.3	13.3	15.7	15.7	15.7	17.1	17.1	124.2
d	20.66	21.06	24.10	26.71	29.65	29.65	29.65	29.83	29.83	
bf	6.500	6.555	9.020	9.960	10.450	10.450	10.450	10.475	10.475	
k1	0.88	0.88	0.94	0.94	1.00	1.00	1.00	1.00	1.00	
Area	1671.8	1700.0	2085.7	2320.2	2527.3	2527.3	2527.3	2540.0	2540.0	20439.6

Table C.1 Calculation of initial cost for S4 (cont.).

Floor	9	8	7	6	5	4	3	2	1	SUM
Column 1	W14 x 48	W14 x 48	W14 x 48	W14 x 48	W14 x 48	W14 x 82	W14 x 82	W14 x 109	W14 x 109	
length(ft)	130	130	130	130	130	130	130	130	150	
lb/ft	48	48	48	48	48	82	82	109	109	
lb	6240	6240	6240	6240	6240	10660	10660	14170	16350	83040
ton	2.8	2.8	2.8	2.8	2.8	4.8	4.8	6.4	7.4	37.7
d	13.79	13.79	13.79	13.79	13.79	14.31	14.31	14.32	14.32	
bf	8.030	8.030	8.030	8.030	8.030	10.130	10.130	14.605	14.605	
k1	0.88	0.88	0.88	0.88	0.88	1.00	1.00	0.88	0.88	
Area	608.8	608.8	608.8	608.8	608.8	705.7	705.7	905.2	1044.5	6405.3

Floor	9	8	7	6	5	4	3	2	1	SUM
Column 2	W14 x 132	W14 x 211	W14 x 211	W14 x 233	W14 x 233	W14 x 257	W14 x 257	W14 x 257	W14 x 257	
length(ft)	104	104	104	104	104	104	104	104	120	
lb/ft	132	211	211	233	233	257	257	257	257	
lb	13728	21944	21944	24232	24232	26728	26728	26728	30840	217104
ton	6.2	10.0	10.0	11.0	11.0	12.1	12.1	12.1	14.0	98.5
d	14.66	15.72	15.72	16.04	16.04	16.38	16.38	16.38	16.38	
bf	14.725	15.800	15.800	15.890	15.890	15.995	15.995	15.995	15.995	
k1	0.94	1.13	1.13	1.19	1.19	1.19	1.19	1.19	1.19	
Area	732.1	781.2	781.2	787.7	787.7	797.2	797.2	797.2	919.9	7181.6

Table C.1 Calculation of initial cost for S4 (cont.).

Floor	9	8	7	6	5	4	3	2	1	SUM
Column 3	W14 x 132	W14 x 233	W14 x 233	W14 x 257	W14 x 257	W14 x 283	W14 x 283	W14 x 311	W14 x 311	
length(ft)	130	130	130	130	130	130	130	130	150	
lb/ft	132	233	233	257	257	283	283	311	311	
lb	17160	30290	30290	33410	33410	36790	36790	40430	46650	305220
ton	7.8	13.7	13.7	15.2	15.2	16.7	16.7	18.3	21.2	138.4
d	14.66	16.04	16.04	16.38	16.38	16.74	16.74	17.12	17.12	
bf	14.725	15.890	15.890	15.995	15.995	16.110	16.110	16.230	16.230	
k1	0.94	1.19	1.19	1.19	1.19	1.25	1.25	1.31	1.31	
Area	915.1	984.6	984.6	996.6	996.6	1006.6	1006.6	1017.4	1173.9	9082.0

Items	Unit Cost ($/sqft)	#, Area, CSF,	Cost	Adjusted Cost by Historical Index
Shear Connectors	1.75	4860	8,505	8,828
Metal Decking	1.86	121500	225,990	234,578
Welded wire Fabric	37	1215	44,955	46,663
Concrete (Lightweight)	1.63	121500	198,045	205,571
Beam fireproofing	1.14	66904	76,270	79,169
Column Fireproofing	1.46	22669	33,096	34,354

Table C.2 Initial cost of 4 cities for S4.

City	Total Cost	City Index	Initial Cost
Los Angeles	1,789,747	1.112	1,990,199
Charleston	1,789,747	0.776	1,388,844
Seattle	1,789,747	1.055	1,888,183
Boston	1,789,747	1.167	2,088,635

Table C.3 1996 Mean BCCD Georgetown Laboratory Cost Estimate by CE 318 class note.

GEORGETOWN LABORATORY COST ESTIMATE (Typical Bay)

1996 MEANS BCCD ITEM	QUANT	UNITS	MEANS INDEX NO.	UNIT COST	TOTAL COST
			STRUCTURAL STEEL SYSTEM		
Steel Beams(Welded)	7.57	Tons	0512550800	$2,375.00	$17,979
Shear Connectors	144	Each	0505600010	$1.75	$252
Steel Columns(Welded)	2.4	Tons	0512550800	$2,375.00	$5,700
Metal Decking 2-in gal	1848	SqFt.	0531045400	$1.86	$3,437
Welded wire fabric	19	CSF	0322070500	$37.00	$703
Concrete (Lightweight)	1848	sqft	0331303300	$1.63	$3,012
Beam fireproofing	1512	SqFt	0725540400	$1.14	$1,724
Column Fireproofing	300	SqFt	0725540700	$1.46	$438
TOTAL					$33,245
UNIT COST/ SQUARE FOOT=					$17.99

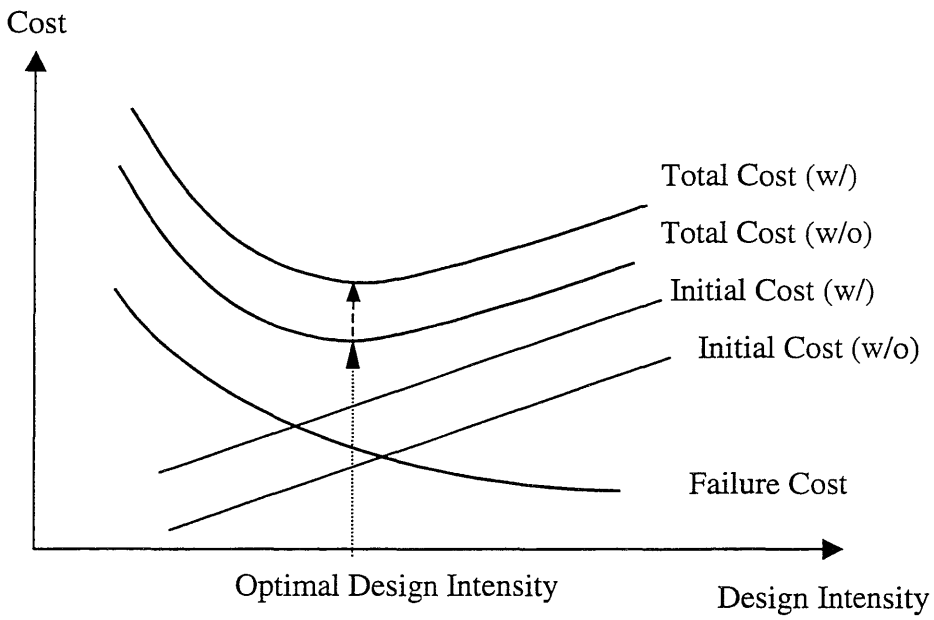

Figure C.1 Optimal design intensity and initial cost with and without cost of nonstructural items.

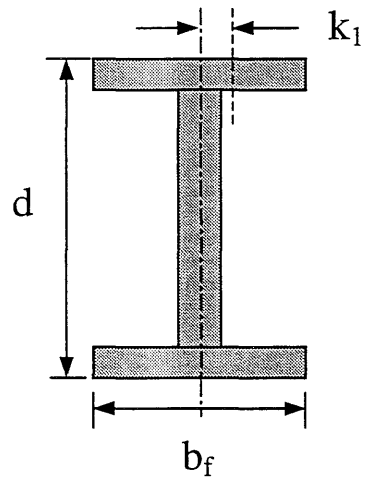

Figure C.2 Shape of steel member assumed for calculating initial cost.

APPENDIX D

MAXIMUM ALONG-WIND DISPLACEMENT

In ASCE 7-98, the equation for the maximum along-wind displacement, $X_{max}(z)$, as a function of height about the ground surface is given by

$$X_{\max}(z) = \frac{\phi(z)\,\rho\,B\,h\,C_{fx}\,\hat{V}_{\bar{z}}^2}{2m_l\,(2\pi n_1)^2} KG \tag{D.1}$$

where $\varphi(z)$ is the fundamental mode shape given by $(z/h)^{\xi}$, ξ is the mode exponent, ρ is air density, B is building width, h is building height, C_{fx} is mean along-wind force coefficient, and $\hat{V}_{\bar{z}}$ is the 3-second gust speed at height $\bar{z}$. $\hat{V}_{\bar{z}}$ is evaluated by

$$\hat{V}_{\bar{z}} = \hat{b}(\bar{z}/33)^{\hat{\alpha}} V \tag{D.2}$$

where $\hat{\alpha}$ and $\hat{b}$ are given in Table 6-4 in ASCE 7-98, V is the 3-sec gust speed in exposure C at the reference height, m_l is modal mass given by

$$m_l = \int_0^h \mu(z)\phi^2(z)dz \tag{D.3}$$

$\mu(z)$ is mass per unit height, n_1 is building natural frequency, K is given by

$$K = (1.65)^{\hat{\alpha}} / (\hat{\alpha} + \xi + 1) \tag{D.4}$$

G is gust effect factor, for rigid structure whose fundamental frequency is greater than or equal to 1 hz. It may be taken 0.85 or calculated by the formula:

$$G = 0.925\left[\frac{1+1.7\,g_Q\,I_{\bar{z}}\,Q}{1+1.7\,g_v\,I_{\bar{z}}}\right] \tag{D.5}$$

For flexible building whose fundamental frequency is less than 1 hz, gust effect factor G is given by

$$G = 0.925\left[\frac{1+1.7\,I_{\bar{z}}\sqrt{g_Q^2Q^2 + g_R^2R^2}}{1+1.7\,g_v\,I_{\bar{z}}}\right] \tag{D.6}$$

where $I_{\bar{z}}$ is intensity of turbulence at height $\bar{z}$, it is given by

$$I_{\bar{z}} = c(33/\bar{z})^{1/6} \tag{D.7}$$

where $\bar{z}$ is the equivalent height of the structure defined as 0.6 h but not less than z_{min} for all building height. z_{min} and c are listed for each exposure in Table 6-4 in ASCE 98-7. g_Q and g_v shall be taken as 3.4 and g_R is given by

$$g_R = \sqrt{2\ln(3600 n_1)} + \frac{0.577}{\sqrt{2\ln(3600 n_1)}} \tag{D.8}$$

The background response Q is given by

$$Q = \sqrt{\frac{1}{1+0.63\left(\frac{B+h}{L_{\bar{z}}}\right)^{0.63}}} \tag{D.9}$$

where $L_{\bar{z}}$ is the integral length scale of turbulence at the equivalent height given by

$$L_{\bar{z}} = l(\bar{z}/33)^{\bar{\varepsilon}} \tag{D.10}$$

in which l and $\bar{\varepsilon}$ are constants listed in Table 6-4 in ASCE 98-7. R, the resonant response factor, is given by

$$R = \sqrt{\frac{1}{\beta} R_n R_h R_B (0.53 + 0.47 R_L)} \tag{D.11}$$

where β is damping ratio, percent of critical, and R_n is given by

$$R_n = \frac{7.47 N_1}{(1+10.3 N_1)^{5/3}} \tag{D.12}$$

where N_l is

$$N_1 = \frac{n_1 L_{\bar{z}}}{\bar{V}_{\bar{z}}} \tag{D.13}$$

in which n_l is building natural frequency. R_h, R_B and R_L can be obtained by the following equation, where the subscript l shall be taken as h, B, and L, respectively.

$$R_l = \begin{cases} \frac{1}{\eta} - \frac{1}{2\eta^2}(1-e^{-2\eta}) & for\ \eta > 0 \\ 1 & for\ \eta = 0 \end{cases} \tag{D.14}$$

$$R_l = R_h \quad setting \quad \eta = 4.6 n_1 h / \overline{V}_{\bar{z}}$$

$$R_l = R_B \quad setting \quad \eta = 4.6 n_1 B / \overline{V}_{\bar{z}}$$

$$R_l = R_L \quad setting \quad \eta = 15.4 n_1 L / \overline{V}_{\bar{z}}$$

where L is horizontal dimension of a building measured parallel to the wind direction, $\overline{V}_{\bar{z}}$ is mean hourly wind speed (ft/sec) at height $\bar{z}$ determined from

$$\overline{V}_{\bar{z}} = b\left(\frac{\bar{z}}{33}\right)^{\overline{\alpha}} V\left(\frac{88}{60}\right) \tag{D.15}$$

where $\overline{b}$ and $\overline{\alpha}$ are constants in Table 6-4 in ASCE 7-98, and V is the basic wind speed in mph.

REFERENCES

Allen, E., *Fundamentals of Building Construction Materials and Methods*, John Wiley & Sons, 1990.

Ambrose, J., *Building Structure*, John Wiley & Sons, 1993.

Ang, A. H.-S. and Leon, D., "Development of Target Reliability for Design and Upgrading of Structures," *Structural Safety*, Vol. 14, No. 1, 1997.

Applied Technology Council, Earthquake Damage Evaluation Data for California, ATC-13, 1985.

Applied Technology Council, Seismic Vulnerability and Impact of Disruption of Lifelines in the Conterminous United States, ATC-25, 1991.

ASCE Standard, *Minimum Design Loads for Buildings and Other Structures*, ANSI/ASCE 7-98, 1999.

Barton C. and Nishenko S., "Natural Disasters: Forecasting Economic and Life Losses," U.S. Geological Survey Fact Sheet, 1999. (http://marine.usgs.gov/fact-sheets/nat-disasters)

Beason, W. L. and Morgan, J. R., "Glass Failure Prediction Model," *Journal of Structural Engineering*, ASCE, Vol. 110, No. 2, pp. 197-212, 1984.

Beason, W. L., Meyers, G., and James, R., "Hurricane Related Window Glass Damage in Houston," *Journal of Structural Engineering*, ASCE, Vol. 110, No. 12, pp. 2843-2857, 1984.

Behr, R. A., Minor, J. E., and Linden, M. P., "Load Duration and Interlayer Thickness Effects on Laminated Glass," *Journal of Structural Engineering*, ASCE, Vol. 112, No. 6, pp. 1441-1453, 1986.

Behr, R. A., Minor, J. E., Linden, M. P., and Vallabhan, C. V. G., "Laminated Glass Units under Lateral Pressure," *Journal of Structural Engineering*, ASCE, Vol. 111, No. 5, pp. 1037-1050, 1985.

Belk, C. A. and Bennett, R. M., "Macro Wind Parameters for Load Combination," *Journal of structural Engineering*, Vol. 117, No. 9, pp. 2742-2756, 1991.

Borcherdt, R. D., "New Developments in Estimating Site Effects Ground Motion," *Chapter 10 in Proceeding of Seminar on New Development in Earthquake Ground Motion Estimation and Implications for Engineering Design Practice*, Applied Technology Council, ATC 35-1, 1994.

Brookshire, D. S., Chang, S. E., Cochrane, H., Olson, R. A., Rose, A., Steenson, J., "Direct and Indirect Economic Losses from Earthquake Damage," *Earthquake Spectra*, Vol. 13, No. 4, pp. 683-702, 1997.

Building Construction Cost Data (BCCD), 54th annual Edition,1996.

Calderone, I. and Melbourne, W. H., "The Behaviour of Glass under Wind Loading," *Journal of Wind Engineering and Industrial Aerodynamics*, Vol. 48, pp. 81-94, 1993.

Colaco, J. P., "Proposed Revision to the Houston Building Code for Wind Loads and Missile Impact," *Proceedings of Specialty Conference, Hurricane Alicia: One Year Later*, Galveston, TX, August 16-17, 1984, ASCE, New York, pp. 187-190, 1984.

Colaco, J. P., "Structural Performance of High-Rise Buildings in Houston During Alicia," *Proceedings of Specialty Conference, Hurricane Alicia: One Year Later*, Galveston, TX, August 16-17, 1984, ASCE, New York, pp. 187-190, 1984.

Collins, K. R., Wen, Y.K. and Foutch D. A., "Dual-level Design: A Reliability-based Methodology," *Earthquake Engineering and Structural Dynamics,* Vol. 25, pp. 1433-1467, 1996.

Costa, F. V., "Expectation Ratio Versus Probability," *Proceedings of the 3rd IFIP WG 7.5 Conference,* Berkeley, California, 1990.

Crandell, J. H., Gibson, M. T., Laatsch, E. M., Nowak, M. S., and Overeem, J. A. V., "Statistically-Based Evaluation of Homes Damaged by Hurricanes Andrew and Iniki," *Proceedings of a Symposium on Hurricanes 1992*, Miami, December, 1993.

Dalgliesh, W. A., "Planning for Codification of Window Glass Research," *Proceedings of Specialty Conference, Hurricane Alicia: One Year Later*, Galveston, TX, August 16-17, 1984, ASCE, New York, pp. 187-190, 1984.

Daneshvaran, S. T., Yao, R. M., Zadeh, M., Wen, Y. K., "A parametric model for efficient hurricane risk analysis of large portfolios," *International Conference of Structural Safety and Reliability (ICOSSAR) '97*, Kyoto, Japan, November, 1997.

Devin, P. A., "Wind Endurance," Civil Engineering, Vol. 67, N 12, 1997.

Eliopoulos, D. F. and Wen, Y. K., "Method of Seismic Reliability Evaluation for Moment Resisting Steel Frames," *Civil Engineering Studies*, Structural Research Series Report No. 562, University of Illinois at Urbana-Champaign, Urbana, Illinois, 1991.

Englehardt, J. D., Peng, C., and Mamini, A., "Economic Risk Analysis of Building Codes," *Proceedings of a Symposium on Hurricanes 1992*, Miami, December, 1993.

Federal Emergency Management Agency, A Benefit-Cost Model for the Seismic Rehabilitation of Buildings, Volume 1 & Volume 2, FEMA-227 & FEMA-228, 1992.

Federal Emergency Management Agency, NEHRP Handbook for the Seismic Evaluation of Existing Building, FEMA-178, 1992.

Federal Emergency Management Agency, HEHRP Guidelines for the Seismic Rehabilitation of Buildings, FEMA-273, 1997.

Ferritto, J. M., "Economic Review of Earthquake Design," *Journal of the Structural Division*, ASCE, Vol. 107, No. ST8, pp. 1413-1425, 1981.

Foutch, D. A. and Yun, S.-Y., personal communication, University of Illinois, Urbana, Illinois, 1999.

Frangopol, D. and Corotis, R. B., Editors, "Reliability-Based Structural System Assessment, Design and Optimization," Special Issue, *Journal of Structural Safety*, Vol. 16, 1994.

Frangopol, D. M., "Structural Optimization Using Reliability," *Journal of Structural Engineering*, ASCE, Vol. 111, No. 11, pp. 2288-2301, 1985.

Gabriel, P., "Alicia One Year Later Changes in the Galveston Building Code," *Proceedings of Specialty Conference, Hurricane Alicia: One Year Later*, Galveston, TX, August 16-17, 1984, ASCE, New York, pp. 187-190, 1984.

Harlan, M. R., "Damage to Engineered Structures at Homestead AFB," *Proceedings of a Symposium on Hurricanes 1992*, Miami, December, 1993.

Ishizaki, H., "Problems in Designing Window Glass against Wind Pressure," *Proceedings of the second U.S.A.-Japan Research Seminar on Wind Effects on Structures*,

Jones, H. L., "Minimum Cost Prestressed Concrete Beam," *Journal of Structural Engineering*, ASCE, Vol. 111, No. 11, pp. 2464-2478, 1985.

Kareem, A. and Stevens, J. G., "Window Glass Performance and Analysis in Hurricane Alicia," *Proceedings of Specialty Conference, Hurricane Alicia: One Year Later*, Galveston, TX, August 16-17, 1984, ASCE, New York, pp. 178-186, 1984.

King, S. A., Kiremidjian, A. S., Basoz, N., Law, K., Vucetic, M., Doroudian, M., Olson, R. A., Eidinger, J. M., Goettel, K. A., and Horner G., "Methodologies for Evaluation the Socio-Economic Consequences of Large Earthquakes," *Earthquake Spectra*, Vol. 13(4), pp. 565-584, 1997.

Kircher, C. A., Nassar, A. A., Kustu O., and Holmes, W. T., "Development of Building Damage Function for Earthquake Loss Estimation," *Earthquake Spectra*, Vol. 13, No. 4, pp. 663-682, 1997.

Kircher, C. A., Reitherman, R. K., Whitman, R. V., and Arnold, C., "Estimation of Earthquake Losses to Buildings," *Earthquake Spectra*, Vol. 13, No. 4, pp. 703-720, 1997.

Liu, S. C. and Neghabat, F., "A Cost Optimization Model for Seismic Design of Structures," *The Bell System Technical Journal*, Vol. 51, No. 10, pp. 2209-2225, 1972.

Liu, S. C., Dougherty, M. R. and Neghabat, F., "Optimal Aseismic Design of Building and Equipment," *Journal of Engineering Mechanics, ASCE*, Vol. 102, No. 3, pp. 395-414, 1976.

Maes, M. A. and K. Breitung, "Reliability-Based Tail Estimation," *IUTAM*, San Antonio, Texas, pp. 335-346, 1993.

Maison, B. F. and Bonowitz, D., "How Safe Are Pre-Northridge WSMFs? A Case Study of the SAC Los Angeles 9-Story Building," Opinion Paper, 1998.

McCormack, T. C., and Rad, F. N., "An Earthquake Estimation Methodology for buildings Based on ATC-13 and ATC-21", *Earthquake Spectra*, 1997, Vol. 13(4), 605-622.

McDonald, J. R., "Impact Resistance of Common Building Materials to Tornado Missiles," *Proceedings of the Sixth U.S. National Conference on Wind Engineering*, University of Houston, Houston, Texas, March 1989.

Metha, K. C., "Hurricane Wind Load Criteria of the ANSI Standard," *Proceedings of Specialty Conference, Hurricane Alicia: One Year Later*, Galveston, TX, August 16-17, 1984, ASCE, New York, pp. 187-190, 1984.

Minor, J. E., "Windborne Debris and the Building Envelope," *Journal of Wind Engineering and Industrial Aerodynamics*, Vol. 53, pp. 207-227, 1994.

Minor, J. E., "Window Glass Design Practices: A Review," *Journal of the Structural Division*, ASCE, Vol. 107, 1981.

Minor, J. E., "Window Glass Failure in Windstorms," *Journal of the Structural Division*, ASCE, Vol. 102, 1976.

Minor, J. E., "Window Glass in Windstorms," *Civil Engineering Report Series*, CE74-01, Department of Civil Engineering, Texas Tech University, Lubbock, Texas, 1974.

Minor, J. E., "Window Glass Performance and Hurricane Effects," *Proceedings of Specialty Conference, Hurricane Alicia: One Year Later*, Galveston, TX, August 16-17, 1984, ASCE, New York, pp. 151-167, 1984.

Minor, J. E. and Beason, W. L., "Window Glass Failures in Windstorms," *Journal of the Structural Division*, ASCE, Vol. 102, 1976.

Minor, J. E. and Behr, R. A., "Improving the Performance of Architectural Glazing in Hurricanes," *Proceedings of a Symposium on Hurricanes 1992*, Miami, December, 1993.

Minor, J. E. and Reznik, P. L., "Failure Strengths of Laminated Glass," *Journal of Structural Engineering*, ASCE, Vol. 116, 1990.

Minor, J. E., Beason, W. L., and Harris, P. L., "Designing for Windborne Missiles in Urban Areas," *Journal of the Structural Division*, ASCE, Vol. 104, pp. 1749-1759, 1978.

Minor, J. E., Metha, K. C., and McDonald, J. R., "Failure of Structures due to Extreme Winds," *Journal of the Structural Division*, ASCE, Vol. 98, pp. 2455-2471,1972.

Neely, E. S., and Neathammer, R., "Computerized Life-Cycle Cost Systems in the Army," *Journal of Computing in Civil Engineering*, ASCE, Vol. 3, No. 1, pp. 93-104, 1989.

Norville, H. S., Bove, P. M., Sheridan, D. L., and Lawrence, S. L., "Strength of New Heat Treated Window Glass Lites and Laminated Glass Units," *Journal of Structural Engineering*, ASCE, Vol. 119, 1993.

Olshansky, R. B., "The Role of Earthquake Hazard Maps in Loss Estimation: A Study of the Northridge Earthquake," *Earthquake Spectra*, 1997, Vol. 13(4), 721-738.

Pantelides, C. P., Horst, A. D., and Minor, J. E., "Postbreakage Behavior of Hear Strengthened Laminated Glass under Wind Effects," *Journal of Structural Engineering*, ASCE, Vol. 119, 1993.

Pantelides, C. P., Horst, A. D., and Minor, J. E., "Post-Breakage Behavior of Architectural Glazing in Windstorms," *Journal of Wind Engineering and Industrial Aerodynamics*, Vol. 41-44, pp. 2425-2435, 1992.

Rifer, W., Osterhaug, B., and Burton, D., "Disaster Debris Management and Diversion from Hurricane Iniki," *Proceedings of a Symposium on Hurricanes 1992, Miami*, December, 1993.

Roehm, J. M., "Standards Related to Curtain Wall," *Proceedings of Specialty Conference, Hurricane Alicia: One Year Later*, Galveston, TX, August 16-17, 1984, ASCE, New York, pp. 187-190, 1984.

Rojahn, C., King, S. A., Scholl, R. E., Kiremidjian, A. S., Reaveley L. D., and Wilson, R. D., "Earthquake Damage and Loss Estimation Methodology and Data for Salt Lake County," Utah (ATC-36), *Earthquake Spectra*, 1997, Vol. 13(4), 623-642.

Rosenblueth, E., "Optimum Design for Infrequent Disturbances," *Journal of structural division*, Proc. of ASCE, pp. 1807-1825, 1976.

Rosenblueth, E., "Toward Optimal Design through Building Codes," *Journal of structural division,* Proc. of ASCE, pp. 591-607, 1976.

Russell, A. D., and Choudhary, K. T., "Cost Optimization of Buildings," *Journal of the Structural Division*, ASCE, Vol. 106, No. ST1, pp. 283-300, 1980.

Structural Engineering Association of California (SEAOC), "Performance Based Seismic Engineering of Building", Vol. 1 and 2, 1995.

Shinozuka, M., Chang, S. E., Eguchi, R. T., Abrams, D. P., Hwang, H. H. M., and Rose, A., "Advances in Earthquake Loss Estimation and Application to Memphis, Tennessee," *Earthquake Spectra*, Vol. 13, No. 4, pp. 739-758, 1997.

Simiu, E. and Cordes, M. R., "Tornado-Borne Missile Speed Probabilities," *Journal of Structural Engineering*, ASCE, Vol. 109, 1983.

Sparks, P. R. and Bhinderwala, S. A., "Relationship Between Residential Insurance Losses and Wind Conditions in Hurricane Andrew," *Proceedings of a Symposium on Hurricanes 1992*, Miami, December, 1993.

Sparks, P. R., Schiff, S. D., and Reinhold, T. A., "Wind Damage to Envelope of Houses and Consequent Insurance Losses," *Journal of Wind Engineering and Industrial Aerodynamics*, Vol. 53, pp. 145-155, 1994.

Structural Engineers Association of California (SEAOC), *Performance Based Seismic Engineering of Buildings*, Volume I, Vision 2000 Report, California, 1995.

Stubbs, N. and Perry, D. C., "Engineering of the Building Envelope "To Do Or Not To Do"," *Proceedings of a Symposium on Hurricanes 1992*, Miami, December, 1993.

Surahman, A., and Rojiani, K. B., "Reliability Based Optimum Design of Concrete Frames," *Journal of Structural Engineering*, ASCE, Vol. 109, No. 3, pp. 741-757, 1983.

Tao, Z., Corotis, R. B., and Ellis J. H., "Reliability-based Bridge Design and Life Cycle Management with Markov Decision Processes," *Structural Safety*, Elsevier, Vol 16 (1+2), pp. 111-132, 1994.

Tsai, C. R. and Stewart, R. A., "Stress Analysis of Large Deflection of Glass Plates by the Finite-Element Method," *Journal of The American Ceramic Society*, 1976.

Twisdale, L. A., "Probability of Facility Damage from Extreme Wind Effects," *Journal of the Structural Division*, ASCE, Vol. 114, NO 10, pp. 2190-2209, 1988.

U.S. Geological Survey, National Seismic Hazards Mapping Project, 1999. (http://geohazards.cr.usgs.gov/eq/fhtml/fwus.shtml)

Vallabhan, C. V. G., "Iterative Analysis of Nonlinear Glass Plates," *Journal of Structural Engineering*, ASCE, Vol. 109, 1983.

Vallabhan, C. V. G., Das, Y. C., Magdi, M., Asik, M., and Bailey, J. R., "Analysis of Laminated Glass Units," *Journal of Structural Engineering*, ASCE, Vol. 119, 1993.

Vallabhan, C. V. G., Minor, J. E., and Nagalla, S. R., "Stress in Layered Glass Units and Monolithic Glass Plates," *Journal of Structural Engineering*, ASCE, Vol. 113, No. 1, pp. 36-43, 1987.

Vanmarcke, E., and Angelides, D., "Risk Assessment for Offshore Structure," *Journal of Structural Engineering*, ASCE, Vol. 109, No. 2, pp. 555-571, 1983.

Vild, D. J., "Glass Design in Hurricane Regions," *Proceedings of Specialty Conference, Hurricane Alicia: One Year Later*, Galveston, TX, August 16-17, 1984, ASCE, New York, pp. 187-190, 1984.

Walter, F., "Critique-Manufactured Housing Session," *Proceedings of a Symposium on Hurricanes 1992*, Miami, December, 1993.

Wardlaw, R. L. and Kind, R. J., "Wind Speeds for Gravel Scour and Paver Lifting on Roofs," *Proceedings of Specialty Conference, Hurricane Alicia: One Year Later*, Galveston, TX, August 16-17, 1984, ASCE, New York, pp. 187-190, 1984.

Warszawski, A., Gluck, J., and Segal, D., "Economic Evaluation of Design Codes-Case of Seismic Design," *Journal of Structural Engineering, ASCE*, Vol. 122, No. 12, pp. 1400-1408, 1996.

Weibull, W., "A Statistical Theory of the Strength of Materials," Ingeniorsvetenskapsakademiens, Handlinger NR151, Stockholm, Sweden, 1939.

Wen, Y. K., *Structural load modeling and combination for performance and safety evaluation*, Elservier Science Publisher, 1990.

Wen, Y. K., "Reliability and Performance Based Design for Seismic Load," Keynote in the Asian-Pacific Symposium on Structural Reliability and its Applications (APSSRA 99), Taipei, Taiwan, Republic of China, Feb. 1999.

Wen, Y. K., and Ang, A. H.-S., "Reliability and Cost-Effectiveness of Structures with Active Control," *Intelligent Structures-2: Monitoring and Control*, Proc. of the International Workshop on Intelligent Systems, Perugia, Italy, 27-29, *Elsevier Applied Science,* June 1991

Wen, Y. K., and Foutch, D. A., "Proposed Statistical and Reliability Framework for Comparing and Evaluating Predictive Models for Evaluation and Design and Critical Issues in Developing Such Framework," Report No. SAC/BD-97/03, *SAC Steel Project,* SAC Background Document, Sacramento, California, August 1997.

Wen, Y. K., and Shinozuka, M., Cost-Effectiveness Issues in Active Structural Control, *Proc. First World Conference on Structural Control*, Pasadena, California, August 3-5, 1994.

Werner, S. D., Taylor C. E., and Moore II, J. E., "Loss Estimation Due to Seismic Risks to Highway Systems," *Earthquake Spectra*, Vol. 13, No. 4, pp. 585-604, 1997.

Whitman, R. V., Anagnos, T., Kircher, C., Lagorio, H. J., Lawson, R. S., and Schneider, P., "Development of a National Earthquake Loss Estimation Methodology," *Earthquake Spectra*, Vol. 13, No. 4, pp. 643-662, 1997.

Woods, A. R. and Blackmore, P. A., "The Effect of Dominant Openings and Porosity on Internal Pressures," *Journal of Wind Engineering and Industrial Aerodynamics*, Vol. 57, pp. 167-177, 1995.